This is to certify that the

dissertation entitled

The Rheology and Morphology of Reactively
Compatibilized Polymer Blends

presented by

Himanshu Asthana

has been accepted towards fulfillment
of the requirements for

Ph.D. _____ degree in Chemical Engineering

_Major professor

Date 12/18/97

PLACE IN RETURN BOX
to remove this checkout from your record.
TO AVOID FINES return on or before date due.

DATE DUE	DATE DUE	DATE DUE
JUN 2009 2008		

1/98 c/CIRC/DateDue.p65-p.14

THE RHEOLOGY AND MORPHOLOGY OF REACTIVELY COMPATIBILIZED POLYMER BLENDS

By

Himanshu Asthana

A DISSERTATION

Submitted to
Michigan State University
in partial fulfillment of the requirements
for the degree of

DOCTOR OF PHILOSOPHY

Department of Chemical Engineering

(1997)

ABSTRACT

THE RHEOLOGY AND MORPHOLOGY OF REACTIVELY COMPATIBILIZED POLYMER BLENDS

By

Himanshu Asthana

The study was conducted to investigate the effect of progressive extents of interfacial reaction on the rheology and morphology of reactively compatibilized polymer blends. Although the interfacial reaction is known to produce a finer morphology, its effect on interfacial tension has not been quantified in earlier studies. The values of equilibrium interfacial tension in blends with progressive extent of reaction were determined in the present study from rheological measurements on blends of maleated polypropylene and nylon 6. Nylon 6 was melt blended in a twin screw extruder with one of several grades of maleated polypropylene which contained progressively increasing extent of maleation to study reactive compatibilization via direct reaction. The results show that the equilibrium interfacial tension falls due to interfacial reaction. However, the corresponding morphological observations indicate that a minimal extent of interfacial reaction (and hence a small reduction in equilibrium interfacial tension) is sufficient to bring about a change in the particle size. The dynamic shear measurements show that interfacial reaction imparts additional rigidity to the blend.

Polypropylene and polystyrene were similarly melt blended with a pre-made elastomeric -[S-EP]- di block copolymer. The data show that the equilibrium interfacial tension falls due to the addition of the compatibilizing agent from 5 mN/ m in non

compatibilized blends to 1 mN/m in non compatibilized blends. However, unlike the directly reacted blends, increasing the amount of the compatibilizing agent did not reduce the interfacial tension. Also, in this case the cross over of the blend storage modulus with the components is at a much higher frequency compared to the directly reacted blends. Due to the solubilization of the matrix in the external block copolymer, the storage modulus curves are non-monotonic. In the directly reacted blends, the storage modulus increased progressively with greater extent of maleation and reaction.

In Loving Memory

of

Shashi Asthana

ACKNOWLEDGEMENTS

TABLE OF CONTENTS

LIST OF TABLES

LIST OF FIGURES

xiii

.

LIST OF SYMBOLS

Ca : Capillary Number.
d : Diameter of the drops, m.
d_u : Diameter of the drops in the unreacted system, m.
d_r : Diameter of the drops in the reacted system, m.
D : Deformation of the drop.
G' : Storage modulus of the material, N/m^2.
G'' : Loss modulus of the material, N/m^2.
G_b^* : Complex modulus of the blend, N/m^2.
G_d^* : Complex modulus of the dispersed phase, N/m^2.
G_m^* : Complex modulus of the matrix, N/m^2.
p : Viscosity ratio, η_d/η_m.
p_r : Viscosity ratio in the reactive system.
p_u : Viscosity ratio in the unreactive system.
q : Rate of growth of the instability.
R_0 : Radius of the filament at t = 0.
$\bar{R}_v$: Volume average radius of dispersed phase, m.
t : Time, s.
t_b : Time for break-up of the filament, s.
t_{coll} : Time for collision of the drops, s.
t_{int} : Time for interaction of the drops, s.
t_{drain} : Time for drainage of the drops, s.
$t_{process}$: Time for process of collision of the drops, s.
t_{ret} : Time for retraction of the drops, s.

Greek Symbols:

α : Amplitude of disturbance, m.
α_0 : Amplitude of the disturbance at time t = 0.
β^* : Sum of surface shear modulus and surface dilatation modulus, N/m^2.
β_s^* : Surface shear modulus, N/m^2.
β_d^* : Surface dilatation modulus, N/m^2.
η_d : Viscosity of the dispersed phase, Pa-s.
γ : Shear rate, 1/s.
Γ^0 : Equilibrium interfacial tension, N/m.
Γ_r : Interfacial tension of the reactive system, N/m.
Γ_u : Interfacial tension of the unreactive system, N/m.
λ : Wavelength of the disturbance, m.
λ_1 : Relaxation time, s.
λ_2 : Retardation time, s.
λ_d : Relaxation time of the dispersed phase, s.
λ_m : Relaxation time of the matrix, s.
λ_D : Beginning of secondary plateau of the blend, s.

λ_P : End of secondary plateau of the blend, s.

λ_M : Beginning of primary plateau of the blend, s.

Ω : Tabulated function.

η : Sum of viscosity of component phases, Pa-s.

η_0 : Zero-shear viscosity, Pa-s.

η_b : Viscosity of the blend, Pa-s.

η_d : Viscosity of the dispersed phase, Pa-s.

η_m : Viscosity of the matrix, Pa-s.

ϕ_d : Volume fraction of the dispersed phase.

ϕ_m : Volume fraction of the matrix.

τ : Time scale of retraction of the filament, s.

τ_s : Shear stress, N/ m^2.

T_r : Torque in mixer in reactive system, N-m.

T_u : Torque in mixer in unreactive system, N-m.

INTRODUCTION

Chapter 1

It is a common industrial practice to mix two or more polymers to make a new material whose properties are an optimum combination of the individual components. When two polymers are mixed, one of the phase (the minor phase) forms the dispersed phase and the other component (the major phase) forms the continuous or the matrix phase. The shape and size of the dispersed phase plays a critical role in the final properties and the processing behavior of the blend [Wu, 1983]. The main issue in blending of polymers is to control the particle shape and size (distribution). Most polymers phase separate on mixing due to the thermodynamic considerations [Sperling, 1992]. Thus, there is a need to compatibilize the components so that they do not phase separate on mixing and at the same time offer control over the particle size of the dispersed phase. Most often, this requires promoting dispersive mixing by the reduction of interfacial tension between the component phases. This may also lead to enhanced adhesion between the component phases which is a result of reduction of interfacial tension between the two phases. There are two common techniques employed to achieve this [Xanthos, 1994]. They are:

1. Addition of an external compatibilizing agent to the mixture.

2. Carry out an in-situ reaction between the complementary groups on the individual components.

These lead to smaller particle sizes, a narrower particle size distribution and improved adhesion. The following section is a brief discussion of the steps involved in the development of morphology in emulsions. A direct analogy can be made to the morphology of polymeric blends.

1.1 DEVELOPMENT OF MORPHOLOGY

The simplest problem to study the development of morphology is that of a break-up of a drop suspended in an infinite continuous phase. There are three main steps involved during this process:

1. Drop deformation.

2. Drop dispersion.

3. Coalescence of drops.

1.1.1 Drop Deformation.

After the seminal work of Taylor [Taylor 1934; Taylor 1938], several researchers have studied the deformation of a drop suspended in another fluid [Cox, 1969; Grace, 1979; Bentley, 1986; Stone, 1994; Tjahjadi et. al., 1996]. The relation governing the deformation of the drop is:

$$D = Ca \frac{[(19p+16)/(16p+16)]}{[(19pCa/40)^2 + 1]^{1/2}} \qquad (1.1)$$

$$\theta = \pi/4 + 0.5\tan^{-1}(19pCa/20) \qquad (1.2)$$

where the capillary number Ca is defined as

$$Ca = \frac{\tau_s d}{\Gamma^0} = \frac{\dot{\gamma}\,\eta_m d}{\Gamma^0} \qquad (1.3)$$

The main results of these studies are :

1. The Ca_{crit} for drop break-up is lowest at a viscosity ratio of unity.

2. Beyond a viscosity ratio of 3.0-3.5, shear is incapable of dispersing the drop. For extensional flow this limit is very high.

3. There is a critical capillary number Ca_{crit} beyond which the drop bursts. In effect, beyond Ca_{crit} interfacial tension forces can not balance the viscous forces.

4. Extensional flow is more conducive to drop dispersion as compared to shear flow.

It is seen that the equilibrium interfacial tension plays a direct role through the capillary number. *For a given flow field, lower interfacial tension facilitates drop deformation (or dispersion) by the action of viscous forces.* In the initial stages of

blending when the particle sizes are large ($Ca \gg Ca_{crit}$) viscous forces dominate

interfacial forces and thus long stretched threads are formed. The mechanism of break-up

of these threads is by Rayleigh instabilities as discussed in the following section.

1.1.2 Break-up of threads by growth of Rayleigh instabilities

Rayleigh presented the first study of the problem of capillary instability of a

cylindrical column [Rayleigh, 1878]. The salient feature of the hypothesis is that the

disturbance, assumed sinusoidal grows if the wavelength of the disturbance $\lambda > 2\pi R_o$.

This situation leads to an increase in the interfacial energy/ area which is

thermodynamically unfavourable. To reduce the interfacial energy the disturbance grows

at an exponential rate such that the thread breaks up into several smaller drops. Larger

number of drops causes the energy to distribute over a larger interfacial area, causing a

reduced interfacial energy/ area and hence thermodynamic stability. The growth of the

disturbance is exponential and given as:

$$\alpha = \alpha_0 \exp(qt) \qquad (1.4)$$

In Equation 1.4, α is amplitude of the disturbance, α_0 amplitude at t=0, t being the time

and q the rate of growth.

$$q = \frac{\Gamma^0 \Omega(\lambda, p)}{2\eta_m R_0} \qquad (1.5)$$

The parameter Ω in Equation 1.5 is a tabulated function [Tomotika 1935; Tomotika

1936]. Experimental investigations have confirmed the validity of these relations

[Rumscheidt and Mason, 1962; Elmendorp, 1986]. From the relations presented above, the time for break-up of the thread is given as [Rumscheidt and Mason, 1962]:

$$t_b = \frac{1}{q} \ln \left[\frac{0.81 R_0}{\alpha_0} \right] \qquad (1.6)$$

The preceding discussion brings out two important parameters for the dispersion of a cylindrical thread - t_b and Ca_{crit}. $Ca > Ca_{crit}$ is a pre-requisite for break-up, which is accomplished only if $t > t_b$. It can be seen that the interfacial tension plays a critical role in this step also. The Equation 1.5 shows that the rate of growth of the disturbance is directly proportional to the equilibrium interfacial tension. A lower interfacial tension means that the disturbance grows at a slower rate. In effect, a lower interfacial tension translates to improved adhesion between the two phases. In addition, the above discussion also shows that the residence time (in case of batch mixers) and / or residence time distribution (in case of continuous reactors) is important during processing. This governs the time of break-up allowed. Besides, the residence time (distribution) also affects the coalescence phenomenon directly.

1.1.3   Coalescence of drops

With increasing concentration of the dispersed phase, the probability of interaction of the drops with each other increases. This leads to collision. But, does each collision necessarily lead to a coalescence of drops? Janssen and co-workers have studied this problem and found that the process is governed by four time scales [Janssen and Meijer, 1995].

1 - time of collision t_{coll}, average time after which the drop collides.

2 - time of interaction t_{int}, duration of collision.

3 - time of drainage of the film t_{drain}.

4 - time of process, $t_{process}$.

The equilibrium interfacial tension is directly involved in the drainage time. Depending on the mobility of the interface it has differing impact. But, in general a reduced interfacial tension leads to an increased drainage time. This suppresses coalescence which prevents smaller drops from forming larger drops and ultimately leads to a reduced particle size.

The study by Janssen et. al. also showed that there is a range of processing parameters which favor coalescence [Janssen and Meijer, 1995]. Coalescence preferentially occurs in regions of small deformation rates, which provide large interaction times. In this process the nature of the interface (of the drops) plays a critical role. Higher interface mobility promotes film drainage increasing probability of coalescence. *Externally added compatibilizing agents or in-situ reaction reduce the interface mobility [Janssen and Meijer, 1995]. This promotes higher drainage times hindering coalescence and stabilizing the morphology.*

The preceding discussion illustrates the importance of interfacial tension in the various steps involved in the break-up of a drop. It is a critical step involved in the development of morphology of polymeric blends. The present work is an attempt to understand the specific role that interfacial tension plays in reactive polymer blends. An

important parameter that characterizes the interfaces is the interfacial tension. The following chapter illustrates the past work that has been done to understand the role of equilibrium interfacial tension in polymeric blends and its role in development of morphology.

Chapter 2

The preceding chapter showed the importance of interfacial tension in the development of morphology. Also, the different equations and experimental observations show that a reduced interfacial tension promotes drop dispersion. This fact has been used to promote compatibilization in polymeric blends. It is achieved either by addition of an external agent or by direct reaction between the complementary groups on the blend components [Xanthos, 1994]. In both cases, an emulsifying action occurs at the interface which leads to a reduced interfacial tension. This chapter discusses the past work that has been done to understand the role of interface and interfacial tension in the development of morphology of polymeric blends.

2.1 SYSTEMS COMPATIBILIZED BY IN-SITU REACTION BETWEEN COMPLEMENTARY GROUPS

It is widely accepted that interfacial reaction promotes dispersive mixing by the reduction of interfacial tension. Experimental evidence is well documented in the literature which shows that the interfacial tension is reduced by the addition of an external agent [Cho et. al., 1996; Elemans et. al., 1991]. However, there is no systematic study on the effect of an in-situ reaction between the polymers on the interfacial tension between them. The study by Wu on a system of nylon 6 blended with non-reactive and reactive (functionalized with less than 1% carboxylic acid) EP-rubbers in a twin screw extruder is

considered a significant step in this direction [Wu 1987]. Wu presented interfacial

tension values based on statistical mechanical theory of polymers. The interfacial tension

was related to the Flory-Huggins χ parameter which in turn was related to the interfacial

thickness. The basis of this was the theoretical development by Helfand and Sapse

[1975].

$$\Gamma^0 \propto \chi^{1/2} \propto L^{-1} \qquad (2.1)$$

Based on the regression analysis of the experimentally measured thickness of the

interface in model systems Wu arrived at the following relation.

$$\Gamma^0 = 7.6 L^{-0.86} \qquad (2.2)$$

Wu then made measurements of the interfacial thickness in nylon 6 - reactive rubber

blends and by using the Equation 2.2 proposed that the interfacial tension drop in a

reactive system could be as much as 30 fold (from 8.8 mN/ m in non-reactive to 0.25 mN/

m in reactive systems). Wu attributed this reduction in interfacial tension to the

emulsifying action of the graft copolymer formed in-situ due to the reaction [Wu 1983].

Although a useful result, it is still not a direct measurement of the interfacial tension in

reactive system. *It is an important purpose of this study to provide experimentally*

measured values of interfacial tension. Also, in the same study Wu proposed that the

droplet breakup behavior of polymeric viscoelastic drops is fundamentally different from

those of Newtonian fluids. On the basis of some empiricism he derived the following

relation.

$$\frac{(\dot{\gamma}\,\eta_m)d}{\Gamma^0} = \frac{\tau_s d}{\Gamma^0} = 4p^{\pm 0.84} \qquad (2.3)$$

The '+' sign applies to systems having the viscosity ratio greater than unity while '-' sign

applies when it is less than unity. The viscosity values are prior to the reaction. *Although*

it is a good starting point for estimating particle sizes based on processing conditions, it

is not a fundamental result. Two important parameters were *estimated* in Wu's analysis.

1. interfacial tension in reactive blends.
2. shear rate.

This study focuses on attempting to remove the discrepancy with regard to the interfacial

tension. Serpe and co-workers [1990] used Wu's relation in their work with

polyethylene-polyamide blends and found that *for differing compositions, their curves*

followed a V-shape trend parallel to Wu's curves but all the points did not fall onto a

single curve. They modified Wu's relation as follows.

$$Ca^* = \frac{\dot{\gamma}\,\eta_b d}{\Gamma^0}(1 - 4(\phi_d \phi_m)^{0.8}) = 4p^{\pm 0.84} \qquad (2.4)$$

In Equation 2.4, ϕ_d and ϕ_m are the volume fractions of the dispersed and the continuous

phases respectively. Note that the *matrix viscosity has been replaced by the blend*

viscosity. Such disagreements necessitate further investigations into the role of interfacial

tension on the blend behavior. This work aims to do this.

Scott and Macosko [1995, Intern. Polym. Proc] investigated the morphology of

reactive blends of nylon with functionalized EP rubbers. They found that the size of the

dispersed phase decreased continuously as the extent of reaction increased. *They*

proposed that differences between the actual size and that predicted by Wu's relation are

due to changes brought about by interfacial tension and coalescence. The shear stress was estimated from T, the torque on the mixer because the shear rate is difficult to determine for the complex flow field. Based on Wu's relation the differences between the reactive and non-reactive blends obey the following relation.

$$\frac{d_u}{d_r} = \frac{T_r}{T_u} \left[\frac{p(T_r)}{p(T_u)} \right]^{0.84} \qquad (2.5)$$

In the empirical relation of Equation 2.5 the differences due to interfacial tension alone have not been delineated. Now, one can also modify the above relation as follows (directly from Wu's relation)

$$\frac{d_u}{d_r} = \frac{\Gamma_u}{\Gamma_r} \frac{(\dot{\gamma}\,\eta_m)_r}{(\dot{\gamma}\,\eta_m)_u} \left[\frac{p_r}{p_u} \right]^{0.84} \qquad (2.6)$$

After making estimates of the shear stresses and (if) interfacial tension values are available, one can comment on the effects due to reaction. This would be addressed in this work.

In a related study Scott and Macosko [1995, Poly. Eng. Sc.] blended non-reactive and reactive EP rubbers (functionalized with Maleic anhydride) with non-functionalized and functionalized Polystyrene (functionalized with vinyl oxazoline). The non-reactive blends showed poor interfacial adhesion and large particle sizes of the dispersed phase. On the other hand, the reactive blends exhibit good adhesion and smaller dispersed domain sizes. Reactive blends were shows to have a higher morphological stability. In addition, increasing the oxazoline content lead to decreased dispersed phase particle size. This may not be the case always. Borggreve and Gaymans [1989] carried out a study on

blends of nylon 6 with EPD rubber. They observed that increasing the maleic anhydride content of functionalized rubber from 0.13 to 0.89 did not have a significant impact on the dispersed phase sizes. A similar observation was made by Scott and Macosko [1995, Polym. Eng. Sc.]. This indicates that in reactively compatibilized systems the development of morphology may depend on factors other than reduction of interfacial tension.

In a similar study Hosoda et. al. [1991] carried out a study of morphological changes in nylon 6 - polypropylene (maleated and unmaleated) blends. Their observations show that the graft copolymer formed after the reaction resides at the interface. Similar observations were reported by Fayt et. al. [1986]. Hosoda and co-workers observed that the thickness of the interface lies between 50-100 Å. Moreover, as the grafted maleic anhydride content in the maleated polypropylene increased, the average particle size of the dispersed phase decreased while the interface thickness remained constant. They concluded that the interface stability per graft copolymer molecule is constant and independent of the degree of the reaction between nylon 6 and maleated polypropylene. The study of Nishio et. al. [1991] on nylon 6 and maleated polypropylene shows that the interface area per unit volume increased linearly with increase in the grafted copolymer content. They hypothesized that a unit area of the interface per unit volume is occupied by a certain amount of the copolymer independent of the sample. The copolymer located at the interface behaves as an emulsifier with a constant concentration per unit interface area.

The brief discussion shows that the interface plays a critical role in the determination of morphology. If one has to understand it holistically, then the interplay of interfacial (tension) forces and viscous forces has to be understood. This in turn is dependent on the processing conditions (shear rate, temperature for example). Moreover, in polymers the situation is further complicated by the elasticity of the components. This work will address the interfacial tension segment of the problem. How does morphology vary/ depend on the interfacial reaction between the polymeric species?

2.2 SYSTEMS COMPATIBILIZED BY THE ADDITION OF AN EXTERNAL AGENT

The components of the blend can be compatibilized by the addition of an external agent. This compatibilization may be of a physical or chemical nature. In physical compatibilization, the compatibilizing agent does not react with the component phases. Instead, there are groups on the compatibilizer which are physically similar to the chemical nature of the components. On the other hand, in chemical compatibilization, a chemical reaction occurs between the external agent and the component phase(s). For example, maleated polypropylene would chemically compatibilize neat polypropylene and nylon 6 [Ide and Hasegawa, 1971]. The maleic anhydride group on the maleated polypropylene can react with amine of the nylon 6. A brief discussion of some relevant past work in this area follows.

Okamoto and Inoue [1993] carried out a study on poly-(ε-caprolactone) blended with two different kind of functionalized rubbers. They were coupled (chemically compatibilized) with an external agent. The aim of that study was to understand the development of morphology and relate it to the extent of interfacial reaction. They concluded that as the residence time in the mixer is increased, the average particle size decreases until a given value and then becomes a constant. The exact behavior depends on the amount of coupling agent added. Expectedly, the average size is less for larger amounts. At the same time, the specific interfacial area increases and saturates at a given value. The interesting observation was regarding the interfacial thickness. As observed by Hosoda et. al. [1991], the interfacial thickness assumed a constant value irrespective of the residence time. Based on their observation with two different kinds of rubber, they hypothesized that coupling reaction is faster at thinner interface, which leads to a faster rate of size reduction in such systems.

Lim and White [1994] studied externally compatibilized blends of polyethylene and nylon 6 in a modular twin screw extruder. The main purpose of their study was to relate the development of morphology along the extruder length. It was found that the rate of decrease of phase morphology scale increases rapidly along the screw length by the addition of the compatibilizing agent while at the same time leading to a finer ultimate morphology. They showed that besides the functionality on the compatibilizing agent, the processing conditions and the properties of the components make a significant difference on the resultant morphology. This observation is supported by the study of Lee and Yang [1995]. They prepared blends of polypropylene with nylon 6 by three different

mixing processes; single step blending, two-step blending with reactive premixing and two-step blending with non-reactive premixing. They found that the single step mixing proved to be the most effective for scaling down the morphology.

Now, the studies cited so far have not studied the effect of interfacial tension on the morphology development by making actual measurements of the interfacial tension. An important focus of the present study is to study this aspect of the problem and attempt to provide this information. Also, as preceding discussion shows, the rheology of the blends is effected by the interfacial reaction. This work will systematically study the effects of reaction on morphology development and rheology of the reactively compatibilized polymeric blends.

THE EFFECT OF INTERFACIAL REACTION ON THE INTERFACIAL TENSION IN REACTIVELY COMPATIBILIZED NYLON 6 - MALEATED POLYPROPYLENE BLENDS

Chapter 3

3.1 INTRODUCTION

Polymers are thermodynamically incompatible. As a result they phase separate on blending [Sperling, 1992]. Compatibilization of polymers is carried out to circumvent this problem. It is achieved primarily in two ways. Firstly, by adding an external compatibilizer which is compatible with the blend components. Secondly, by an in-situ reaction of the complementary groups on the components. Both techniques compatibilize by directly influencing the interface between the polymers. Reduction of equilibrium interfacial tension plays a significant role in the process of compatibilization. It has been shown that addition of an external compatibilizer leads to a reduction in equilibrium interfacial tension [Elemans et. al. 1990]. An important aim of this study is to investigate the effect of interfacial reaction on the interfacial tension in blends compatibilized via reaction of complementary reactive groups. The values available in the literature are indirect and based on empirical relations [Wu, 1987]. The relation requires the use of morphological parameters. In recent studies it has been shown that besides equilibrium interfacial tension, suppression of coalescence also plays an important role in the development of morphology [Sundraraj and Macosko, 1993; O'Shaughnessy and Sawhney, 1996]. That is, the morphological parameters alone are

16

insufficient to characterize the equilibrium interfacial tension. Thus, there is a need for directly measured values of equilibrium interfacial tension.

The reaction product located at the interface leads to a fundamental change in the rheological behavior of the blend as has been shown in this study and Chapter 4. Due to the 'occupied interface' and the physical links' that are established between the component phases, the elasticity of the system is enhanced. In light of this observation it can be concluded that the composition of the interface is critical in determining the rheological behavior of the blend.

The materials chosen in this study contain additives which are incorporated in the polymers as processing aids. They are usually low molecular weight materials. Being low molecular weight materials they have a thermodynamic drive to rise to the interface. Another question being investigated in this study relates to the effects of the presence of these low molecular weight materials at the interface? Can they behave as surfactants?

3.1.1 Emulsion Models

The rheological behavior of the polymeric blends has been explained on the basis of emulsion models. Three emulsion models have usually been applied to polymeric systems. They are due to Oldroyd [Oldroyd, 1953], Choi and Schowalter [Choi and Schowalter, 1975] and Palierne [Palierne, 1990]. The models of Oldroyd, and of Choi and Schowalter were formulated for a mixture of Newtonian fluids with monodisperse spherical inclusions. Interestingly, both models predict a non-zero storage modulus of the blend especially in the low frequency region. This is a direct result of the interfacial

tension between the blend components. It leads to long time relaxation processes of the

dispersed phase which are of the order of mechanical relaxation of the drop shape

[Scholz et. al., 1989] as shown in Equation 3.1.

$$\lambda_D \sim f(k)\frac{R\eta_m}{\Gamma^0} \qquad (3.1)$$

These models show that the rheological behavior, especially the storage modulus is

sensitive to the interfacial tension in the low frequency region.

The general form of the models of Oldroyd and of Choi and Schowalter is

$$G' = \eta_a \frac{\omega^2(\lambda_1 - \lambda_2)}{1 + \omega^2\lambda_1^2} \qquad (3.2)$$

$$G'' = \eta_a \frac{\omega(1 + \omega^2\lambda_1\lambda_2)}{1 + \omega^2\lambda_1^2} \qquad (3.3)$$

The definition of the parameters λ_0, λ_1, λ_2 and η_a for the models have been shown in

Table 3.1. These models have been used by several workers to determine the interfacial

tension in the polymeric systems [Scholz et. al., 1989; Graebling and Muller, 1991;

Gramespacher and Meissner, 1992].

To account for the viscoelastic properties of the component phases, Palierne

proposed an emulsion model for a mixture of two viscoelastic fluids [Palierne 1990]. It

accounts for the distribution in particle size and interactions and is applicable for a wide

range of volume fractions of the dispersed phase. The model explicitly takes into account

the rheological behavior of the component phases and the interfacial tension. The

relation is shown in Equation 3.4.

$$G_b^* = G_m^* \left[\frac{1 + \dfrac{3}{2} \sum_i \dfrac{\phi_i E_i}{D_i}}{1 - \sum_i \dfrac{\phi_i E_i}{D_i}} \right] \qquad (3.4)$$

where,

$$E_i = 2(G_d^* - G_m^*)(19G_d^* + 16G_m^*) + \frac{48\beta_d^* \Gamma^o}{R^2} + \frac{32\beta_s^* (\Gamma^o + \beta_d^*)}{R^2} + \frac{8\Gamma^o}{R}(5G_d^* + 2G_m^*) + \frac{2\beta_d^*}{R}(23G_d^* - 16G_m^*) + \frac{4\beta_s^*}{R}(13G_d^* + 8G_m^*)$$

$$(3.5)$$

and

$$D_i = (2G_d^* - 3G_m^*)(19G_d^* + 16G_m^*) + \frac{48\beta_d^* \Gamma^o}{R^2} + \frac{32\beta_s^* (\Gamma^o + \beta_d^*)}{R^2} + \frac{40\Gamma^o}{R}(G_d^* + G_m^*) + \frac{2\beta_d^*}{R}(23G_d^* + 32G_m^*) + \frac{4\beta_s^*}{R}(13G_d^* + 12G_m^*)$$

$$(3.6)$$

An important feature of this model is its treatment of the interfacial tension as a sum of two parts. A static part which is the equilibrium interfacial tension Γ^o and a frequency dependent complex part $\beta^*(\omega)$. In turn, $\beta^*(\omega)$ consists of two complex moduli - the surface dilatation modulus and the surface shear modulus. Both these properties are characteristics of the interface. The surface dilatation modulus is a result of the non-uniformity of the interfacial tension over the interface while surface shear modulus is the resistance of the interface to the deformation. The preceding models lacked any parameter(s) besides the equilibrium interfacial tension which characterized the properties

associated with the interface. These parameters attain significance as it has been shown

that in externally compatibilized systems, the interface is no more unimolecular layer

thick. It is a region of finite thickness with its own associated properties [Germain et. al.,

1991]. In reactively compatibilized systems also a reaction product is being formed at

the interface. The 'bare' interface is being 'occupied'. This leads to an interface of finite

thickness which has the potential of altering the behavior of the blend significantly.

Thus, the need to incorporate the properties of the interface in the model. Palierne's

model is a step in this direction. It should be pointed out that Oldroyd's model is retained

from Palierne's model. Under such circumstances,

$$G^{*}(\omega) = G_{m}^{*}(\omega) \frac{1 + 3\sum_{i} \phi_{i} H_{i}(\omega)}{1 - 2\sum_{i} \phi_{i} H_{i}(\omega)} \qquad (3.7)$$

where,

$$H_{i}(\omega) = \frac{(4\Gamma^{0}/R_{i})(2G_{m}^{*} + 5G_{d}^{*}) + (G_{d}^{*} - G_{m}^{*})(16G_{m}^{*} + 19G_{d}^{*})}{(40\Gamma^{0}/R_{i})(G_{m}^{*} + G_{d}^{*}) + (2G_{d}^{*} + 3G_{m}^{*})(16G_{m}^{*} + 19G_{d}^{*})} \qquad (3.8)$$

Based on the above model the terminal relaxation time of the emulsion whose

components are represented by single relaxation time Maxwellian model is given by

Equation 3.9 [Graebling and Muller, 1990].

$$\tau = \tau_N + 120\left(\frac{k\Gamma^0}{R\eta_m}\right)\frac{\lambda_m(X-1)}{(19k+16)^2}\tau_N + \lambda_m \qquad (3.9)$$

The parameter τ_N is the terminal relaxation time of an emulsion of two Newtonian fluids whose viscosities are same as the viscosities of the viscoelastic phases. It is given by Equation 3.10.

$$\tau_N = \frac{5}{8}\left(\frac{R\eta_m}{\Gamma^0}\right)\phi_d \frac{(19k+16)^2}{50(k+1)^2 + 5\phi_d(5k+2)(k+1) - 3\phi_d^2(5k+2)^2} \qquad (3.10)$$

The basis of the equilibrium interfacial tension measurements is the secondary plateau in storage moduli which is a result of the interfacial forces. Thus, to determine interfacial tension from the rheological measurements, it is essential to capture as much secondary plateau as possible.

3.2 EXPERIMENTAL

3.2.1 Materials

Nylon 6 (PA6) (BASF Ultramid, B3SQ661), neat polypropylene (PP) (Montell Polyolefins, Profax 6501) and maleated polypropylene (PP-MA) (Uniroyal Chemicals, PB3150) were used in this study. The Nylon 6 was reported to contain lubricants for processing ease. The Maleic anhydride content of the PB3150 was reported to be 0.8 wt. % as per the manufacturer. PA6 was blended with PP and PP-MA respectively. PA6 was the matrix and PP (or PP-MA) were the dispersed phases. Blending was carried out in a ZSK-30 twin screw extruder at a temperature of 230 °C for all the zones. To minimize the effects of moisture, the materials were dried under a nitrogen blanket for 6-8 hours prior to blending. The extrudate strands were pelletized and dried. Three blend compositions of differing weight fractions of PP and PP-MA (10, 20, 30 weight percent respectively) were prepared. A density of 1.14 g/cc for PA6 and 0.93 g/cc for polypropylene was used. In the reactive system the amine group of the PA6 reacts with the maleic anhydride of the polypropylene [Ide and Hasegawa, 1974]. The blends will be referred to in the text with the components and their weight fractions in the parenthesis.

3.2.2 Rheological

Rheological characterization was carried out on an RMS-800 rheometer (from Rheometrics Scientific, Inc.) using a 50 mm parallel plates arrangement. The disks were prepared by compression molding the pellets in a Carver press under a force of 6 tons and 230 °C. The pellets were pre-dried in a vacuum oven for 10-12 hours. The instrument oven was purged with dry nitrogen during measurements to avoid degradation. A frequency range of 0.05 - 50 rad/ s and strains of 10-15% were chosen. It was ensured that the testing was carried out in linear viscoelastic limits.

3.2.3 Morphological

The samples for morphological examination were prepared by pre-notching the disks used in rheological measurements, heating them to 230 °C in the rheometer oven and placing them directly in the liquid nitrogen at that temperature. Those were then fractured under liquid nitrogen. This ensured that the morphological information used in the analysis was as close to the one under investigation. These samples were then examined in Phillips Electroscan 2020 environmental scanning microscope. Water vapor at a pressure of 2-3 Torr was used as the imaging gas. The size of the disperse phase was measured directly from the micrographs. The volume average radii were calculated for the blends and used in the analysis.

3.3 RESULTS AND DISCUSSION

3.3.1 Blend Morphology

Figures 3.2a through 3.2c show the morphology of the non-reactive blends while Figures 3.2d through 3.2f show the morphology of the reactive blends. For the non-reactive blends the particles are spherical with a broad particle size distribution. Their size increases progressively with increasing volume fraction of the dispersed phase. Such a behavior can be attributed to coalescence. On the other hand, in case of reactive blends, the particle size is reduced, the particle size distribution is narrowed and the effect of volume fraction is minimal. Coalescence is reduced in reactive blends due to the increased stability and the reduced mobility of the interface [Sundraraj and Macosko, 1995; O'Shaughnessy and Sawhney, 1996; Janssen and Meijer, 1995]. Table 3.2 summarizes the volume average particle sizes.

3.3.2 Rheology

Table 3.3 shows the zero-shear viscosity η_o and the corresponding relaxation time of the components. The zero-shear viscosity was determined from the flat portion of the η' vs ω curve. The values were confirmed by the following relation.

$$\eta_o = (\lim \omega \to 0)\frac{G''(\omega)}{\omega} \qquad (3.11)$$

Relaxation time was determined by

$$\lambda = (\lim \omega \to 0)\frac{G'(\omega)}{\omega^2 \eta_o} \qquad (3.12)$$

Figures 3.3a and 3.3b show the storage and loss moduli of the blend components respectively. The storage modulus of PA6 is lower than those of the dispersed phases PP and PP-MA over the frequency range under investigation. The lower relaxation time of the PA6 is significant to the study since it minimizes the effects of the relaxation of the matrix. It should be noted that the relaxation time of the dispersed phases are almost same in the non-reactive and reactive systems.

Figures 3.4a and 3.4b compare the storage and loss moduli for the non-reactive blends respectively. The storage moduli curves are characterized by a distinct plateau. This plateau becomes more pronounced as volume fraction of the dispersed phase increases. This is in accordance with the predictions of the model [Graebling et. al., 1990]. Figures 3.5a and 3.5b show a similar comparison for reactive systems. These blends are also characterized by a plateau in storage moduli curves which occurs at a lower frequency compared to the non-reactive blends. The full width of this plateau has not been captured due to limits of the instrument. According to the model, the plateau moves to lower frequency if

• the interfacial tension is reduced

• viscosity ratio is increased

The effect of the viscosity ratio 'k' (from 1.7 in the non-reactive system to 0.7 in reactive system) should be to shift the plateau to higher frequencies. However, the shift is toward the lower frequency. Thus, the change in position can be attributed to a reduction in equilibrium interfacial tension (due to interfacial reaction). Before proceeding to quantify the extent of change in equilibrium interfacial tension, it is in order to observe the rheological behavior of the blend with respect to its components.

Figures 3.6 is a comparison of the storage moduli curves of the PA6/ PP (90/ 10) blend with its components. The storage modulus of the blend follows the trend of the dispersed phase till a certain frequency after which it falls between them. This effect is due to the interfacial tension forces. At lower frequencies the relaxation of the dispersed droplets dominate the rheological behavior. The shape retaining interfacial tension forces dominate the viscous forces. At higher frequencies the effect of equilibrium interfacial tension is reduced and the visco-elastic properties of the components, especially the matrix dominate the behavior. Similar behavior was observed for PA6/ PP (80/ 20) and PA6/ PP (70/ 30) blends as shown in Figures 3.7 and 3.8 respectively.

In the case of PA6/ PP-MA (90/ 10) blend the storage modulus follows the dispersed phase behavior till a certain frequency after which it is higher than the components. Refer to Figures 3.9. But, as the weight fraction of the dispersed phase was raised (to 80/ 20 and 70/ 30 respectively), the behavior changed. The storage modulus of the blend was consistently higher than the components over the complete frequency range under investigation. This is shown in Figures 3.10 and 3.11 respectively. This observation shows that there is a fundamental change brought about in the rheological behavior of the blend as a result of the interfacial reaction. As the reaction proceeds, the

'bare interface' is being 'occupied' by the reacted moiety. The interfacial reaction leads to the formation of a product located at the interface which has a significant effect on the rheological behavior of the blend. In PA6/PP-MA (90/10) system the observations show that the process (of imparting elasticity) has just started. To sum up,

- In non-reactive systems $G'_b > G'_d$ at low ω, and $G'_b < G'_d$ at high ω.

- In reactive systems, $G'_b > G'_d$ over the complete frequency range under investigation.

At this stage two important questions need to be answered.

1. What is the extent of the reduction in interfacial tension due to reaction, if any?

2. How does one explain the increased storage modulus in reactive blends over the complete frequency range?

To determine the solution to these, one needs to determine the value of equilibrium interfacial tension.

3.3.3 Interfacial Tension Values

The thermodynamic models which explain the behavior of the interface can be used for providing the initial estimates of the values. The most notable work in this direction is due to Helfand and Tagami [1971]. According to these researchers the following relation can be used for determining the equilibrium interfacial tension between two asymmetric polymer melts.

$$\Gamma^0 = k_B T (\rho_0 \chi)^{1/2} \left[\frac{\beta_A + \beta_B}{2} + \frac{1}{6} \frac{(\beta_A - \beta_B)^2}{\beta_A + \beta_B} \right] \tag{3.13}$$

The parameter χ is estimated from the Hilderbrand solubility parameters. The relation is

$$\chi = \frac{1}{\rho_0 k_B T} (\delta_A - \delta_B)^2 \tag{3.14}$$

The temperature dependence of χ in Equation 3.14 leads to the temperature dependence of Γ^0. A major limitation of this equation is the lack of data on χ in the literature. The values for the materials used in this work have been shown in Table 3.4 [Brandrup and Immergut, 1989]. These values yield an equilibrium interfacial tension value of 28 mN/m.

Another independent estimate for the value of interfacial tension can be made from the polar and dispersive components of the individual phase. For nylon 6 and polypropylene, the values are listed in Table 3.5 [Wu, 1987]. The equation used to estimate the equilibrium interfacial tension is

$$\Gamma_{12} = \Gamma_1^0 + \Gamma_2^0 - \frac{4\Gamma_1^d \Gamma_2^d}{\Gamma_1^d + \Gamma_2^d} - \frac{4\Gamma_1^p \Gamma_2^p}{\Gamma_1^p + \Gamma_2^p} \tag{3.15}$$

This yields a value of 10 mN/m. The two values have a difference of ~150%. Which of them is correct? In Chapter 4 it has been shown that the equilibrium interfacial tension

between nylon 6 and polypropylene is 8 mN/ m. This value agrees well with the value of 10 mN/ m estimated from the polar and dispersive components of the individual phases.

In this work rheological technique was employed to determine the value of equilibrium interfacial tension in the system under investigation. Equation 3.7 and 3.8 were used. Storage moduli curves were used for this purpose. As discussed in the Introduction section, these are most sensitive to the changes in the rheology brought about by the effect of interfacial tension and morphological parameters, especially in the low frequency region. The model curves were generated from the experimentally obtained storage and loss moduli curves for the blend components. The morphological observations were made directly from the micrographs. The curves generated from the model were matched with the experimentally obtained curves. The ratio ($\Gamma^0/ \bar{R}_v$) was used as the variable to fit the model curve to the experimental curve. The secondary plateau and the frequency region below it were the main focus of attention while varying the ratio.

The Figures 3.12 and 3.13 show a comparison between the model and the experimentally obtained G' and G" curves based on the models of Oldroyd and of Choi and Schowalter for PA6/ PP(90/10) blend. Since the models were developed for emulsion of Newtonian fluids, the model curves are characterized by a single transition only. Thus, the limited use of these models. Table 3.6 shows the values of the relaxation time λ_1 and the retardation time λ_2 from the relations of Table 3.1 for the two models. Since these models are incomplete, there is a need to use Palierne's model which accounts for the viscoelastic properties of the components.

Figure 3.14 shows the result of such a fit for PA6/ PP (70/ 30) by using Palierne's model. A value of 4 mN/m for equilibrium interfacial tension yields a good fit between the models and the experimentally obtained curves. This value gave good results for PA6/ PP (80/ 20) and PA6/ PP (90/ 10) too, as shown in Figures 3.15 and 3.16. However, in the 90/ 10 system there was a discrepancy in the lower frequency region. The model and experimental curves do not match well in this region. A similar observation was made by Graebling and co-workers [1993]. This can be attributed to the polydispersity in the particle size of the dispersed phase. The relaxation time of the monodisperse emulsion increases with particle radius. Due to the polydispersity in particle sizes, there is a resultant dispersity in the relaxation times, which leads to this discrepancy. Such effects would be most pronounced toward low frequency region where the long time relaxation processes are dominant.

The results thus far indicate that the interfacial tension between nylon 6 and non-reactive polypropylene under investigation is 4 mN/ m. This value is 50% lower than a similar reported value of 8 mN/ m in nylon 6 - polypropylene system determined by similar technique as shown in Chapter 4. What is the cause of this difference? The main difference between the two studies is in the nature of the nylon 6. Although both have the same molecular weight (M_n of 18,000), but the nylon 6 in this study contained low molecular weight lubricating agents. Due to thermodynamic considerations these have a tendency to migrate to the interface region. As a result they have the potential of acting as surfactants and hence reduce the equilibrium interfacial tension. This is supported by the theory presented by Broseta and co-workers [1990]. They showed on theoretical

grounds that the equilibrium interfacial tension is lowered by the presence of small chains at the interface according to Equation 3.16.

$$\Gamma^0 \approx \Gamma_\infty^0 \left[1 - \frac{\pi^2}{6w_n} + ... \right]$$

(3.16)

In this equation w_n signifies the degree of incompatibility.

Now, what happens when the system is reactive? Figure 3.17 shows the fit between the model curve and the experimentally obtained storage moduli curve for PA6/ PP-MA (90/ 10) system. A value of 1 mN/m for Γ^0 was used. There is an acceptable fit in the low frequency region, while in the high frequency region, the model curve falls below the experimentally obtained curve. The situation deteriorates further in the case of higher volume fractions. Figure 3.18 shows the case for PA6/ PP-MA (80/ 20). There is no match even for values as low as 0.1 mN/ m. Similar observation was made in PA6/ PP-MA (70/ 30) blend. This means that at this stage, an additional phenomenon besides the role of equilibrium interfacial tension reduction seems to be coming into play. There is an enhanced elasticity in the system due to reaction. This additional elasticity is volume fraction dependent as well as frequency dependent. The model (using the equilibrium interfacial tension alone) provides lower values of the moduli as compared to the experimentally obtained curves. The enhanced elasticity seems to be playing an increasingly important role in the reactive systems and needs to be accounted for in the model. This needs a closer look and understanding. It is worthwhile to focus on the physical events occurring in the blends to understand the phenomenon.

3.3.4 Physical Phenomenon

The position of the secondary plateau is an important indicator of the interfacial events in the polymer blend. But, what is the physical process that leads to this plateau? The physical events in this region are an interplay of the interfacial forces and the viscous forces. In the low-frequency region of the dynamic behavior of the polymer melts the long-time relaxation processes dominate. The mechanical relaxation of the droplets after deformation is one such phenomenon. Interfacial tension plays an important role in this behavior. It has been shown that the time required for the deformed droplets to return to their original shape is of the same order as the mechanical relaxation times [Scholz et. al., 1989]. The parameter λ_D in Figure 3.1 is the shortest relaxation time of the emulsion corresponding to the relaxation of the droplets back to the original spherical shape. Below this frequency (i.e. higher relaxation times) the interfacial forces dominate the viscous forces. The long time relaxation processes dominate in the terminal region.

In the region λ_D to λ_P, the interfacial forces and viscous forces are of the same order. The shape deforming viscous energy is being spent in overcoming the resistance offered by the shape retaining equilibrium interfacial tension. This leads to time-scales of relaxation that result in a secondary plateau in the storage modulus curve which lead to a secondary plateau. A similar phenomenon has been observed in dispersed systems where the energy is spent in overcoming Van der Waals kind of forces. These forces cause a yield stress kind of phenomenon [Matsumoto et. al., 1975]. The equilibrium interfacial tension causes a similar resistance. It should be reminded that a well-defined plateau as

per the model occurs in the blend if the component phases were assumed to be ideal Maxwellian elements with a single relaxation time. However, in real systems, there is a distribution of relaxation times.

Beyond λ_p there is enough energy in the system to overcome the interfacial tension resistance and flow of the materials start. The role of long time relaxation processes is reduced. The short time relaxation processes start playing an increasing role, as in the transition zone. Effects due to equilibrium interfacial tension alone do not fall in this category.

The discussion presented till now is valid for a 'bare interface'. In such a situation, the interfacial force competes with viscous forces. The interfacial tension forces are well-defined as the interface between the matrix and the dispersed phase is too. However, if the interface is 'occupied', say, due to the products of the interfacial reaction then the effects due to this region will also participate in the inter-play of forces. The interface is not demarcated as sharply. It has a finite thickness and is occupied by a new product (of reaction). This should contribute to the rheological and morphological behavior of the blend. The extent of impact should depend on the 'extent of coverage' of the interface, i.e., how much product is at the interface. This is supported in the rheological observations made for the reactive system. As the volume fraction of the dispersed phase is increased, the deviation from the model predictions also increase. O'Shaughnnesy and Sawhney [1996] have shown theoretically that after a critical extent of the coverage of the interface, the reaction is 'switched-off'. They showed that as the reaction products crowd the interface, the interface thickness becomes larger than the

unperturbed chain dimensions. The interface can no longer be considered 'uni-molecular' layer thick.

It has been shown by Fayt and co-workers [1986] that in the externally compatibilized systems the copolymer resides at the interface. This is a physical layer with its own associated visco-elastic properties. It has a characteristic relaxation time (and spectrum) of its own which enhances elasticity. Thus, it provides resistance to deformation. We believe that in the system under investigation this phenomenon is occurring. The layer around the dispersed phase in reactive blends acts as a reinforcing agent which supports the stress transfer mechanism. This leads to a good stress transfer from the matrix to the particles which increases the elasticity of the system and hence the storage modulus. On the other hand, in non-reactive blends no such layer is present to offer additional resistance which maintains the storage moduli values within those estimated by the models developed for 'bare' interface.

In the micrographs for non-reactive blends (refer to Figure 3.2a through 3.2c), it is clear that there is a lack of good adhesion between the spherical particles and the matrix. This causes poor stress transfer from the matrix to the particles. In reactive blends (Figures 3.2d through 3.2f), the adhesion is improved. There are physical and chemical links between the two phases due to interfacial reaction. The properties of the graft copolymer layer govern the behavior of the blend. The interface cannot be treated as 'bare' anymore. It is occupied by the reacted moiety.

But, how does one quantify the enhanced elasticity? The following section addresses this issue by incorporating the surface shear modulus of the interface [Palierne, 1990]. This leads to the resistance to the deformation of the interface. In other words,

this is a cause for the additional elasticity which is seen in the storage moduli of the

reactive blends. To use the surface shear modulus, estimates of this value had to be made

as direct measurements of this property are not possible yet.

3.3.5 Estimates of surface shear modulus

A parallel was drawn between the reactive blends and lightly cross-linked rubbers.

In this formalism [Ferry, 1961] (refer to Figure 3.20),

$$\beta_s^* = \beta_s^{'} + i\beta_s^{"} \qquad (3.17)$$

For $\omega\lambda_\beta < 1$

$$\beta_s^{'} = \beta_o$$
$$\beta_s^{"} = \beta_o\omega\lambda_\beta \qquad (3.18)$$

For $\omega\lambda_\beta > 1$

$$\beta_s^{'} = \beta_s^{"} = \beta_o\sqrt{\omega\lambda_\beta} \qquad (3.19)$$

The Equations 3.17 thru 3.19 show that two parameters are crucial - β_o and λ_β. In the

theroy of rubber elasticity, β_o (N/m^2) is the equilibrium modulus in the range of

infinitesimal deformations. To draw a parallel in case of the modulus associated with the interface (N/m), it can be thought of as a product of a bulk modulus and a characteristic length. This bulk modulus could be different from either of the individual components and also different in each blend depending on the volume fraction. On the other hand, the choice for the characteristic length falls clearly on the interfacial thickness. Experimental evidence suggest, the interfacial thickness attains a constant value in the early stages of mixing [Okamoto et. al., 1993]. Work by Hosoda and co-workers [1991] shows that the interfacial thickness is ~50 °A (50 x 10^{-10} m). Increasing extents of reaction increases the amount of reactive copolymer in the interface region. That is, an effect of increased reaction should be enhanced elasticity. In fact, this is what is observed. The deviation from the base model increases as the volume fraction of the maleated polypropylene is increased.

On the other hand, λ_β is a characteristic relaxation time. It corresponds to a frequency until which the elastic recoil is accomplished after the removal of stress [Ferry, 1961]. In the theory, λ_β refers to the longest relaxation time possible in the system. The parameter λ_p is a good candidate for this (refer to Figure 3.1). In Figure 3.8 it is seen that at a frequency of ~0.2 rad/s the secondary plateau ends and the effect of equilibrium interfacial tension starts to diminish (the region after λ_p in Figure 3.1). This yields a value of λ_β to be 5 s.

The result of incorporating a surface shear modulus is a change in the form of $H_i(\omega)$ of Equation 3.8. The new equation assumes the form [Palierne, 1990]:

$$H_i(\omega) = \frac{(4\Gamma^0 / R_i)(2G_m^* + 5G_d^*) + (G_d^* - G_m^*)(16G_m^* + 19G_d^*) + (16\beta_s^* \Gamma^0 / R^2) + (2\beta_s^* / R)(13G_d^* + 8G_m^*)}{(40\Gamma^0 / R_i)(G_m^* + G_d^*) + (2G_d^* + 3G_m^*)(16G_m^* + 19G_d^*) + (32\beta_s^* \Gamma^0 / R^2) + (4\beta_s^* / R)(13G_d^* + 12G_m^*)}$$

$$(3.20)$$

Figures 3.19 and 3.20 show the result of incorporating a value of β_0 for the 80/ 20 and 90/ 10 reactive systems. For 70/ 30 reactive system this parameter did not improve the situation significantly. It should be reminded that these values are approximations only. There are no experimental values available in the literature at this stage. If the interfacial thickness is assumed to be ~50 °A, these values of β_0 yield a bulk modulus of ~10^6 N/m. Table 3.7 shows the results of the values of the equilibrium interfacial tension and the estimated values of the surface shear modulus.

Now, Wu has proposed a relation based on empirical grounds which can be used to make estimates of the particle sizes if the properties of the materials and the processing conditions are known [Wu, 1987]. It is shown in Equation 3.21.

$$\frac{\eta_m \dot{\gamma} d}{\Gamma^0} = 4p^{\pm 0.84}$$

$$(3.21)$$

If this equation is used to determine the ratio of particle sizes in non-reactive and reactive

systems with the same matrix properties and processing conditions the relation obtained

is

$$\frac{d_u}{d_r} = \frac{p_u^{0.84}}{p_r^{-0.84}} \left(\frac{\Gamma_u^0}{\Gamma_r^0} \right)$$

(3.22)

The subscript u and r signify non-reactive and reactive systems respectively. The ratio

d_u/d_r from the above relation is 3.00. However, the actual ratios vary from 8 to 24

depending on the volume fraction. Thus, there are effects other than reduction in

equilibrium interfacial tension which play a role in development of morphology of

polymeric blends [Sundraraj and Macosko, 1993; O'Shaughnessy and Sawhney, 1996].

Also, it is interesting to observe the behavior of the blend as per the theoretical

description in the Newtonian limit. As suggested by Graebling and co-workers [1993],

in the Newtonian limit, the following approximations are useful.

$$\lambda_D \approx \left(\frac{R\eta_m}{4\Gamma^0} \right) \left[\frac{(19k + 16)((2k + 3) - 2\phi(k - 1))}{10(k + 1) - 2\phi(5k + 2)} \right]$$

(3.22)

$$G_P \approx \left(20 \frac{\Gamma^0}{R} \phi \right) \frac{1}{[(2k + 3) - 2\phi(k - 1)]^2}$$

(3.23)

$$\lambda_P^2 = \frac{\eta_m \lambda_m}{G_P} g(k,X,\phi) \qquad (3.24)$$

where,

$$g(k,X,\phi) = \left[\frac{3(1-\phi)(1-X)}{(2k+3)-2\phi(k-1)} + \frac{((2k+3)+3\phi(k-1))((2k+3X)-2\phi(k-X))}{((2k+3)-2\phi(k-1))^2} \right]$$

$$\underline{\qquad\qquad} (3.25)$$

Based on these equations and the data in Table 3.2 and 3.3, the λ_D, λ_P and G_p obtained are presented in Table 3.8.

The discussion above shows that interfacial tension reaction leads to a reduction in interfacial tension and is accompanied by an enhancement in elasticity. Based on the estimates in the value of β_0, the elasticity enhancement is increased as the volume of the dispersed phase is increased. This is similar to the phenomenon compatibilized by external agents. Okamoto and co-workers [1993] postulated that increasing the extent of reaction leads to the accumulation of the products at the interface. The observations in this work show that this seems to be the case and that it results in an enhancement in elasticity. Also, the role of the equilibrium interfacial tension is decreased once this 'finite thickness' layer is formed around the dispersed phase. An interesting question that arises then is that what happens to the interfacial properties as the reactivity of the system is progressively altered. Does the interfacial tension go down in steps as the extent of reaction is increased? Or does it depend on the reactivity of the system? The results of such a study have been reported in Chapter 4.

CONCLUSIONS

It has been shown in this chapter that the interfacial reaction between nylon 6 and polypropylene leads to a reduction in the equilibrium interfacial tension. The value of interfacial tension drops from 4 mN/ m in non-reactive system to 1 mN/ m in reactive system. This reduction in equilibrium interfacial tension is accompanied by an enhancement in elasticity in the reactive blends. In addition, it is observed that the presence of the low molecular weight lubricating agents reduces the interfacial tension due to their presence at the interface as compared to the similar system without any agents.

Observations show that the equilibrium interfacial tension alone is insufficient to account for the rheological behavior over the complete frequency range. Toward the lower frequencies and until a certain volume fraction, the results are in agreement with the model while in the higher frequency range the agreement is not good. A possible cause of this behavior is that with the progress of the reaction, the interface is being 'occupied' with the reaction product which imparts additional elasticity to the system. This has been accounted for by considering surface shear modulus in addition to the interfacial tension.

Table 3.1: The comparison between the models of Oldroyd and of Choi and Schowalter for an emulsion of Newtonian fluids [Graebling and Muller, 1990].

	Oldroyd	Choi and Schowalter
η_a	$1 + \phi \dfrac{(5k+2)}{2(k+1)} + \phi^2 \dfrac{(5k+2)^2}{10(k+1)^2}$	$1 + \phi \dfrac{(5k+2)}{2(k+1)} + \phi^2 \dfrac{5(5k+2)^2}{8(k+1)^2}$
λ_1	$\lambda_0 \left[1 + \phi \dfrac{(19k+16)}{5(k+1)(2k+3)} \right]$	$\lambda_0 \left[1 + \phi \dfrac{5(19k+16)}{4(k+1)(2k+3)} \right]$
λ_2	$\lambda_0 \left[1 - \phi \dfrac{3(19k+16)}{10(k+1)(2k+3)} \right]$	$\lambda_0 \left[1 + \phi \dfrac{3(19k+16)}{4(k+1)(2k+3)} \right]$
λ_0	$\left(\dfrac{\eta_m R}{\Gamma^0} \right) \left[\dfrac{(19k+16)(2k+3)}{40(k+1)} \right]$	

Table 3.2: The volume average radii of different blends.

Material	R_v (μm)
PA6/ PP (90/ 10)	4
PA6/ PP (80/ 20)	8
PA6/ PP (70/ 30)	12
PA6/ PP-MA (90/ 10)	0.5
PA6/ PP-MA (80/ 20)	0.5
PA6/ PP-MA (70/ 30)	0.5

Table 3.3: The zero-shear viscosities and the corresponding relaxation times of the components of the blend.

Material	η_o (Pa-s)	Relaxation time, λ (s)
PA6	690	0.01
PP	1150	0.35
PP-MA	490	0.28

Table 3.4: The data used for determination of interfacial tension from thermodynamics.

	δ_i (cal/cc)$^{1/2}$	$\rho_i \times 10^{-21}$ (monomer/cc)	$\beta_i \times 10^{-14}$
PA6	13.6	6.06	6.25
PP	8.3	8.9	6.67

Table 3.5: The polar and dispersive component of the component phases [Wu, 1987; Paul, 1978].

	Γ (mN/ m)	Γ^p (mN/ m)	Γ^d (mN/ m)
PA6	29.6	9.9	19.7
PP	21.0	0	21.0

Table 3.6: A comparison of the parameters of the models of Oldroyd and of Choi and Schowalter for emulsion of Newtonian fluids.

	Oldroyd				Choi and Schowalter			
	λ_0	λ_1	λ_2	η_a	λ_0	λ_1	λ_2	η_a
PA6/PP (90/10)	1.9	2.0	1.8	865	1.9	2.8	2.0	944
PA6/PP (80/20)	3.9	4.5	3.1	1070	3.9	7.3	4.4	1380
PA6/PP (70/30)	5.9	7.0	4.0	1305	5.86	13.3	7.5	2010
PA6/PP-MA (90/10)	0.6	0.7	0.6	835	0.6	1.0	0.7	890
PA6/PP-MA (80/20)	0.6	0.8	0.5	1000	0.6	1.4	0.8	1220
PA6/PP-MA (70/30)	0.6	0.8	0.4	1187	0.6	1.8	0.9	1680

Table 3.7: The interfacial tension values for different blends.

Material	Γ^0 (mN/m)	β_0 (mN/m)	τ (s)
PA6/ PP (90/ 10)	4	0	0.3
PA6/ PP (80/ 20)	4	0	1.3
PA6/ PP (70/ 30)	4	0	3.0
PA6/ PP-MA (90/ 10)	1	0.5	0.2
PA6/ PP-MA (80/ 20)	1	0.5	0.3
PA6/ PP-MA (70/ 30)	1	0.5	0.5

Table 3.8: The values of λ_D, λ_P and G_P based on the Newtonian limit. The value of interfacial tension used is 4 mN/m for non-reactive and 1 mN/ m for reactive blend.

	λ_D (s)	λ_P (s)	G_P (Pa)
PA6/PP (90/10)	2	0.77	63
PA6/PP (80/20)	4.5	1.0	67
PA6/PP (70/ 30)	7.5	1.2	70
PA6/PP-MA (90/10)	0.72	0.33	238
PA6/PP-MA(80/20)	0.8	0.31	462
PA6/PP-MA(70/30	0.9	0.3	672
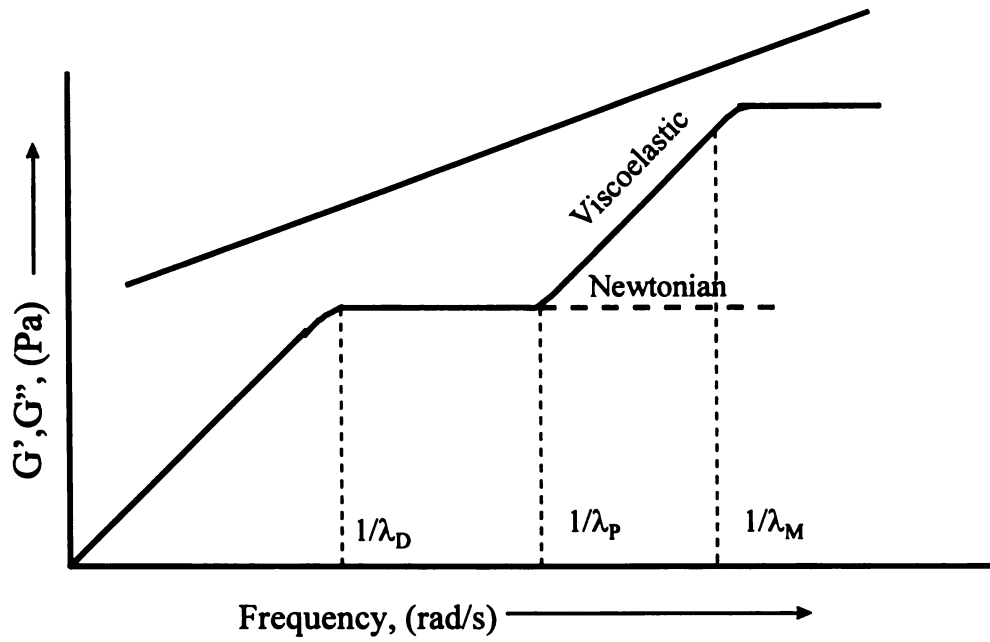
Figure 3.1: The storage and loss moduli for a blend of Newtonian and viscoelastic fluids.

Notice the appearance of a secondary plateau in viscoelastic blend which is a result of

interfacial effects [Graebling et. al., 1993].
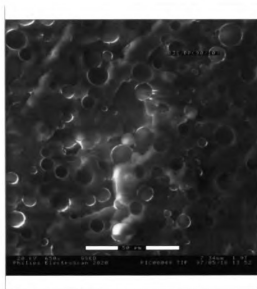
Figure 3.2a: Micrograph showing the morphology of B3S/ PP (90/ 10).
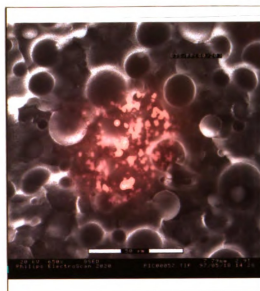
Figure 3.2b: Micrograph showing the morphology of B3S/ PP (80/ 20).
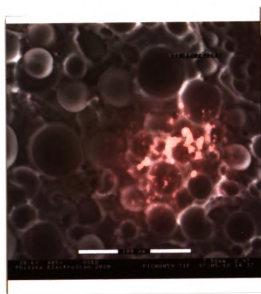
Figure 3.2c: Micrograph showing the morphology of B3S/ PP (70/ 30).

Figure 3.2d: Micrograph showing the morphology of B3S/ 3150 (90/ 10).
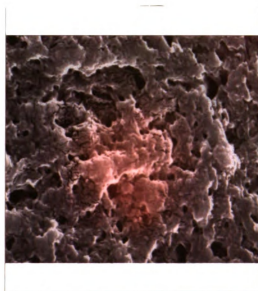
Figure 3.2e: Micrograph showing the morphology of B3S/ 3150 (80/ 20).
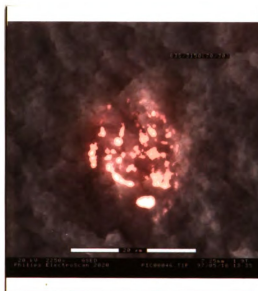
Figure 3.2f: Micrograph showing the morphology of B3S/ 3150 (70/ 30).
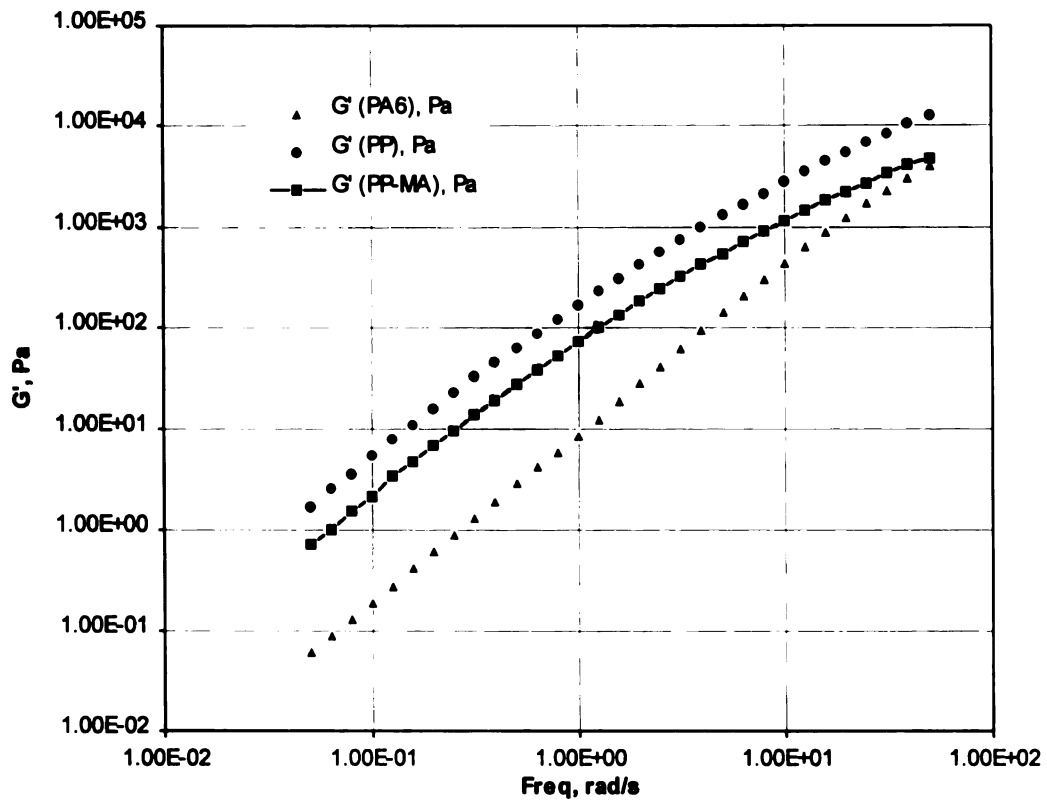
Figure 3.3a: Comparison of the storage moduli of the components of the blend.
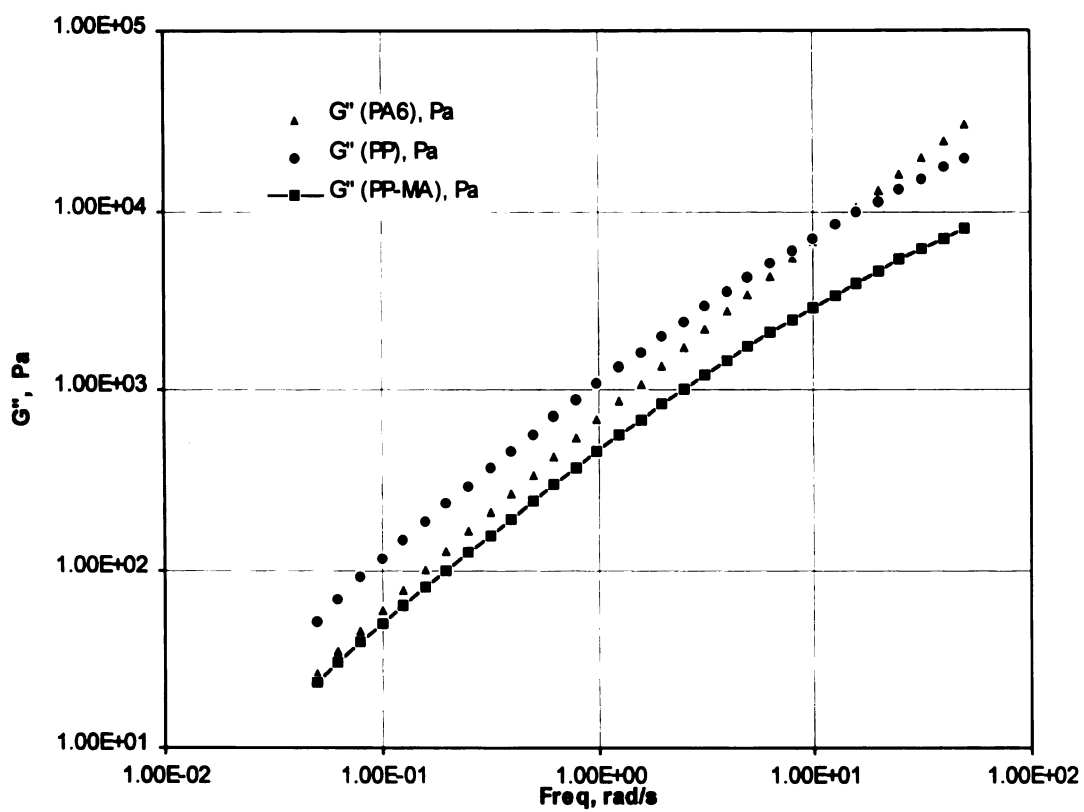
Figure 3.3b: Comparison of the loss moduli of the components of the blend.
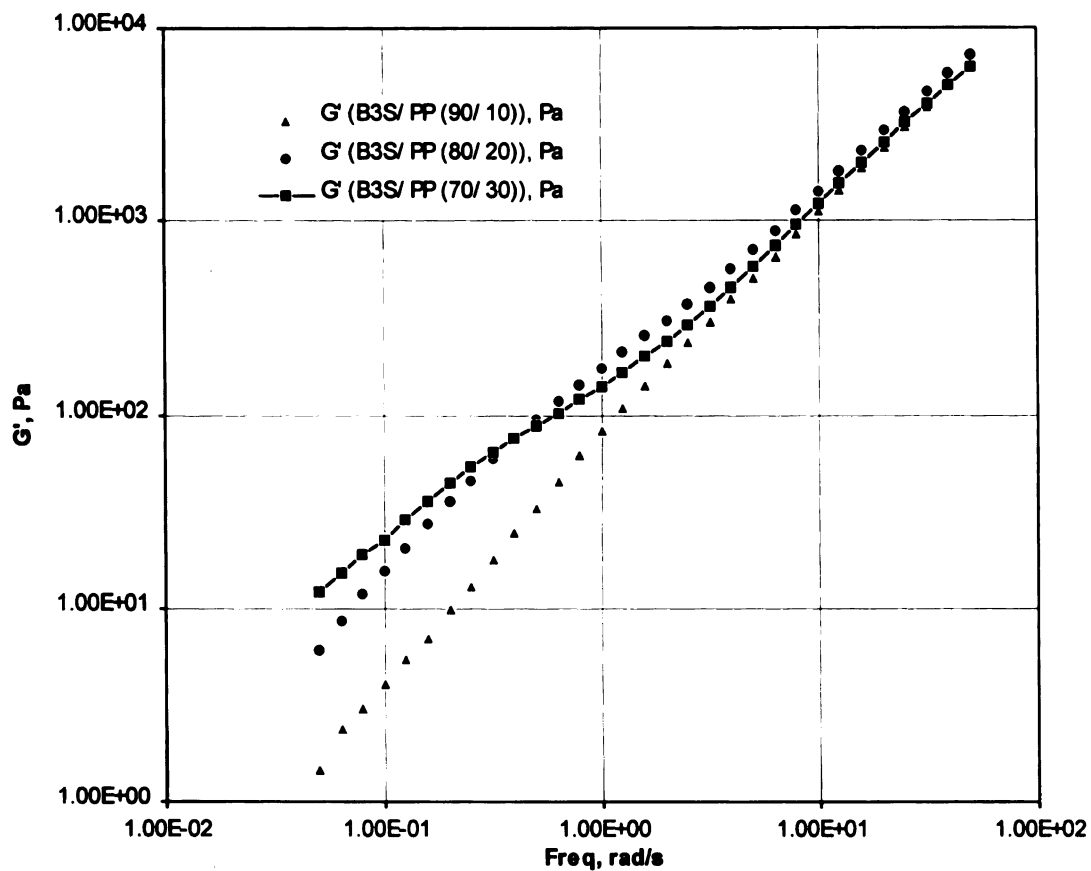
Figure 3.4a: Comparison of the storage moduli of the non-reactive blends for varying weight fractions.
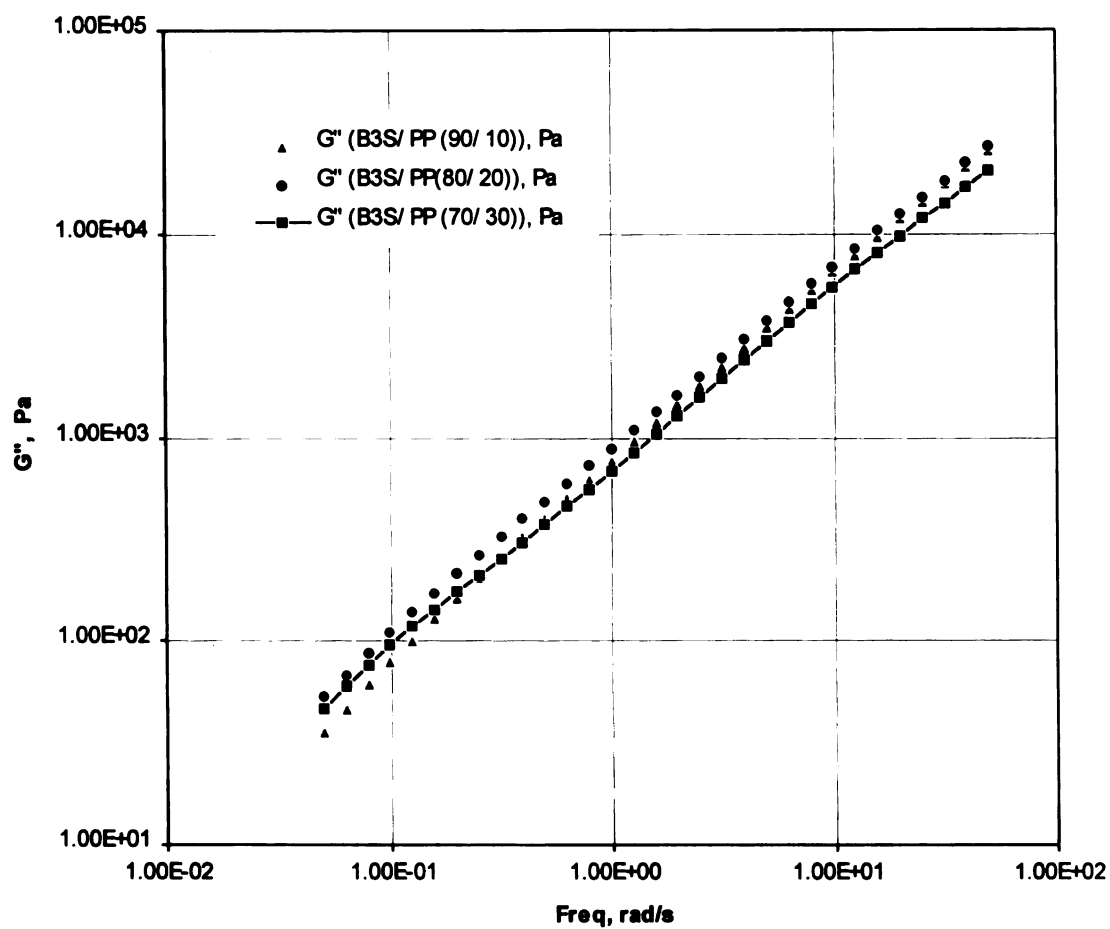
Figure 3.4b: Comparison of the loss moduli of the non-reactive blends for varying weight fractions.
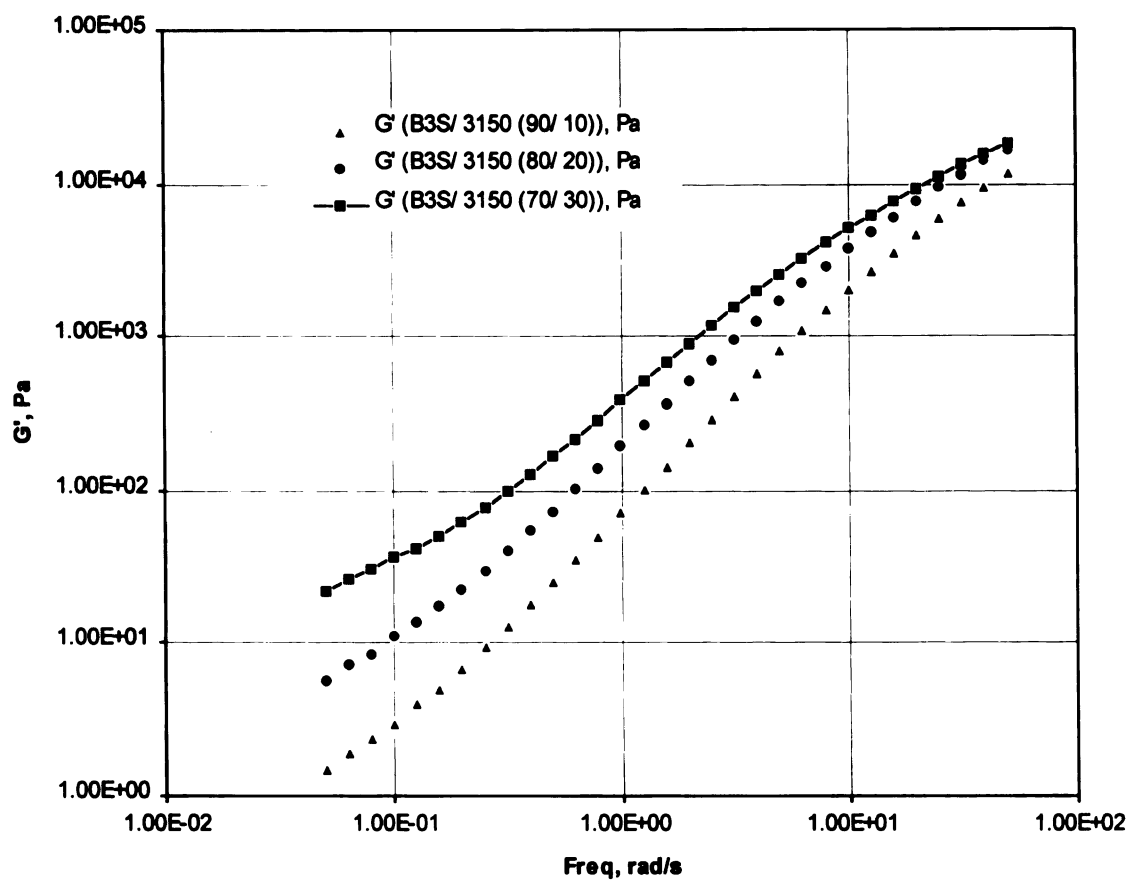
Figure 3.5a: Comparison of the storage moduli of the reactive blends for varying weight fractions.
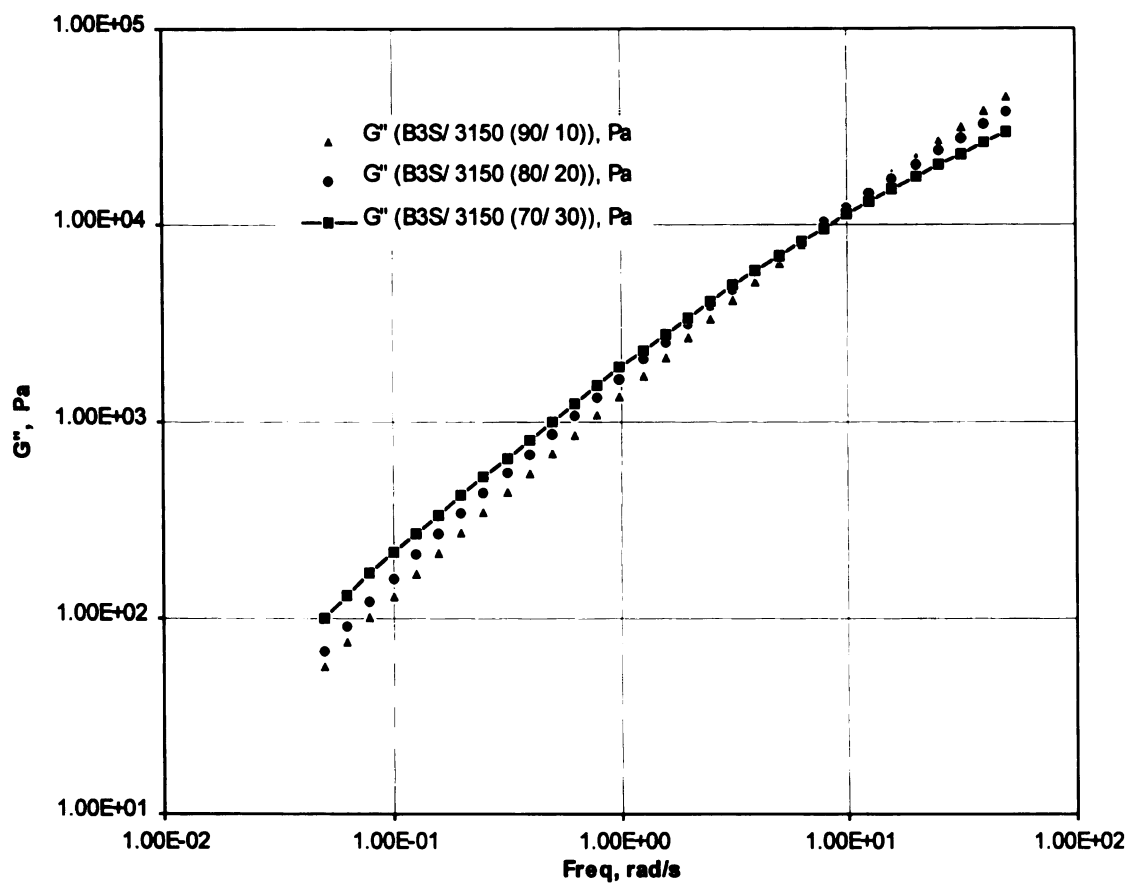
Figure 3.5b: Comparison of the loss moduli of the reactive blends for varying weight fractions.
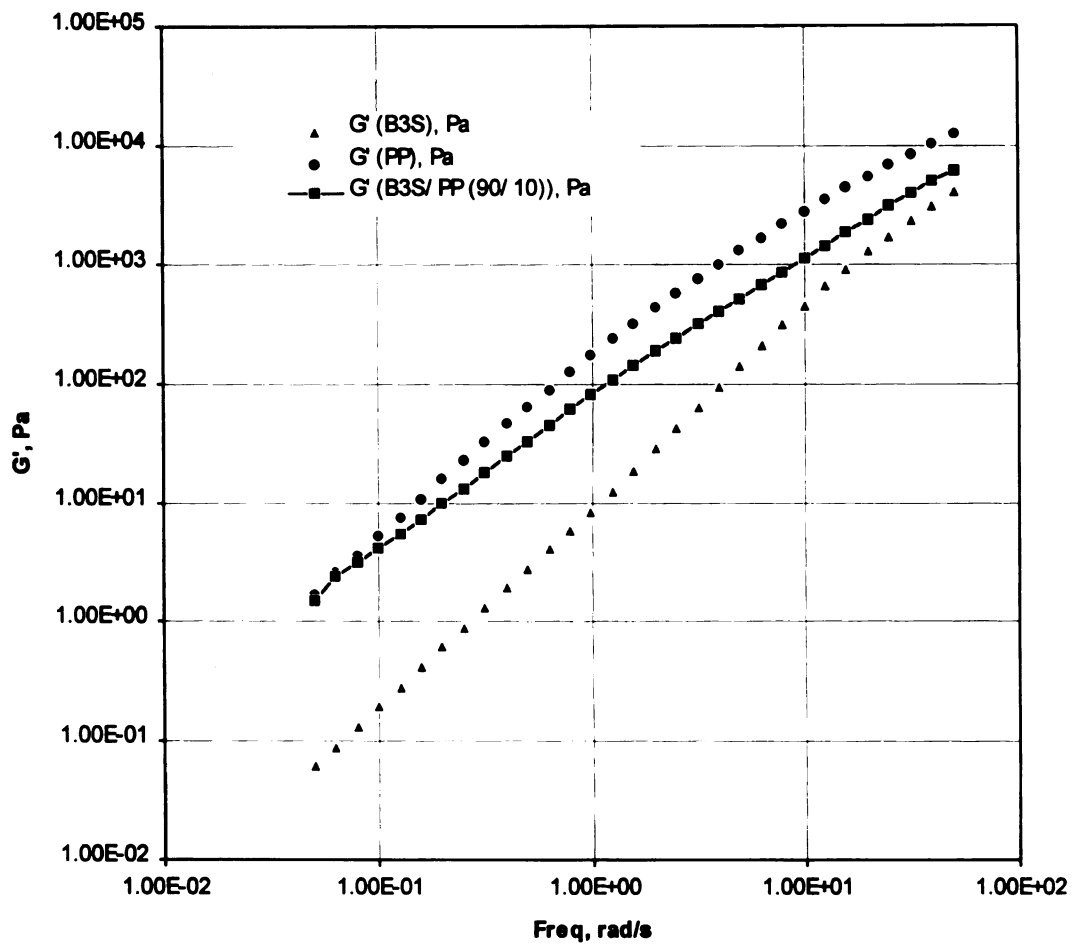
Figure 3.6: Comparison of the storage moduli of the PA6/ PP (90/ 10) blend with the components.
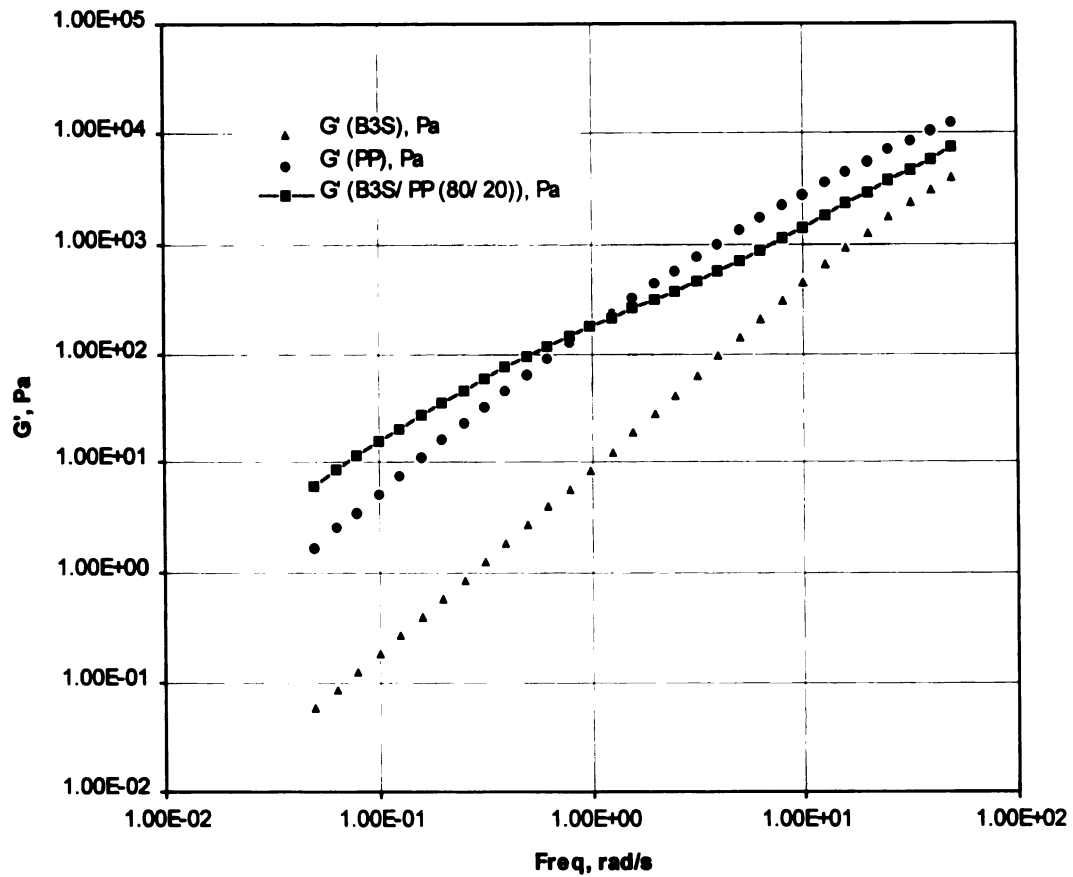
Figure 3.7: Comparison of the storage moduli of the PA6/ PP (80/ 20) blend with the components.
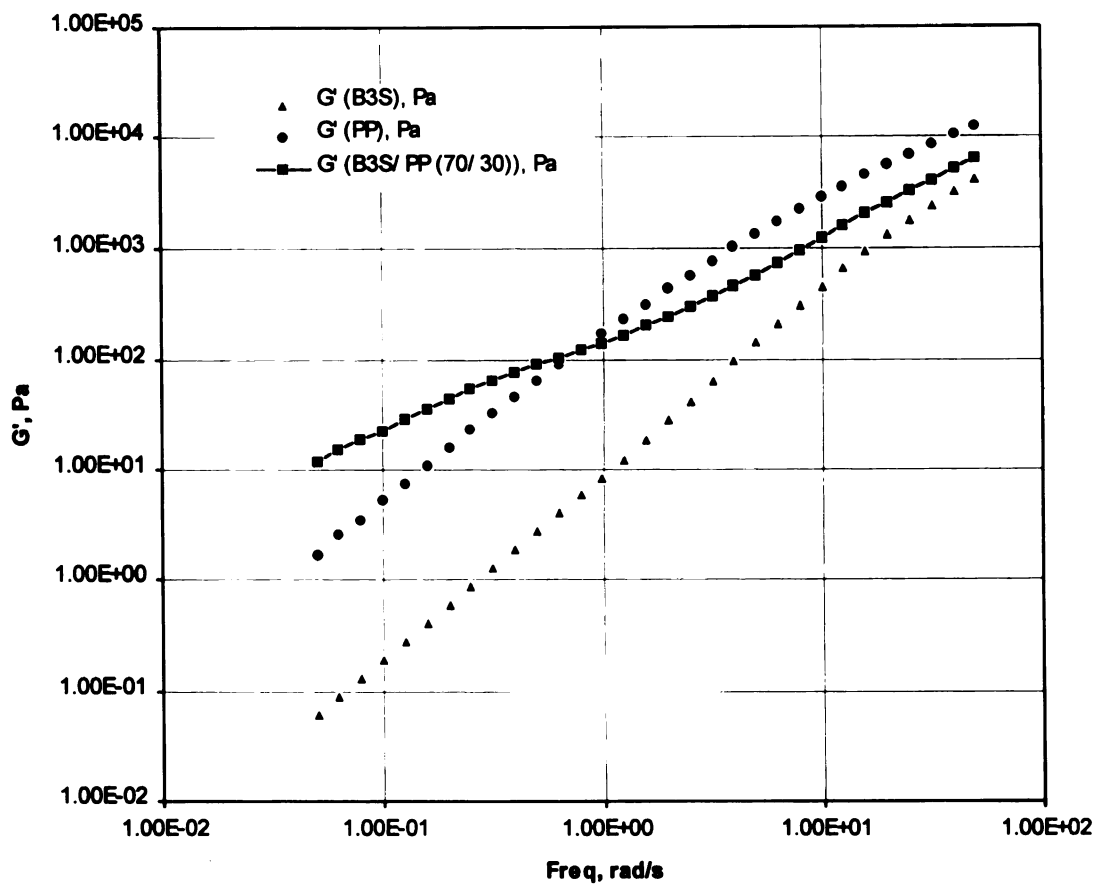
Figure 3.8: Comparison of the storage moduli of the PA6/ PP (70/ 30) blend with the components.
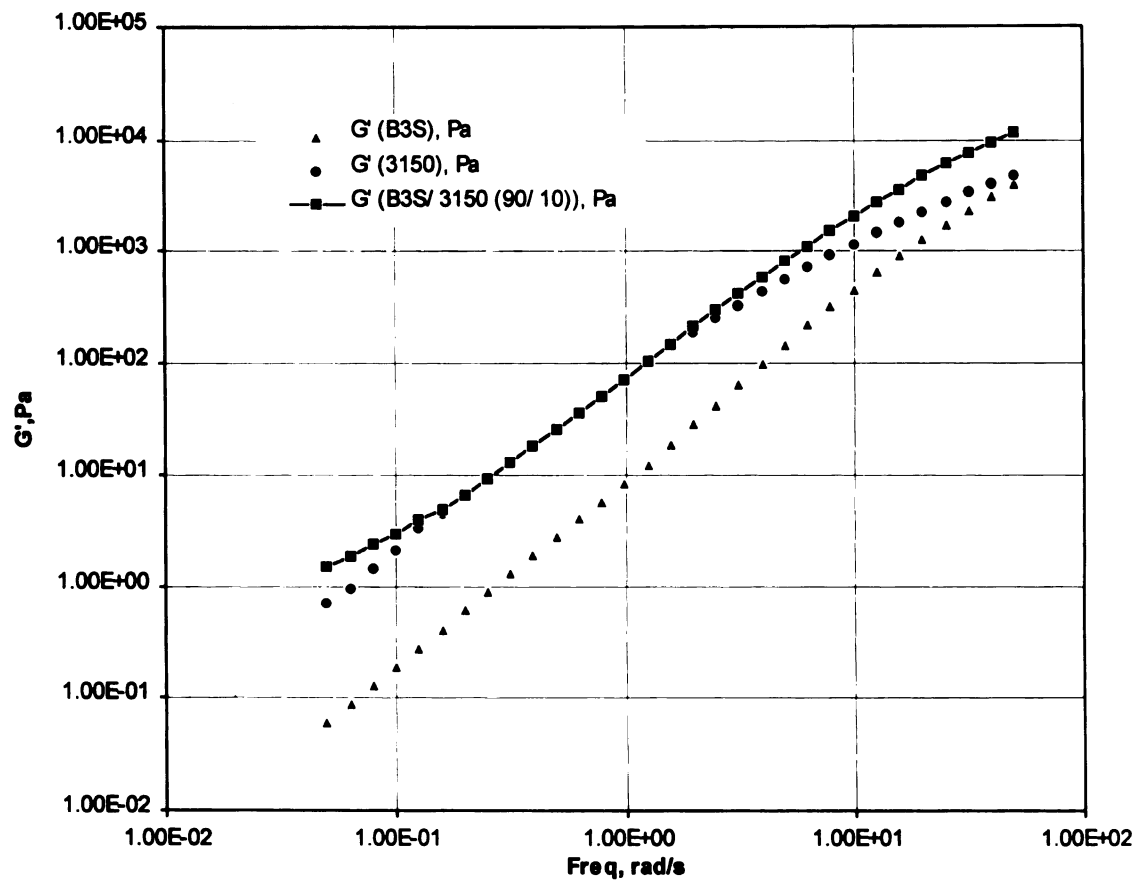
Figure 3.9: Comparison of the storage moduli of the PA6/ PP-MA (90/ 10) blend with the components.
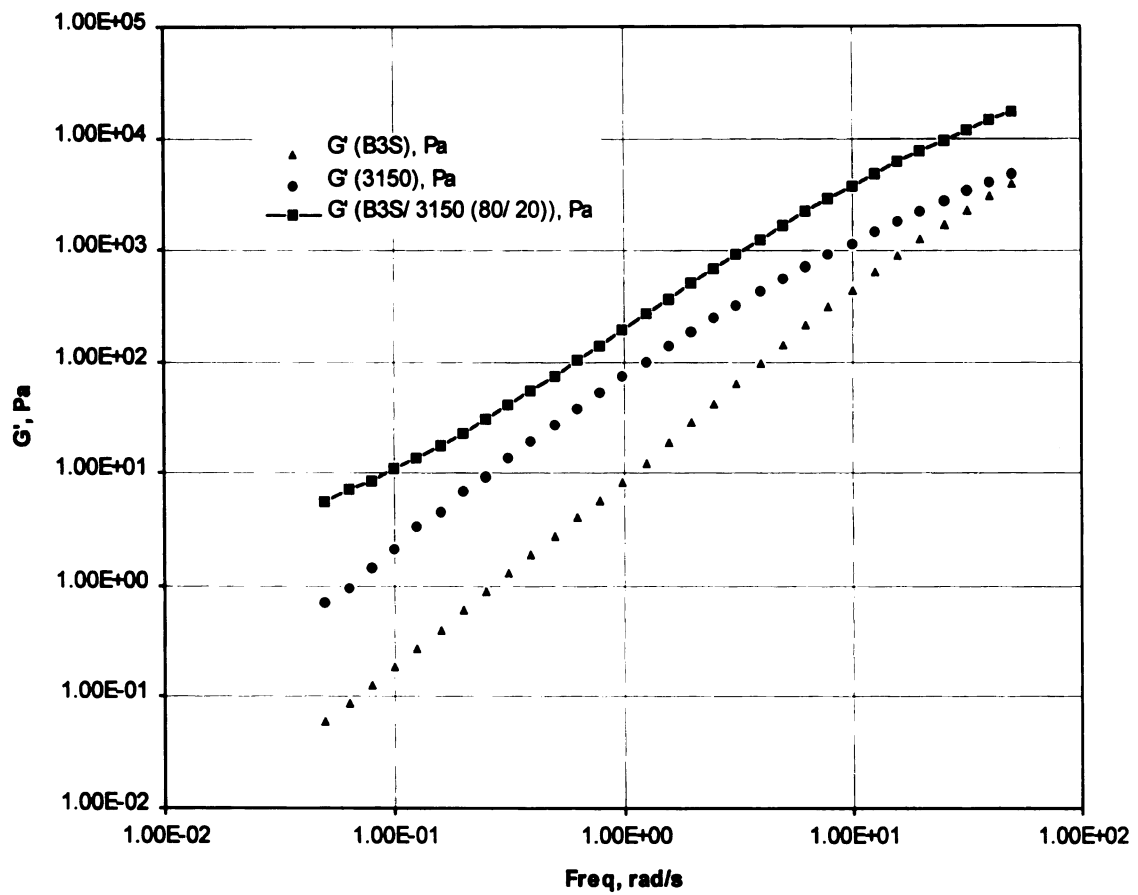
Figure 3.10: Comparison of the storage moduli of the PA6/ PP-MA (80/ 20) blend with the components.
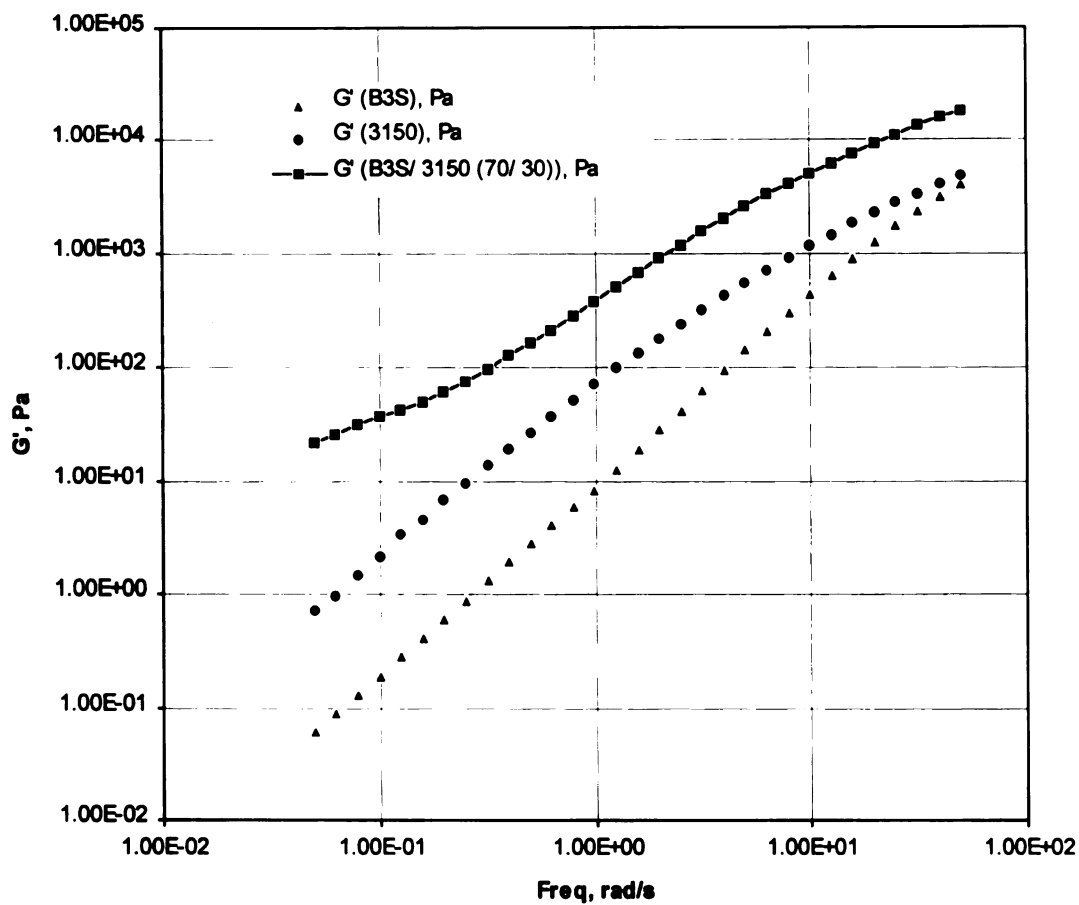
Figure 3.11: Comparison of the storage moduli of the PA6/ PP-MA (70/ 30) blend with the components.
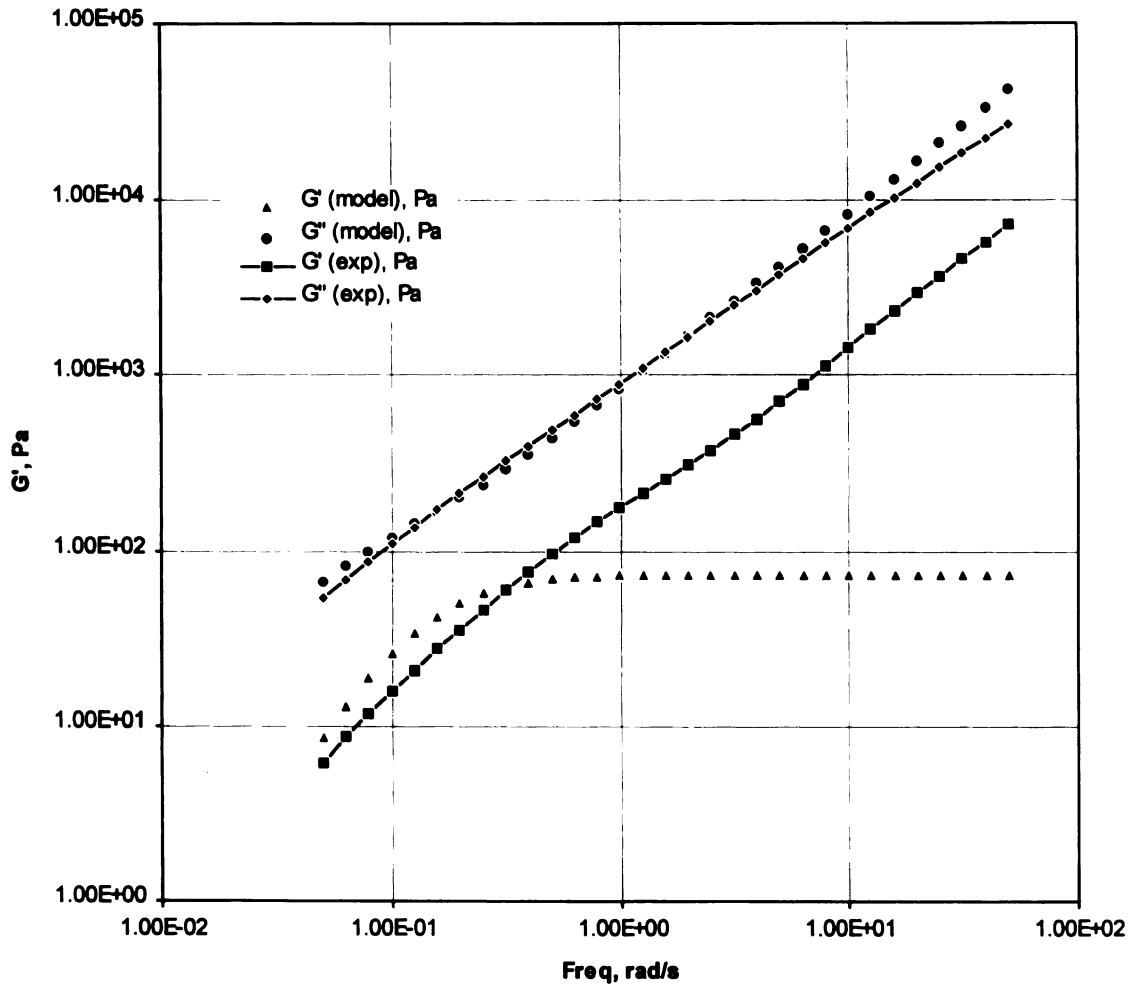
Figure 3.12: Comparison of the storage and loss moduli values obtained from the Choi and Schowalter model with that obtained experimentally for PA6/ PP (80/ 20) ($\Gamma^0 = 4$ mN/ m, R = 8 μm).
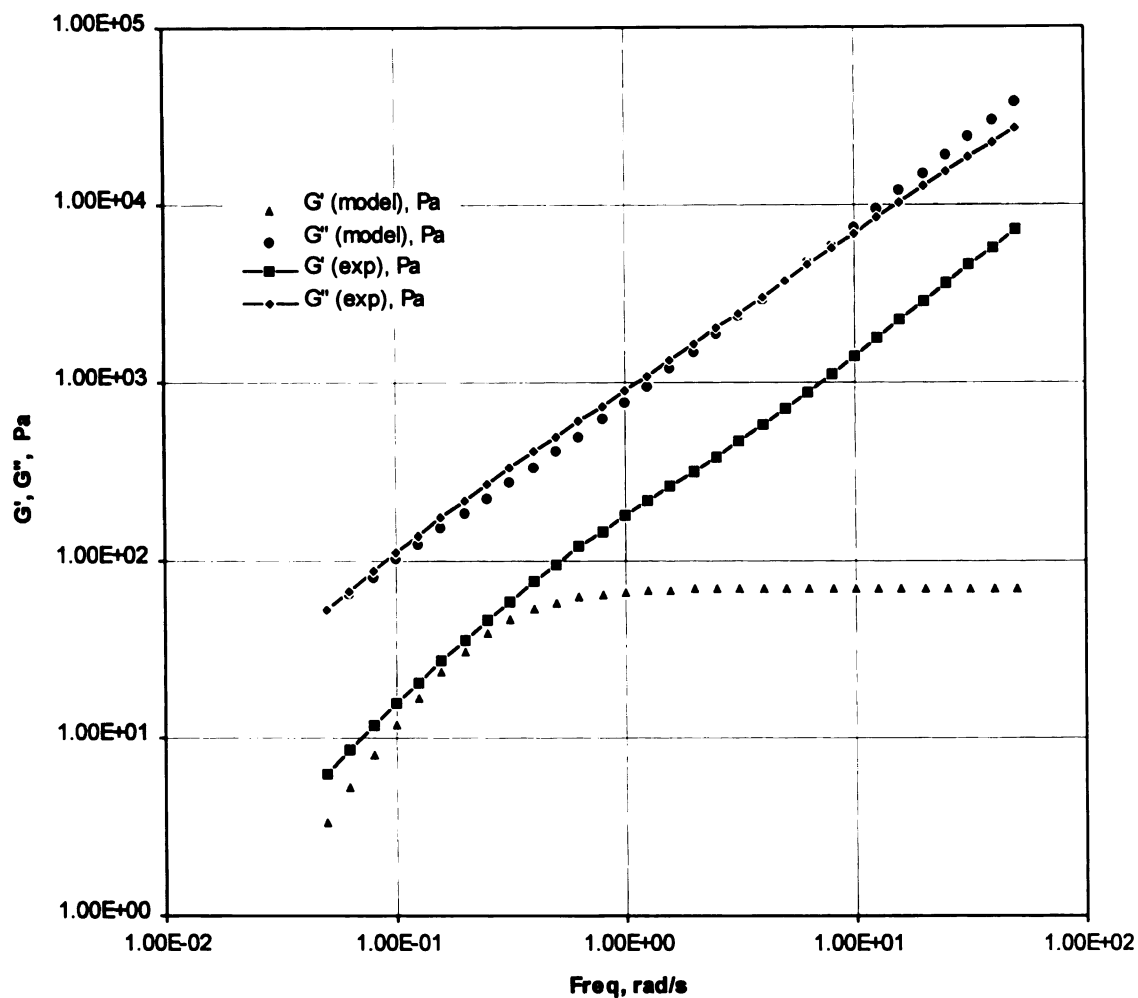
Figure 3.13: Comparison of the storage and loss moduli values obtained from the Oldroyd model with that obtained experimentally for PA6/ PP (80/ 20) (Γ^0 = 4 mN/ m, R = 8 μm).
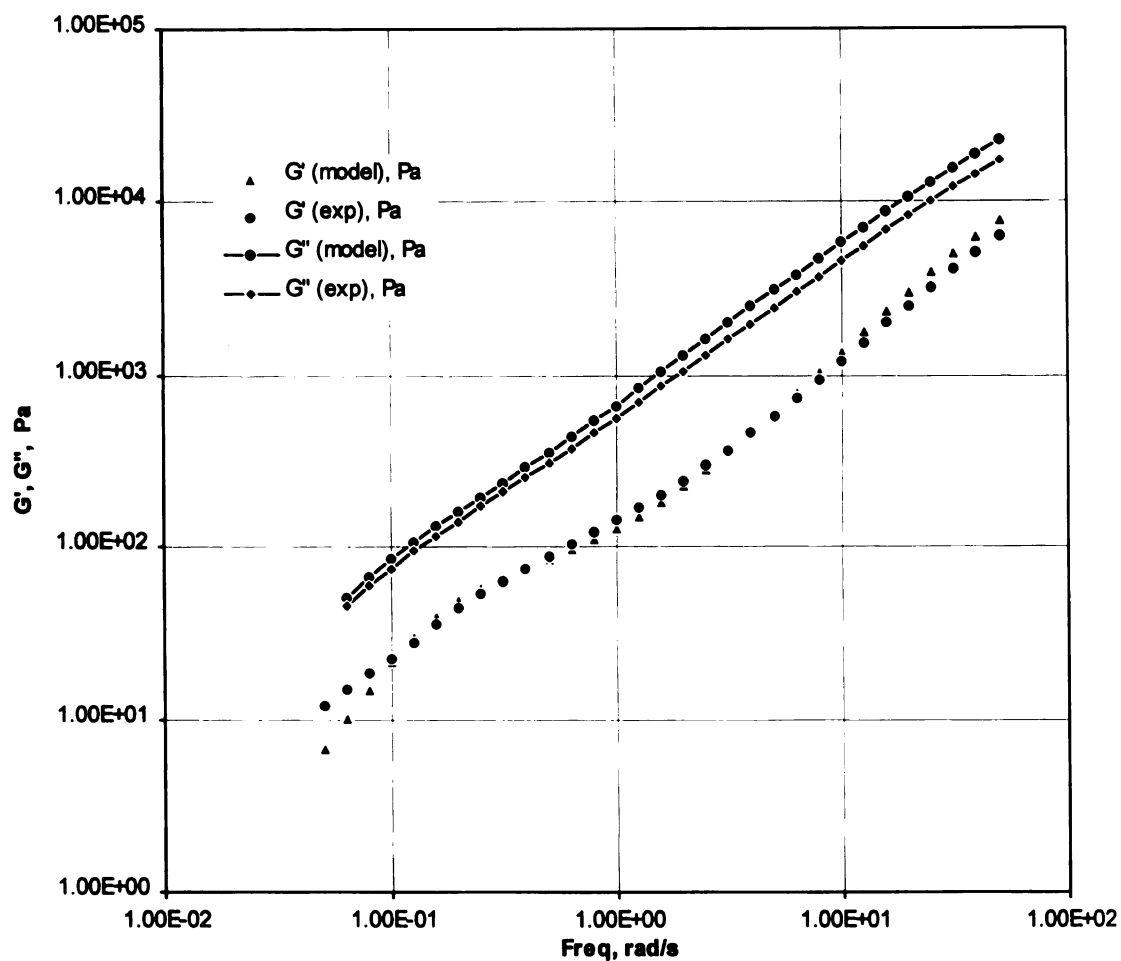
Figure 3.14: Comparison of the storage and loss moduli values obtained from the model with that obtained experimentally for PA6/ PP (70/ 30) (Γ^0 = 4 mN/ m, R = 12 μm).
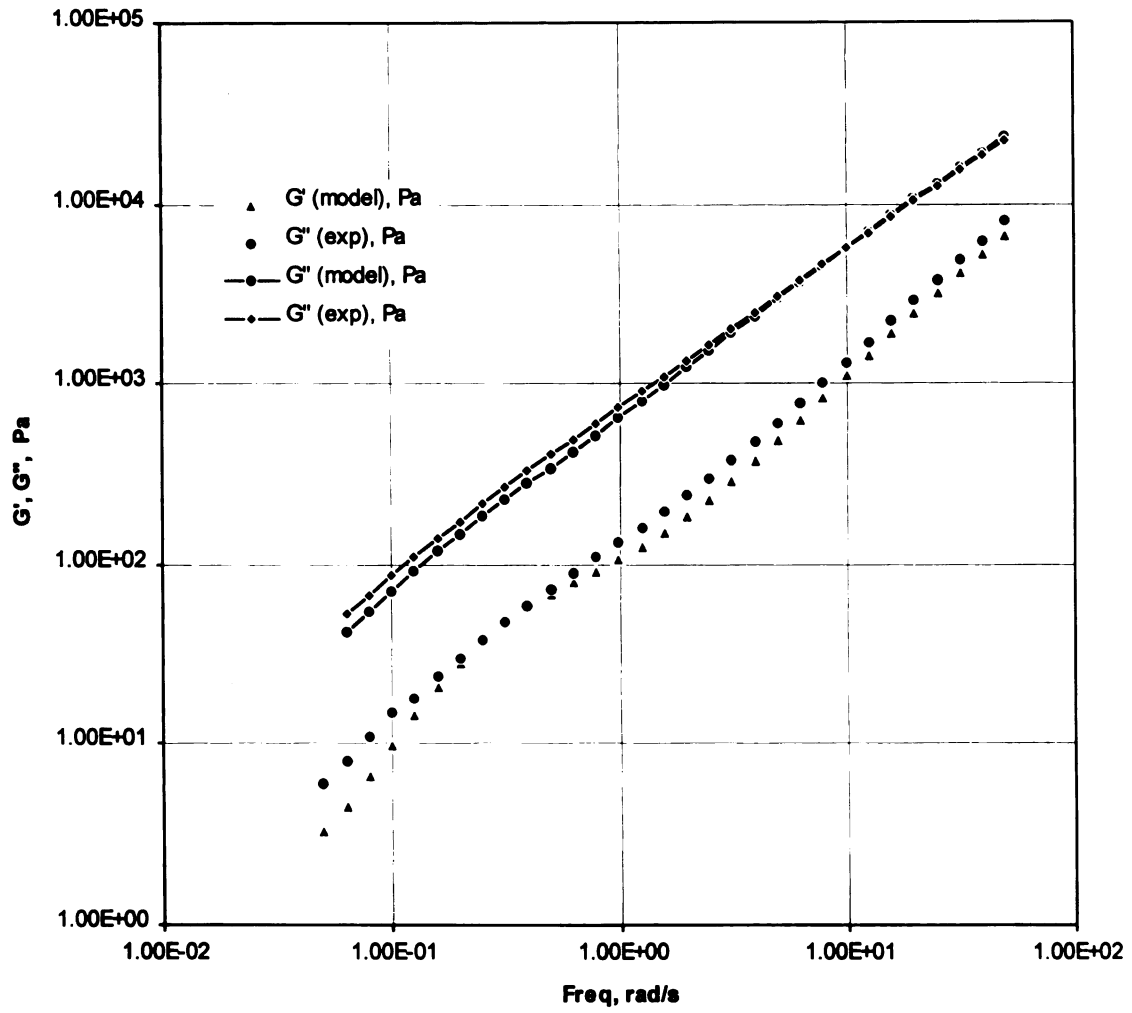
Figure 3.15: Comparison of the storage and loss moduli values obtained from the model with that obtained experimentally for PA6/ PP (80/ 20) (Γ^0 = 4 mN/ m, R = 8 μm).

Figure 3.16: Comparison of the storage and loss moduli values obtained from the model with that obtained experimentally for PA6/ PP (90/ 10) (Γ^0 = 4 mN/ m, R = 4 μm).
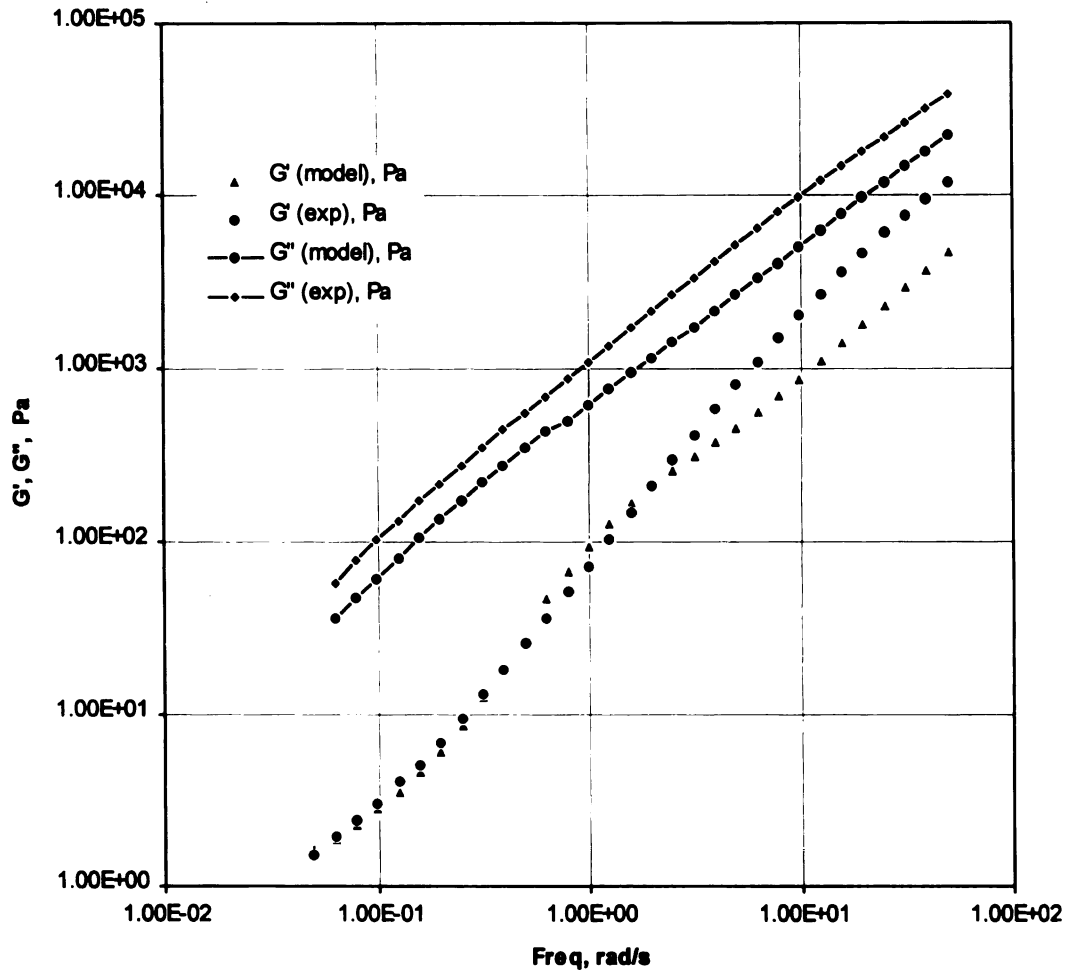
Figure 3.17: Comparison of the storage and loss moduli values obtained from the model with that obtained experimentally for PA6/ PP-MA (90/ 10) (Γ^0 = 1 mN/ m, R = 0.5 μm).

Figure 3.18: Comparison of the storage and loss moduli values obtained from the model with that obtained experimentally for PA6/ PP-MA (80/ 20) (Γ^0 = 1 mN/ m, R = 0.5 μm).

Figure 3.19: Comparison of the storage and loss moduli values obtained from the model with that obtained experimentally for PA6/ PP-MA (90/ 10) ($\Gamma^0 = 1$ mN/ m, R = 0.5 μm, $\beta_0 = 0.5$ mN/ m, $\omega_\beta = 0.2$ rad/ s).
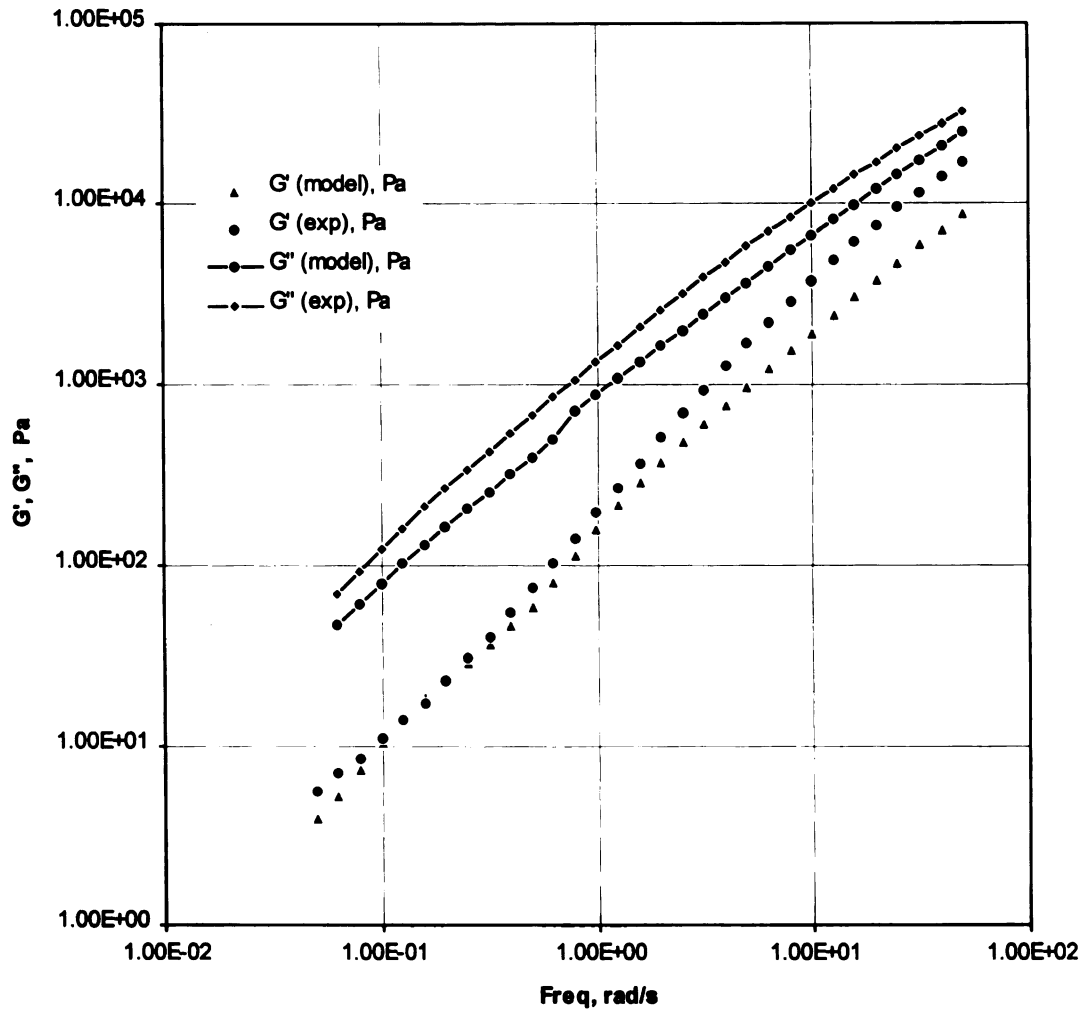
Figure 3.20: Comparison of the storage and loss moduli values obtained from the model with that obtained experimentally for PA6/ PP-MA (80/ 20) ($\Gamma^0 = 1$ mN/ m, R = 0.5 µm, $\beta_0 = 0.5$ mN/ m, $\omega_\beta = 0.2$ rad/ s).

THE EFFECT OF PROGRESSIVE EXTENT OF INTERFACIAL REACTION ON THE RHEOLOGY AND MORPHOLOGY OF NYLON 6 - MALEATED POLYPROPYLENE BLENDS

4.1 INTRODUCTION:

Blending of polymers is a popular method of improving their end-use properties [Paul et. al, 1988]. However, most polymers are thermodynamically incompatible which leads to their phase separation on blending. *Compatibilization* of polymer blends is carried out to reduce the degree of incompatibility and stabilize the system. This can be achieved by addition of a pre-made block copolymer to the system or by carrying out an in-situ reaction between the complementary groups of the blend components. Both techniques promote dispersive mixing which leads to a reduced particle size.

Experimental evidence suggests that the addition of premade block copolymers leads to a reduction of interfacial tension [Cho et. al., 1996; Elemans et. al., 1990]. In the area of reactive blending experimental results showing the quantitative effects of interfacial reaction on interfacial tension are limited. In a study on blending of nylon 6 with non-reactive and reactive rubbers Wu [1987] predicted that the interfacial tension could drop from 8 mN/m in non-reactive system to 0.25 mN/m in reactive system. The prediction was based on a statistical mechanical theory of polymer interfaces due to Helfand and Tagami [1971]. The theory predicts the relation shown in Equation 4.1.

$$\Gamma^0 \propto \frac{1}{L} \qquad (4.1)$$

where Γ^0 is the equilibrium interfacial tension and L is the interfacial thickness. The

Helfand theory was developed for a 'bare interface'. That is, an interface which has not

been occupied by a copolymer or a reacted moiety. On the basis of interfacial thickness

and interfacial tension in model experimental systems Wu arrived at the following

modified result.

$$\Gamma^0 \propto \frac{1}{L^{0.86}} \qquad (4.2)$$

This empirical rule was then combined with measurements of interfacial thickness in

nylon 6 - reactive rubber blends to obtain a value of 0.25 mN/m for interfacial tension in

these systems. One of the aims of this study is to obtain values of interfacial tension

independent of thickness in reactively blended polymer systems.

An important effect of the interfacial reaction is the modification of the interface

from a 'bare interface' to an 'occupied interface'. As the extent of interfacial reaction

increases, the interface is progressively occupied. Fayt et. al. [1989] have reported that

the addition of a block copolymer leads to a broader interface. The interface is not

unimolecular thick, but has a finite dimension. In a recent theoretical paper

O'Shaughnessy and Sawhney [1996] conclude that besides reducing interfacial tension,

an 'occupied interface' also suppresses coalescence. This is a direct result of steric

hindrance provided by the 'occupied interface' and leads to a stabilization of the

morphology. The experimental evidence presented by Sundraraj and Macosko [1995]

corroborates this conclusion. This study will investigate the effect of increased occupation of the interface by successively increasing the extent of reaction. Thus, to sum up, there are two important issues being investigated in this work.

- What is the effect of interfacial reaction on the interfacial tension in polymeric blends?

- What is the effect of 'progressive crowding' at the interface on the rheological behavior of the blend?

In this study, nylon 6 has been blended with polypropylene which has been maleated to different extents. Increasing extents of maleation lead to increasing extents of interfacial reaction and hence 'progressive crowding' at the interface.

4.2 BACKGROUND

4.2.1 Emulsion Models

The classic theory of rheology of emulsions focuses on dilute emulsions of spherical, Newtonian drops - see e.g. Frankel and Acrivos [1967] and Choi and Schowalter [1975]. The parameters in this theory are the capillary number Ca and the viscosity ratio k. They are defined in Equations 4.3 and 4.4 respectively.

$$\text{Ca} = \frac{\eta_m \dot{\gamma} d}{\Gamma^0} = \frac{\text{Viscous Forces}}{\text{Interfacial Forces}} \tag{4.3}$$

$$k = \frac{\eta_d}{\eta_m} = \frac{\text{Viscosity of the dispersed phase}}{\text{Viscosity of the matrix}} \tag{4.4}$$

These two parameters determine the deformation of the drop D, the ratio of the major axis to minor axis of the distorted spherical drop. Frankel and Acrivos point out that the bulk stress in a flowing emulsion can be predicted well only if the shapes of the dispersed phase agree well with the predicted shapes.

Theories and computational results on concentrated emulsions have been reported by Palierne [1990] for dynamic shear with very small deformation from spherical; by Loewenberg and Hinch [1996] for shear flows with appreciable departures from spherical shape for the dispersed phase; and by Sangani and Mo [1994] for shear flows of emulsion with nearly spherical dispersed phase. The first two cover only a moderate concentration range - up to 0.3 while the last study accounts for lubrication effects that arise in very

concentrated suspension and emulsions. The Palierne theory has an added distinction of being formulated for viscoelastic constituents. However, it is incorrect to use the Palierne model for large deformation response of emulsions. Table 4.1 is a summary of the available theory and computations of emulsion rheology in the literature.

Of these, three models have been applied widely to polymeric systems to explain their rheological behavior. They are due to Oldroyd [1953], Choi and Schowalter [1975], and Palierne [1990]. The equilibrium interfacial tension leads to long time relaxation processes affecting the dynamic moduli in the low frequency region. These long time relaxation processes are associated with the mechanical relaxation of the dispersed phase [Scholz et. al., 1989]. The important physical parameters governing the relaxation processes are the viscosity ratio k, the particle size R, the equilibrium interfacial tension Γ^0, the matrix viscosity η_m and λ_D, the relaxation time for the drop shape.

$$\lambda_D \sim f(k)\frac{R\eta_m}{\Gamma^0} \qquad (4.5)$$

The model due to Palierne accounts for the viscoelastic nature of the component phases, non-dilute emulsion and the particle size distribution. These factors were not accounted for in the models of Oldroyd and of Choi and Schowalter. The relation for the complex modulus of the blend is

$$G^* = G_m^* \left[\frac{1 + \frac{3}{2}\sum_i \frac{\phi_i E_i}{D_i}}{1 - \sum_i \frac{\phi_i E_i}{D_i}} \right] \qquad (4.6)$$

where,

$$E_i = 2(G_d^* - G_m^*)(19G_d^* + 16G_m^*) + \frac{48\beta_d^* \Gamma^o}{R_i^2} + \frac{32\beta_s^*(\Gamma^o + \beta_d^*)}{R_i^2} + \frac{8\Gamma^o}{R_i}(5G_d^* + 2G_m^*) + \frac{2\beta_d^*}{R_i}(23G_d^* - 16G_m^*) + \frac{4\beta_s^*}{R_i}(13G_d^* + 8G_m^*)$$

$$(4.7)$$

and

$$D_i = (2G_d^* - 3G_m^*)(19G_d^* + 16G_m^*) + \frac{48\beta_d^* \Gamma^o}{R_i^2} + \frac{32\beta_s^*(\Gamma^o + \beta_d^*)}{R_i^2} + \frac{40\Gamma^o}{R_i}(G_d^* + G_m^*) + \frac{2\beta_d^*}{R_i}(23G_d^* + 32G_m^*) + \frac{4\beta_s^*}{R_i}(13G_d^* + 12G_m^*)$$

$$(4.8)$$

The sub-script 'i' refers to the ith particle fraction. As Equations 4.6 thru 4.8 show, this model explicitly accounts for the rheological properties of the component phases, the volume fraction, the morphology and the interfacial tension. An interesting feature of this model is its treatment of the interfacial tension as a sum of two parts - an equilibrium interfacial tension Γ^o and a frequency dependent complex part $\beta^*(\omega)$. In turn, $\beta^*(\omega)$ consists of two complex moduli - surface dilatation modulus and surface shear modulus. Both these properties are characteristics of the interface. The surface dilatation modulus is associated with a non-uniform interface while the surface shear modulus is the resistance of the interface to the shear deformation. The surface shear modulus is related to the layer thickness of the interphase. If, $\beta^*(\omega)$ equals 0, the model takes the reduced form shown in Equation 4.9.

$$G^{*}(\omega) = G^{*}_{m}(\omega) \frac{1 + 3\sum_{i} \phi_{i} H_{i}(\omega)}{1 - 2\sum_{i} \phi_{i} H_{i}(\omega)} \qquad (4.9)$$

where,

$$H_{i}(\omega) = \frac{(4\Gamma^{0}/R_{i})(2G^{*}_{m} + 5G^{*}_{d}) + (G^{*}_{d} - G^{*}_{m})(16G^{*}_{m} + 19G^{*}_{d})}{(40\Gamma^{0}/R_{i})(G^{*}_{m} + G^{*}_{d}) + (2G^{*}_{d} + 3G^{*}_{m})(16G^{*}_{m} + 19G^{*}_{d})} \qquad (4.10)$$

4.2.2 Determination of the Interfacial Tension from Emulsion Rheology

Several groups have used these models to study the rheology of polymeric blends and determine the equilibrium interfacial tension [Scholz et. al., 1989; Graebling et. al., 1991; Gramespacher et. al. 1992; Graebling et. al, 1993]. The models of Oldroyd and of Choi and Schowalter describe only the low frequency region of the dynamic storage modulus curve. Graebling and co-workers [1993] showed that Palierne's model maybe used to describe the dynamic moduli over a broader frequency range. If each of the blend components is described by a single relaxation time Maxwell model, and if a monodisperse particle size distribution is assumed, Equation 4.9 leads to the dynamic behavior depicted in Figure 1 of paper by Graebling et. al. [1993]. The appearance of the low frequency plateau is striking. This is associated with the shape relaxation of the disperse shape domains as shown by λ_{D} in Equation 4.5. The location and magnitude of the secondary plateau determines the accuracy with which interfacial tension can be

estimated from such data. The location of the secondary plateau is sensitive to some emulsion parameters as itemized below.

- As the viscosity ratio k is raised, the secondary plateau moves toward lower storage moduli and lower frequency.

- As the interfacial tension is reduced, the secondary plateau shifts toward lower frequencies and its width increases. Particle size has the opposite effect.

- As the volume fraction of the disperse phase is increased, the secondary plateau becomes more pronounced in width and shifts toward higher frequencies.

- As the ratio of component relaxation times X is decreased, the secondary plateau becomes ill-defined.

4.3 EXPERIMENTAL

4.3.1 Materials

Nylon 6 (Ultramid B3 from BASF Corporation), neat polypropylene (Profax

6501 from Montell Corporation) and three different grades of maleated polypropylene (

PB3001, PB3002, PB3150, from Uniroyal Chemicals) were used in the study. The three

grades of maleated polypropylene contained different amounts of maleic anhydride

functionality on polypropylenes of different molecular weight distribution. The maleic

anhydride content of PB3001, PB3002, PB3150 was reported to be 0.15 wt. %, 0.3 wt. %

and 0.8 wt. % respectively.

4.3.2 Blending

Blends were prepared with nylon 6 as the matrix and different polypropylenes as

the dispersed phase. To minimize the effects of moisture, the materials were dried under

a nitrogen blanket for 6-8 hours at a temperature of 120 °C. Each pair of blends

contained 10 wt%, 20 wt% and 30 wt% of the disperse phase respectively. Blends were

prepared in a ZSK-30 twin screw extruder at a temperature of 230 °C for all the zones.

The extrudate strands were pelletized and dried. The blends will be referred to in the text

with the components and their respective weight fractions in the parenthesis.

4.3.3 Rheological

Rheological characterization was carried out on an RMS-800 rheometer (from Rheometrics Scientific, Inc.) using a 50 mm parallel plate arrangement. The disks were prepared by compression molding the pellets in a Carver press under a force of 6 tons and 230 °C. The pellets were pre-dried in a vacuum oven for 10-12 hours. The instrument oven was purged with dry nitrogen during measurements to avoid degradation. A frequency range of 0.05-50 rad/s and strains of 10-15% were applied during the measurements. A strain sweep was carried out to determine the viscoelastic limits on the strain.

4.3.4 Morphological

The samples for morphological examination were prepared by placing the pre-notched disks in the RMS 800 oven, heating them to 230 °C and placing them directly in liquid nitrogen. Those were then fractured under liquid nitrogen. These samples were then examined in a Phillips Electroscan 2020 environmental scanning microscope. Water vapor at a pressure of 2-3 Torr was used as the imaging gas. The measurements were made directly from the micrographs and the volume average radii were calculated.

4.4 RESULTS AND DISCUSSION

4.4.1 Blend Morphology

Figures 4.1a thru 4.1l show the micrographs of the different blends. Table 4.2 summarizes the volume average radii of the disperse phase in the blends. For the non-reactive blends it is observed that the particles are spherical with a broad particle size distribution. Also, their size increases progressively with increasing volume fraction of the dispersed phase. This behavior is attributed to the effects of coalescence. On the other hand, in the case of reactive blends the particle size is reduced, the particle size distribution is narrowed and the effect of volume fraction of the dispersed phase is minimized. The data show that the particle size in reactive blends does not vary significantly with progressive extent of reaction or with volume fraction of the disperse phase. This suggests that the stability imparted to the interface is independent of the extent of coverage. Also, in reactive blends the probability of formation of micelles is low as compared to the blends compatibilized by an external agent. In externally compatibilized systems the compatibilizer may phase separate above a critical concentration. Chapter 5 discusses the rheology and morphology of externally compatibilized blends.

4.4.2 Rheology

Table 4.3 shows the zero-shear viscosity η_0 and the corresponding relaxation time of the components. It should be noted that the relaxation time of the matrix is significantly lower than that of the disperse phase. This is important to identify the

relaxation changes brought about by the changes occurring at the interface. The values were determined using the dynamic shear data. Figures 4.2a and 4.2b show the storage and loss moduli of the blend components. It is worth pointing out that the molecular weights of the different maleated polypropylenes are not the same. To observe the broad rheological changes brought about by the interfacial reaction, two important issues need to be addressed at this stage:

- What is the effect of increased weight fraction of the disperse phase, for a given disperse phase component ?

- What is the effect of increased extent of maleation (causing progressive extents of reaction) for the same weight fraction of the disperse phase ?

Figures 4.3a and 4.3b show a comparison of the storage and loss moduli of the non-reactive blends with increasing weight fraction of the disperse phase. In Figure 4.3a, the width of the secondary plateau and the associated plateau modulus become more pronounced with increasing weight fraction of the dispersed phase. As the weight fraction is increased, the G' values around the low frequency also increase. These features are in accordance with theoretical predictions [Graebling et. al., 1993]. It is also observed that at higher frequencies, the curves converge. That is, the effects due to the interface contribution are reduced. Also, as shown in Figure 4.3b, there are no significant changes in the loss moduli behavior. This is also in accordance with the theory. The remaining discussion shall focus on trends in the storage moduli.

The effect of the increased weight fraction of the disperse phase in the reactive blend is illustrated in Figure 4.4. It is the same as Figure 4.3a but for B3/ 3001 blend which is also the least reactive. For B3/ 3001 (80/ 20) blend, there is a lift at low frequencies. Also, the curves indicate that an additional elasticity is imparted to the blends with increasing weight fraction of the disperse phase. A comparison with the plots for non-reactive blends shows that the frequency range over which this additional elasticity is significantly enhanced is greater in reactive blends. It appears that the interface in B3/ 3001 blends has a pronounced effect over a larger frequency range as compared to the non-reactive blends. This pattern was observed in all the reactive blends. In the following sections we shall examine the possible reasons for this.

Next, we examine how blend rheology is affected by the increased extent of maleation (and hence the increased extent of reaction) if the weight fraction of the dispersed phase is maintained constant. Figure 4.5 shows a comparison of the storage moduli for the 80/20 blends with varying extents of maleation in polypropylene. An increased extent of maleation (and interfacial reaction) leads to progressively higher elasticity over a larger frequency range. When compared to the non-reactive blend it is seen that the elasticity of the non-reactive system is higher as compared to the elasticity of the reactive system toward the lower frequencies, but lower at the higher frequencies. This can be explained on the basis of the Equation 4.5. It shows that the longest relaxation times correspond to the mechanical relaxation of the dispersed phase [Scholz et. al., 1989]. The size of the disperse phase in the non-reactive blend is much larger compared to the size in reactive blends. The larger size of the droplets leads to longer

relaxation times and larger storage modulus. However, at higher frequencies, where the

long time relaxation processes play a less significant role, the size of the droplets does not

control the relaxation behavior. It is the product of the interfacial reaction which will

control the relaxation phenomenon.

The Figure 4.6 compares the storage modulus of the B3/ PP (80/ 20) blend with

that of its components. It is observed that the storage modulus of the blend lies above the

respective component values until a certain value, after which it falls between them.

Figure 4.7 shows a similar comparison for B3/ 3001 (80/ 20) blend. The storage modulus

of the blend falls between those of the components for the entire frequency range. In the

B3/ 3002 (80/ 20) blend (Figure 4.8), the blend storage modulus falls between those of

the components for the major part of the frequency range but above the component values

at high frequencies. This trend is further enhanced in B3/ 3150 (80/ 20) blend (Figure

4.9), where the blend modulus is consistently higher than those of the components over

the entire frequency range. That is, the interfacial reaction causes a fundamental change

in the rheological behavior of the blend. Progressive extents of reaction lead to a

progressive increase in elasticity. In the following section the effect of interfacial

reaction on the interfacial tension shall be discussed in greater detail which is an

important aim of this study.

4.4.3   Determination of the interfacial tension

To determine the value of the interfacial tension, Equation 4.9 and 4.10 have been

used. Figure 4.10 shows a comparison of the storage and loss moduli obtained from the

model with the experimentally obtained values for the non-reactive B3/ PP (80/20) blend.

The agreement between the model and the experimental value is good for a value of 8

mN/m. This value gives a good fit for 90/ 10 and 70/ 30 non-reactive blends also.

Now, what is the effect of interfacial reaction on the interfacial tension in reactive

blends? Figure 4.11 shows a comparison of the model and the experimentally obtained

values of the storage and the loss moduli in B3/ 3001 (90/10) system. This is the least

reactive system as it is the least maleated. A value of 7 mN/m gives a good fit between

the model and the experimentally obtained values. In B3/3001 (80/20) blend, a

secondary plateau toward the low frequency appears, as shown in Figure 4.4. Figure 4.12

shows a comparison of the model and the experimentally obtained values for B3/ 3001

(80/ 20) blend. They do not agree well, especially in the lower frequency range. The

interfacial reaction has created a fundamental change in the behavior of the reactive

system as compared to the non-reactive system. The change is imparting an additional

elasticity to the system which is not accounted for by the model in the form it has been

used until now. This discrepancy is enhanced as the weight fraction of the 3001 is

increased further. The effect of elasticity enhancement is so pronounced that there is

disagreement over the complete frequency range for any value of equilibrium interfacial

tension in all the reactive blends for 70/ 30 blends as shown in Figure 4.13 for B3/ 3001

(70/ 30) blend. In further discussion, the discussion shall be limited to 90/ 10 and 80/ 20

blends.

A more discriminating fit maybe obtained by extracting the contribution of the

interface to the dynamic storage modulus. To delineate this contribution, the following

quantity was defined and computed from the storage moduli curves for both the predicted

and experimental values.

$$G_{int}^{'} = G_{blend}^{'} - [\phi G_{d}^{'} + (1-\phi)G_{m}^{'}]$$ (4.11)

It should be stated at this stage that the storage modulus in the low frequency limits is the

main focus of discussion as this is most susceptible to the changes in the interface. Figure

4.14 compares G'$_{int}$ obtained from model prediction and from experimental data for the

B3/3001 (80/20) curve in the low frequency range. It is seen that there is reasonable

agreement in the lower frequency range for an equilibrium interfacial tension value of 7

mN/ m which is the same as in Figure 4.11. Similar comparison was carried out for B3/

3002 (80/ 20) and B3/ 3150 (80/ 20) blends as shown in Figures 4.15 and 4.16 to obtain

equilibrium interfacial tension values of 7 mN/ m and 4 mN/ m respectively.

To explain the discrepancy observed in the data above, it is important to

understand the physical events occurring at the interface with progressive extent of

reaction. As the interfacial reaction occurs, the interface goes from being a 'bare

interface' to an 'occupied interface'. Increased extent of reaction leads to a 'crowding' at

the interface. This increased occupancy of the interface and the links established due to

reaction cause the interface to take progressively long times to relax thus causing an

enhanced elasticity.

Thus, it is crucial to account for the contributions being imparted by the interface.

Until this stage, the only property characterizing the interface has been the equilibrium

interfacial tension. This does not account for the 'crowding' effects explicitly. In this

respect the modifications of Palierne's model are useful [Palierne, 1990]. It accounts for the surface dilatation modulus $\beta_d^*(\omega)$ and the surface shear modulus $\beta_s^*(\omega)$. The origin of these two quantities lies in the non-uniformity of the interface and the resistance to the shear deformation respectively. In this study it will be assumed that the interface is uniformly occupied by the reaction products and the surface dilatation modulus can be ignored. However, the reaction product does resist shear deformation, and the surface shear modulus $\beta_s^*(\omega)$ should be accounted for. The quantity $\beta_s^*(\omega)$ itself consists of the storage and loss moduli - $\beta'_s(\omega)$ and $\beta''_s(\omega)$ respectively. However, there are no experimental techniques available to measure these quantities. In the present work, the estimates shall be made from the theory of lightly cross-linked rubber [Ferry, 1961]. The reaction products are thought to behave as lightly cross-linked rubber. In the framework of this theory,

For $\omega\lambda_\beta < 1$

$$\beta'_s = \beta_0$$
$$\beta''_s = \beta_0\omega\lambda_\beta$$

(4.12)

For $\omega\lambda_\beta > 1$

$$\beta'_s = \beta''_s = \beta_0\sqrt{\omega\lambda_\beta}$$

(4.13)

The two important parameters in these equations are β_0 and λ_β (see to Figure 4.15). The quantity β_0 is the low frequency, long time limit of G' and λ_β corresponds to the frequency until which elastic recoil of the system occurs. For λ_β the transition point (in

the experimental curve) till which the additional elasticity is exhibited is a good choice.

It is the inherent elasticity of the system. Incorporating the quantity $\beta_s^*(\omega)$ in the

Equation 4.9 leads to improvement in the agreement between the experimental and model

curve in reactive blends. This has been shown in Figure 4.18 and 4.19 for B3/ 3150 (80/

20) blend. Similar improvements were observed in other reactive systems. Table 4.2

shows the values of the equilibrium interfacial tension and the approximate value of the

β_0 for the different blends.

The progressive extents of reaction leads to progressive 'coverage' of the

interface. This leads to a reduction in equilibrium interfacial tension and an enhancement

in elasticity. But, the important question at this stage is that how much coverage of the

interface is critical to cause a reduction in interfacial tension? This will be discussed in

the following section.

4.4.4   The issue of extent of coverage

Table 4.3 shows the material properties of the materials used in the study. From

these values, the values in Table 4.4 have been derived. It is seen that the amount of

amine functionality available for interfacial reaction is much more than the amount of

maleic anhydride. This is important as it ensures that the interfacial reaction goes to

completion and is not limited by the amount of reactive sites available. That is, whatever

maleic anhydride is in the interface is completely reacted. Also, it is seen that in the

disperse phase the number of maleic anhydride groups per chain available for reaction

increase from 1 per chain in PB3001 to 3.4 in PB3150. This is a significant difference

and will help in delineating the effect of progressively increasing extent of reaction.

Assuming complete reaction and uniformity of -MAH chains in the bulk of the dispersed

particle and the interface, it can be estimated that

$$\frac{\text{no. of g - moles of - MAH in the interface}}{\text{kg - mixture}} = \left(\frac{\text{Volume of interface}}{\text{Volume of particle}}\right)\left(\frac{\text{no. g - moles of - MAH}}{\text{kg - mixture}}\right)$$

Assuming the particle radius to be R and the interface thickness to be ΔR,

$$\frac{\text{Volume of interface}}{\text{Volume of the particle}} \sim \frac{4\pi R^2 \Delta R}{\dfrac{4\pi R^3}{3}} \sim \left(\frac{3\Delta R}{R}\right)$$

Let,

$$c = \frac{\text{no. of g - mole of - MAH}}{\text{kg PP - MA}}$$

If, w is the weight fraction of dispersed PP-MA in the blend

$$\frac{\text{no. of g - mole of - MAH}}{\text{kg - mixture}} = cw$$

Using above,

$$\frac{\text{no. of graft chains of amine - MAH in the interface}}{\text{kg - mixture}} = cwN_A\left(\frac{3\Delta R}{R}\right)$$

$$\text{Area occupied by the particle interface per kg - mixture} = \left(\frac{4\pi R^2}{\dfrac{4\pi R^3}{3}}\right)\left(\frac{w}{\rho_d}\right)$$

Therefore,

$$\Sigma = \frac{\text{Area occupied by grafts in the interface / kg - mixture}}{\text{no. graft chains of amine - MAH in the interface / kg - mixture}} = \frac{1}{\rho_d \Delta R c N_A}$$

The value of Σ was determined for the respective reactive blends and have been shown in

Table 4.5. As the extent of maleation increases, Σ reduces as it should, because the

number of grafts increases due to increased reaction as the number of maleic anhydride

group available per chain increases from 1 to 2 to 3.4 respectively. Combining this with

the estimates of the equilibrium interfacial tension it is seen that it drops continuously

with increasing reaction and increasing occupation of the interface. The reactive blends

with progressively increasingly extents of interfacial reaction show departure from the

model at higher frequencies also. This means, that the product of the interfacial reaction

plays a significant role in the rheological behavior of the blend even at higher

frequencies. Its effect is not limited to low frequencies alone.

4.5   CONCLUSION

This study has investigated the effects of interfacial reaction on the interfacial

tension in reactive polymeric blends. It has been shown that interfacial reaction leads to a

reduction in particle size of the dispersed phase and a reduction in interfacial tension.

Morphological observations show that a minimal amount of interfacial reaction is

required to reduce the particle size. Also, increased reaction does not necessarily cause

progressive reduction in particle size. Interfacial reaction progressively drops from 8

mN/ m in non-reactive blends to 7 mN/ m to 4 mN/ m in reactive blends with different

extents of reaction. The number of reactive sites for grafts per maleated polypropylene chain goes from 1 to 2 to 3.4 respectively in these systems. Rheological observations show that besides a reduction in interfacial tension, there is an enhancement in the elasticity of the reactive blends as compared to the non-reactive blends. This is due to the fundamental difference brought about by the product of the interfacial reaction. To account for this, surface shear modulus has been used as proposed by the model of Palierne [1990].

In order to understand the effects of interfacial reaction on the behavior of the reactive blend, the effects of the visco-elastic nature of the polymeric components need to be eliminated. In the present study, the disperse phases were of varying visco-elastic properties. It is suggested that studies be carried out with disperse phases of same visco-elastic properties, but varying amounts of reactive sites.

Table 4.1: Emulsion Rheology models available in the literature.

Type of Flow	Limit of Concentration	Limit of Deformation	Theory or Approach	Authors
Shear-time varying	<0.02	=0 (Spherical drops)		Oldroyd
Shear-time varying	<0.02	<0.05	Asymptotic expansion	Frankel and Acrivos
Steady Shear	0.02	<0.6	Boundary Integral	Kennedy and Pozrikidis
Steady Shear	0.1	< 0.05	Method of Reflections	Choi and Schowalter
Oscillatory Shear	<0.3	Very small	Self consistent cell	Palierne
Steady Shear	<0.30	<0.6	Boundary Integral periodic B.C.	Lowenberg and Hinch
Steady Shear	up to max packing	<0.05	Multipole expansion periodic B.C.	Sangani and Mo

Table 4.2: The volume average radii of the dispersed phase in the various blends.

Blend	Radius (μm)	Γ^0 (mN/ m)	β_0 (mN/ m)
B3/PP (90/10)	8.75	8	-
B3/PP (80/20)	10.7	8	-
B3/PP (70/30)	16.5	8	-
B3/3001(90/10)	0.8	7	-
B3/3001(80/20)	0.8	7	0.1
B3/3001(70/30)	0.6	7	0.1
B3/3002(90/10)	0.5	7	-
B3/3002(80/20)	1.1	7	-
B3/3002(70/30)	0.7	7	-
B3/3150(90/10)	0.6	4	0.1
B3/3150(80/20)	1.5	4	0.1
B3/3150(70/30)	1.2	4	-

Table 4.3: The material properties of the materials used in this study.

Material	η_0 (Pa-s)	Relaxation time (s)	M_n (kg/ kg-mole)	N
B3	860	0.002	18,000	160
PP	1150	0.35	54,000	1286
3001	3000	1.1	76,000	1714
3002	1970	1.3	63,000	1500
3150	490	0.28	42,000	1000

Table 4.4: The values for reactive sites in the materials used in the study.

Material		n (no. -MAH/ chain)
B3	15.74 (g-mole amines/ kg-B3)	-
3001	0.015 (g-mole -MAH/ kg-3001)	1
3002	0.030 (g-mole -MAH/ kg-3002)	2
3150	0.080 (g-mole -MAH/ kg-3150)	3.4

Table 4.5: The values of the extent of coverage of the interface in different blends.

	$\Sigma \times 10^{18}$ (m^2/ grafts)	$\Sigma / n \times 10^{18}$ (m^2/ chain -PP-MA)	Γ_0 (mN/ m)
B3/ 3001	24	24	7
B3/ 3002	12	6	7
B3/ 3150	4.5	1.3	4

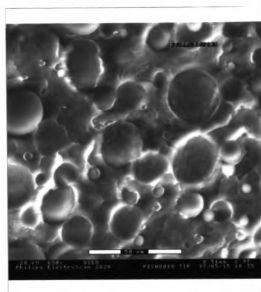Figure 4.1a: Micrograph showing the morphology of B3/ PP (90/ 10).

Figure 4.1b: Micrograph showing the morphology of B3/ PP (80/ 20).

Figure 4.1c: Micrograph showing the morphology of B3/ PP (70/ 30).

Figure 4.1d: Micrograph showing the morphology of B3/ 3001 (90/ 10).

Figure 4.1e: Micrograph showing the morphology of B3/ 3001 (80/ 20).
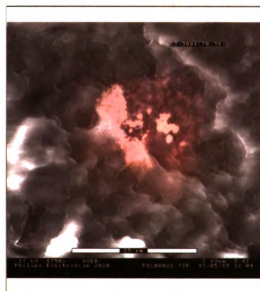
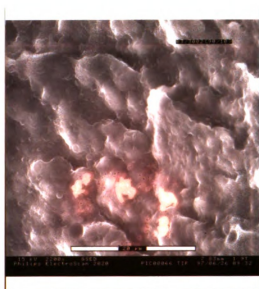Figure 4.1f: Micrograph showing the morphology of B3/ 3001 (70/ 30).

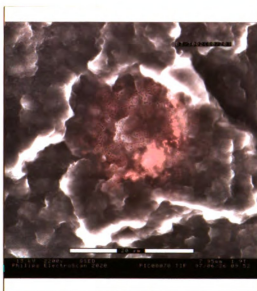Figure 4.1g: Micrograph showing the morphology of B3/ 3002 (90/ 10).

Figure 4.1h: Micrograph showing the morphology of B3/ 3002 (80/ 20).
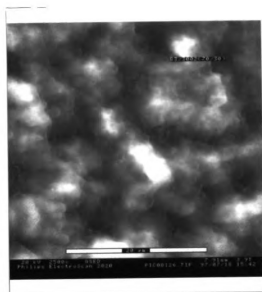
Figure 4.1i: Micrograph showing the morphology of B3/ 3002 (70/ 30).
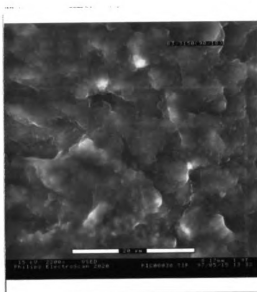
Figure 4.1j: Micrograph showing the morphology of B3/ 3150 (90/ 10).

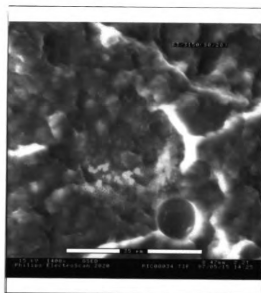Figure 4.1k: Micrograph showing the morphology of B3/ 3150 (80/ 20).
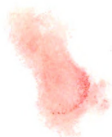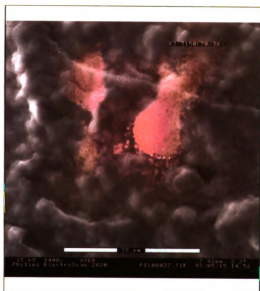
Figure 4.1l: Micrograph showing the morphology of B3/ 3150 (70/ 30).
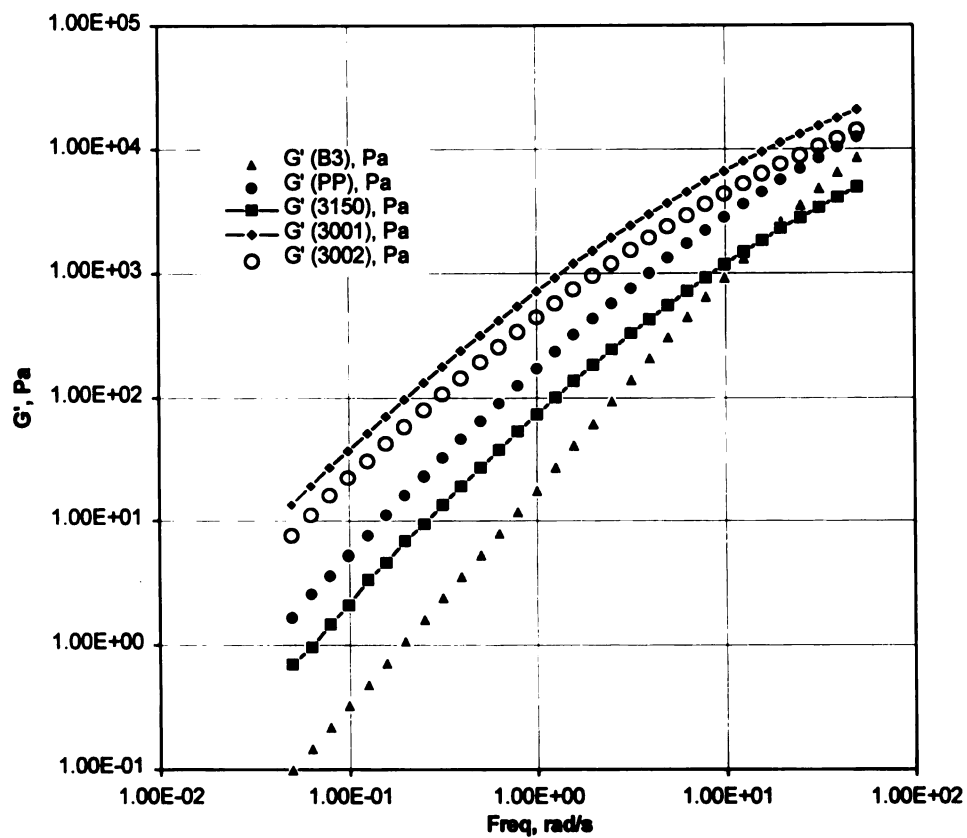
Figure 4.2a: Comparison of the storage moduli of the components of the blend.
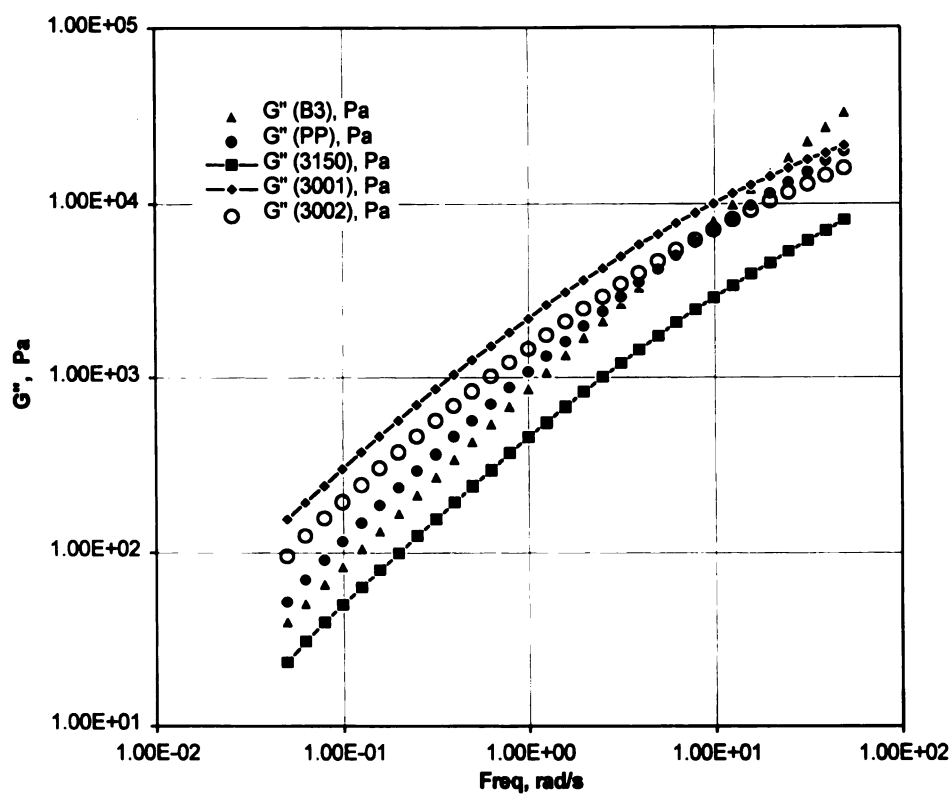
Figure 4.2b: Comparison of the loss moduli of the components of the blend.
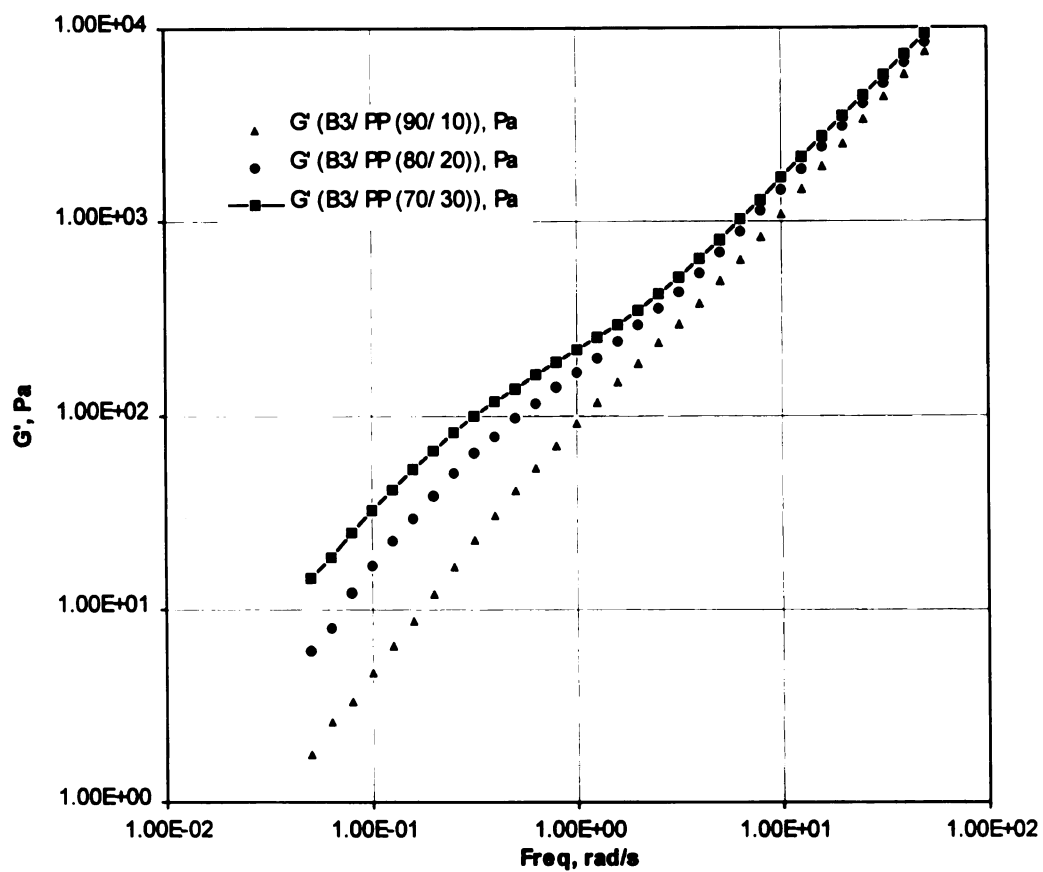
Figure 4.3a: Comparison of the storage moduli of the non-reactive blends for varying weight fractions of the dispersed phase.
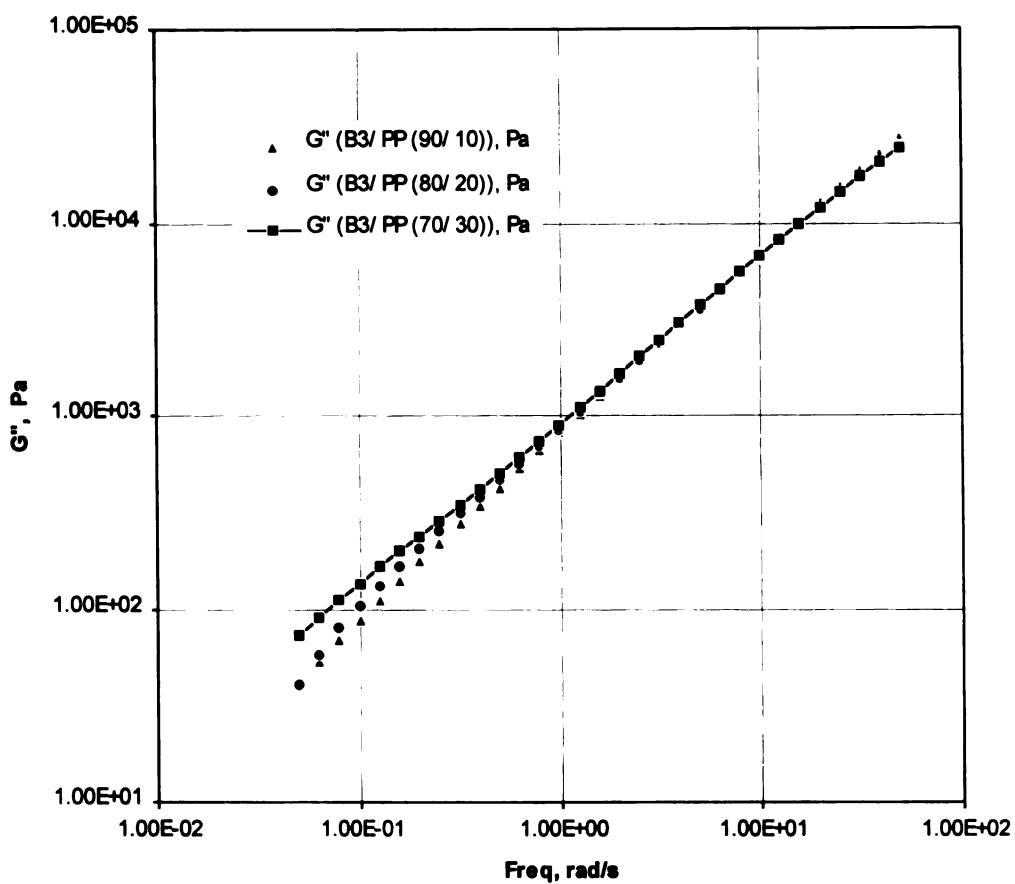
Figure 4.3b: Comparison of the loss moduli of the non-reactive blends for varying weight fractions of the dispersed phase.
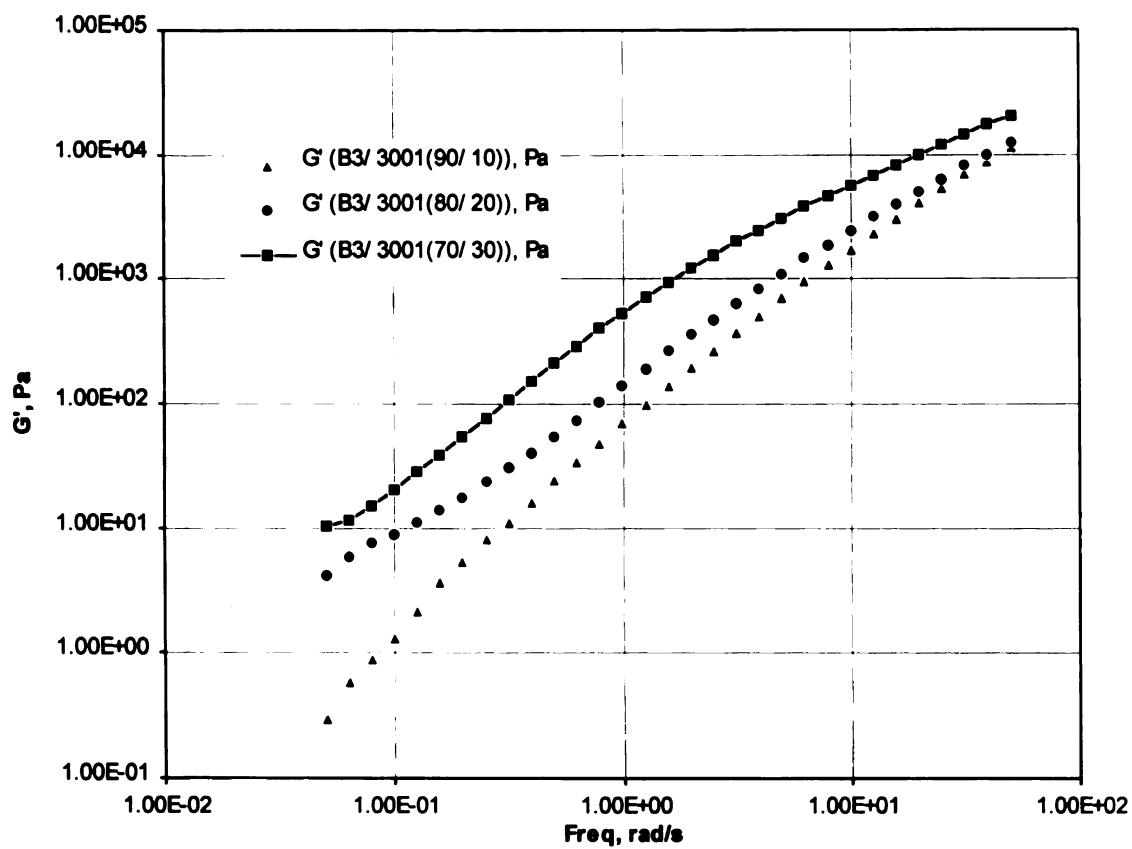
Figure 4.4: Comparison of the storage moduli of the B3/ 3001 blend for varying weight fractions of the dispersed phase.
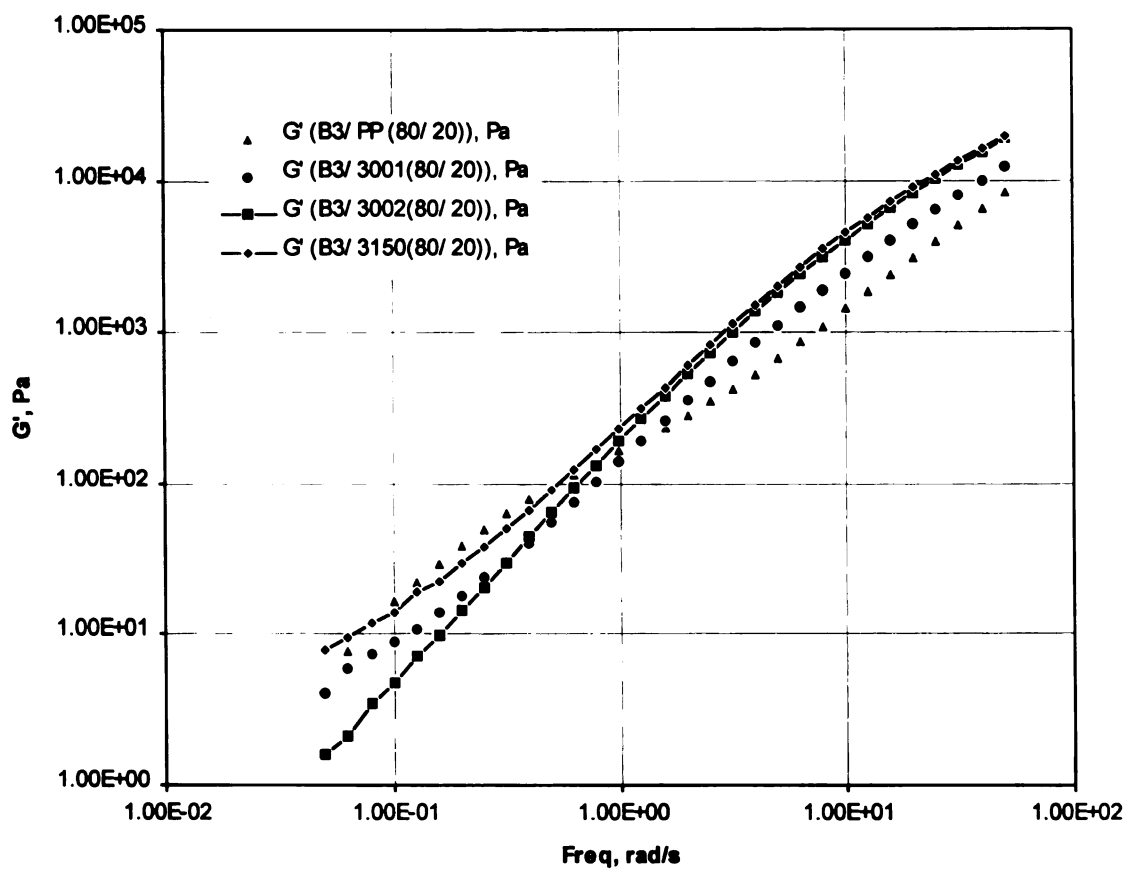
Figure 4.5: Comparison of the storage moduli of the 80/ 20 blends for the different dispersed phases.
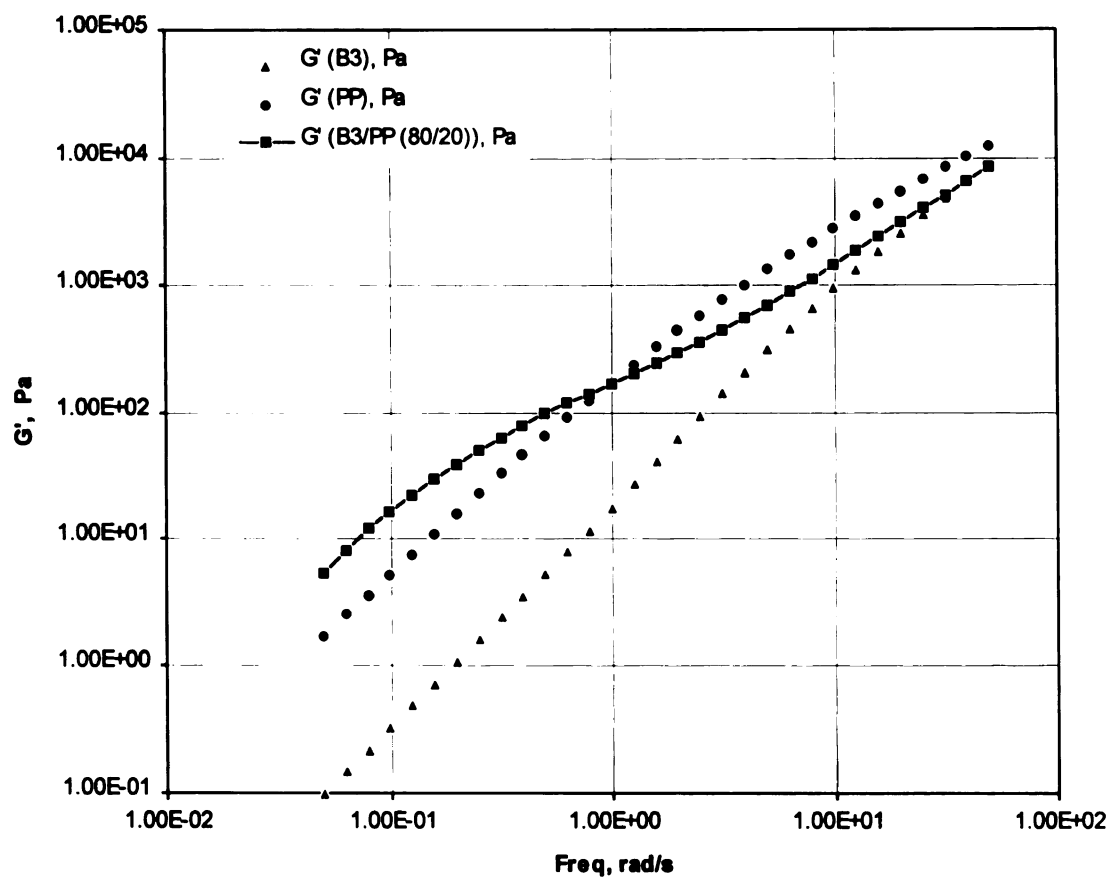
Figure 4.6: Comparison of the storage moduli of the B3/ PP (80/ 20) blend with the components.
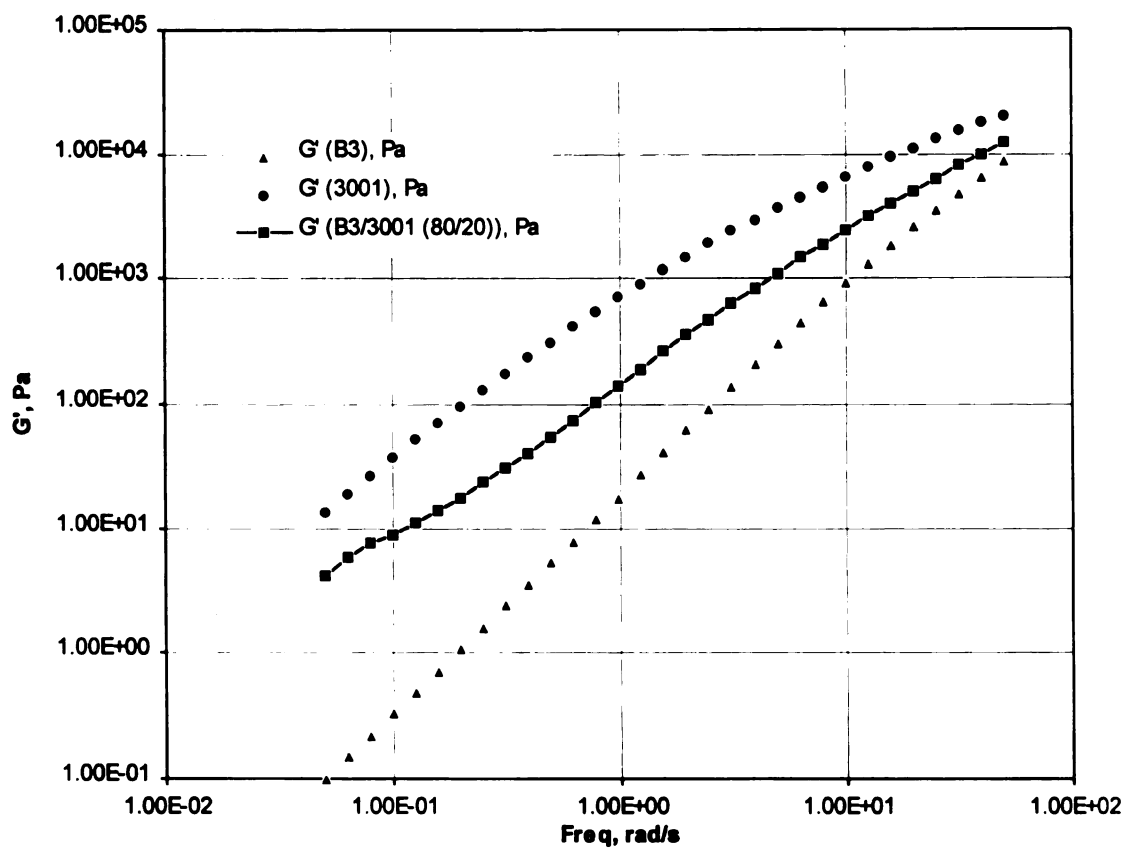
Figure 4.7: Comparison of the storage moduli of the B3/ 3001 (80/ 20) blend with the components.
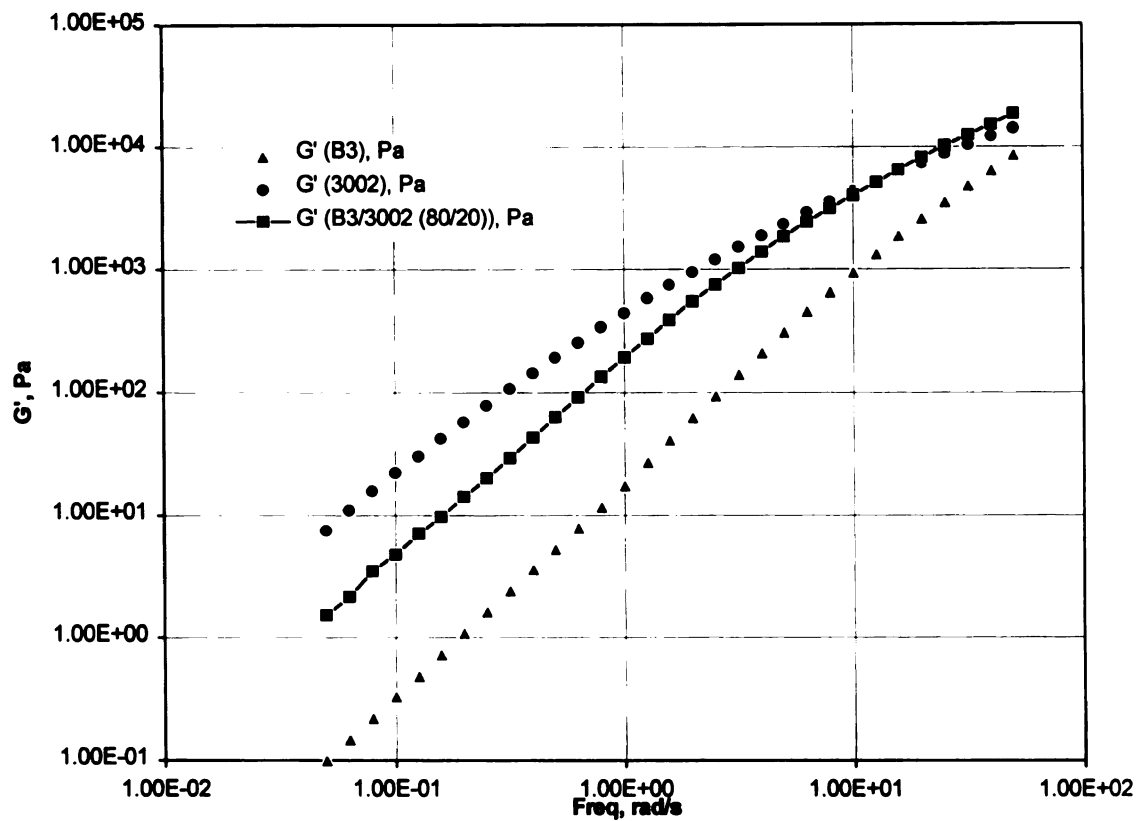
Figure 4.8: Comparison of the storage moduli of the B3/ 3002 (80/ 20) blend with the components.
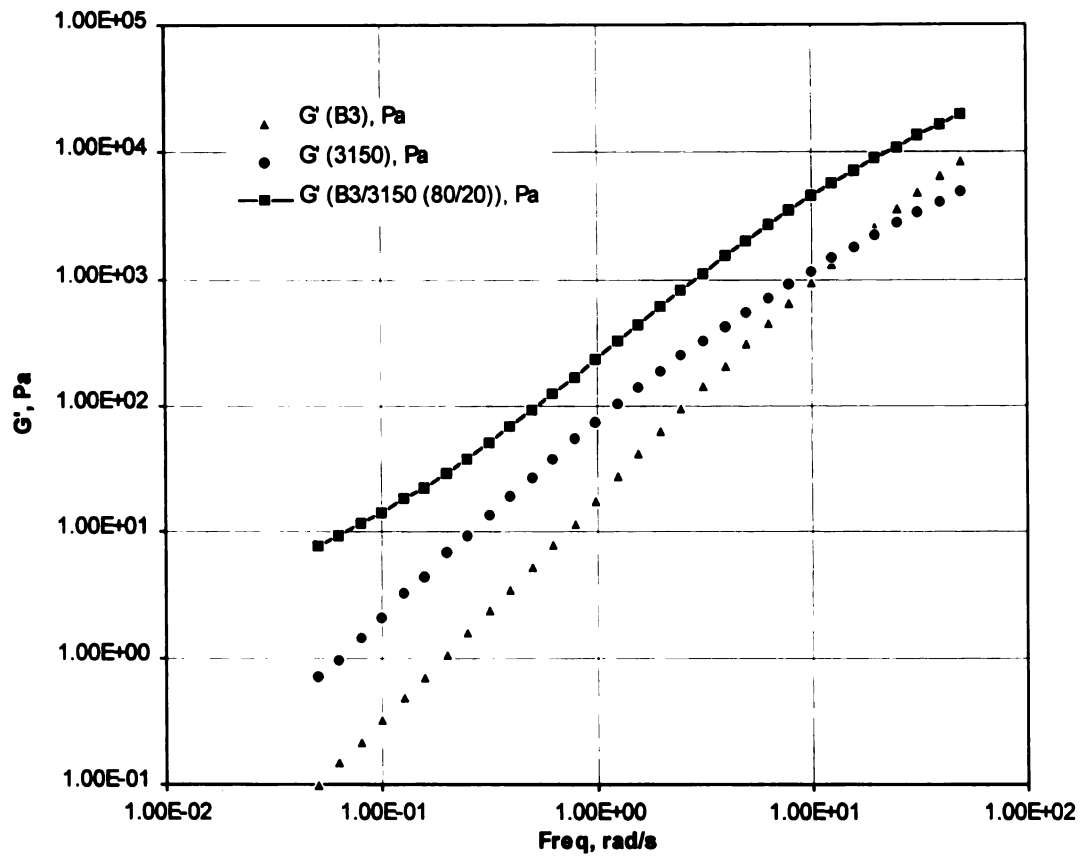
Figure 4.9: Comparison of the storage moduli of the B3/ 3150 (80/ 20) blend with the components.
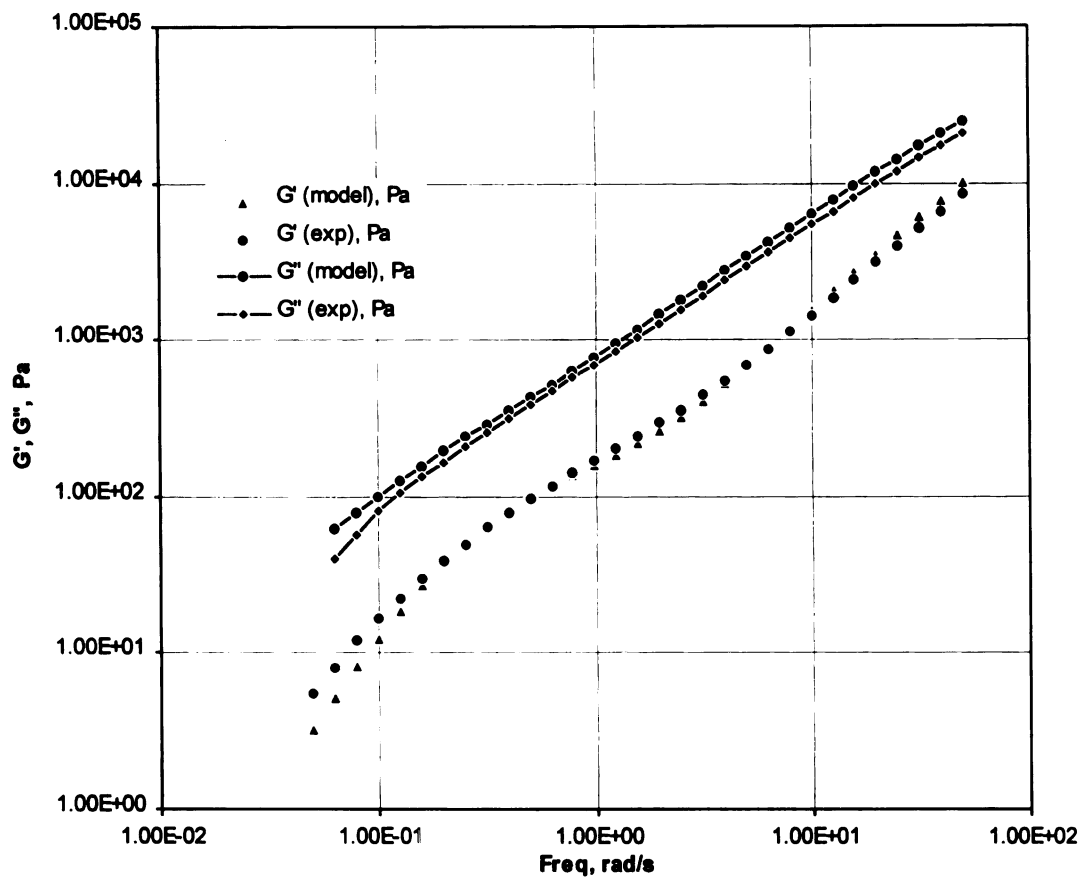
Figure 4.10: Comparison of the storage and loss moduli values obtained from the model with that obtained experimentally for B3/ PP (80/ 20) blend (Γ^0 = 8 mN/ m, R = 10.7 µm).
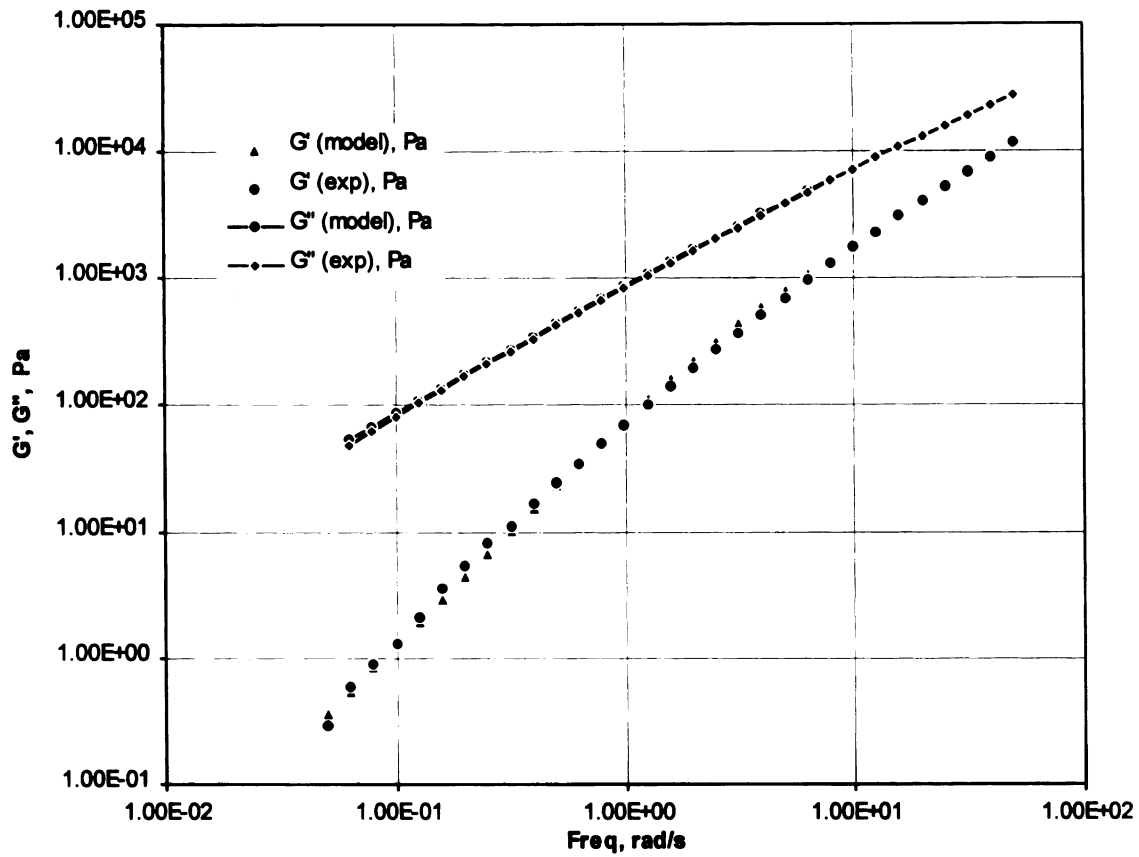
Figure 4.11: Comparison of the storage and loss moduli values obtained from the model with that obtained experimentally for B3/ 3001 (80/ 20) blend (Γ^0 = 7 mN/ m, R = 0.8 μm).
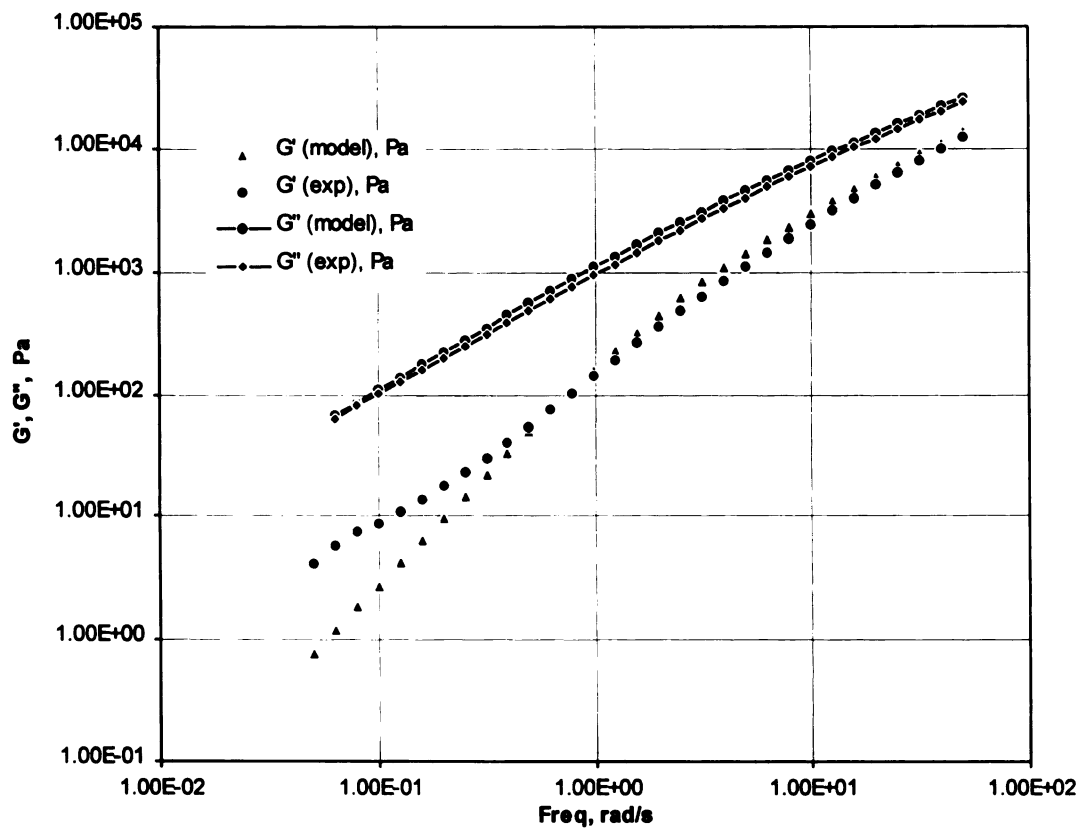
Figure 4.12: Comparison of the storage and loss moduli values obtained from the model with that obtained experimentally for B3/ 3001 (80/ 20) blend (Γ^0 = 7 mN/ m, R = 0.8 μm).
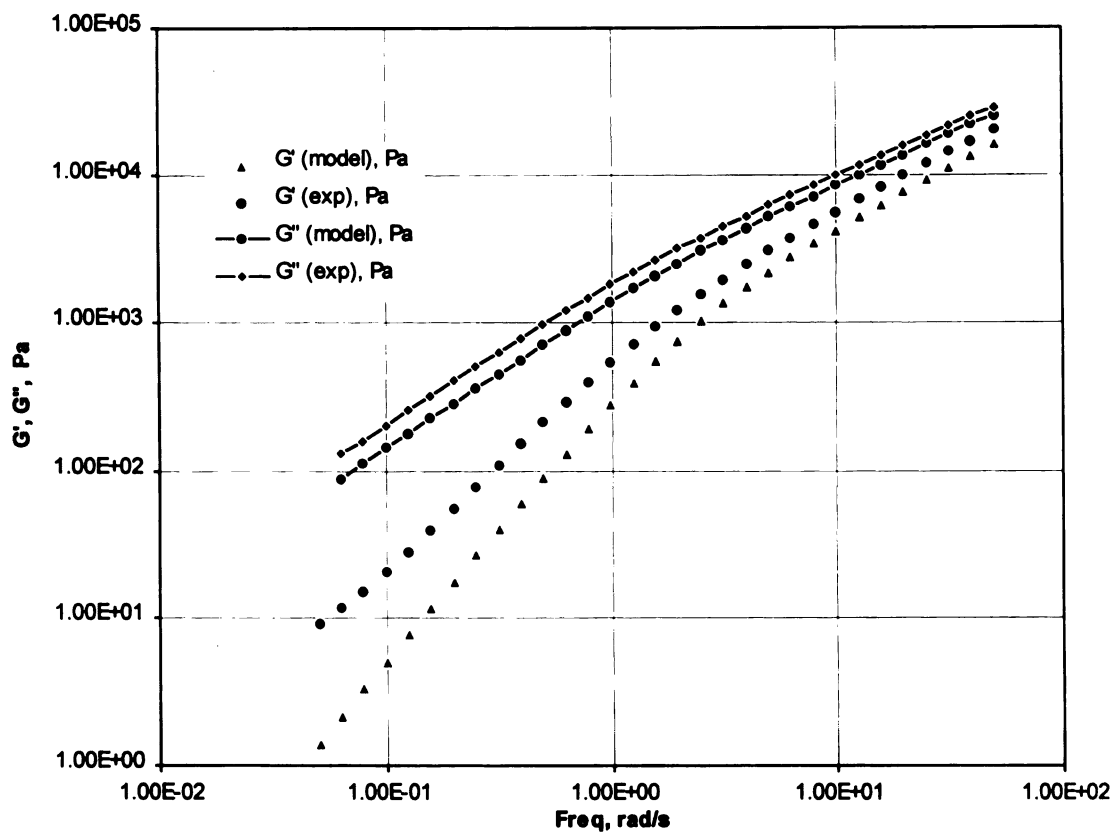
Figure 4.13: Comparison of the storage and loss moduli values obtained from the model with that obtained experimentally for B3/ 3001 (70/ 30) blend ($\Gamma^0 = 7$ mN/ m, R = 0.8 µm).
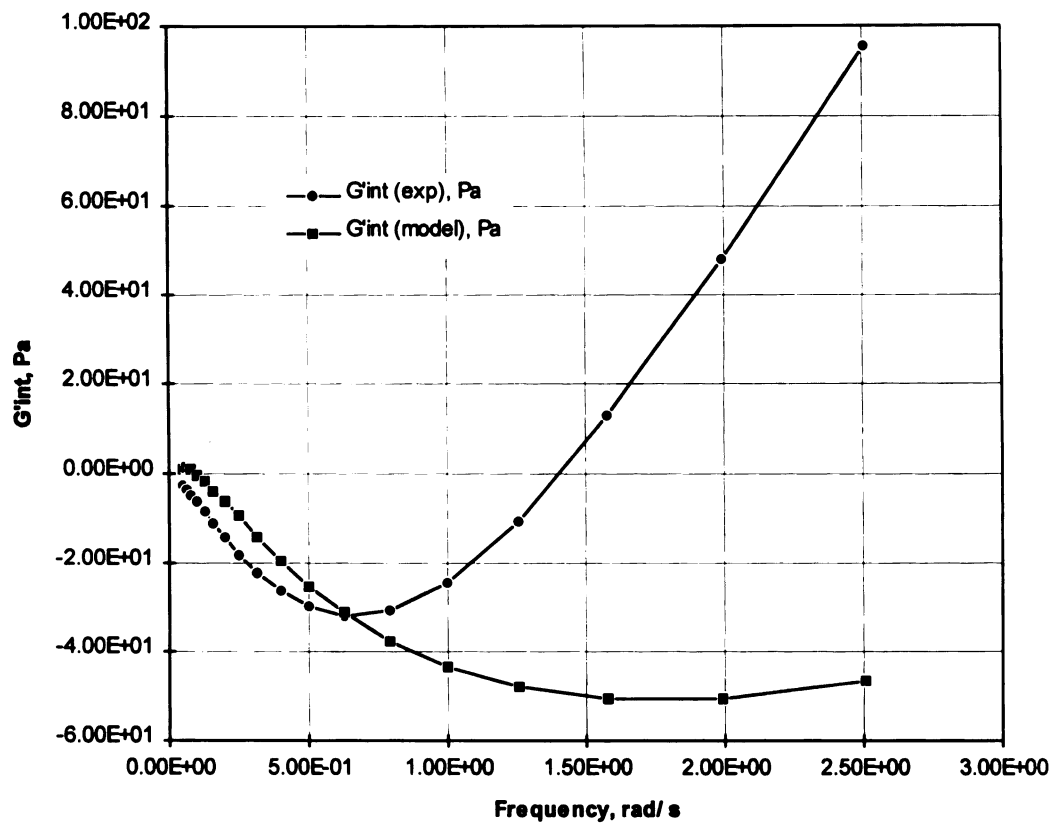
Figure 4.14: Comparison of the G'_{int} values obtained from the model with that obtained experimentally for B3/ 3001 (80/ 20) ($\Gamma^0 = 7$ mN/ m, R = 0.8 μm).
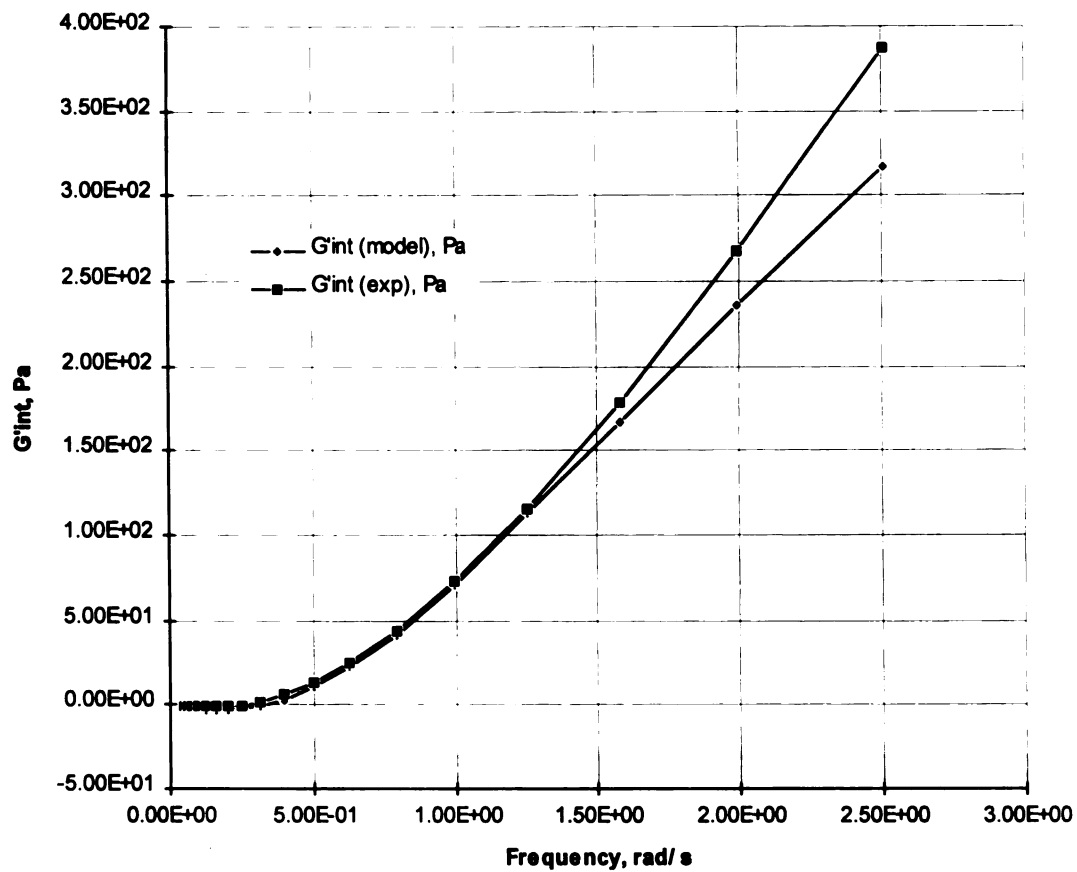
Figure 4.15: Comparison of the G'_{int} values obtained from the model with that obtained experimentally for B3/ 3002 (80/ 20) (Γ^0 = 7 mN/ m, R = 0.8 μm).
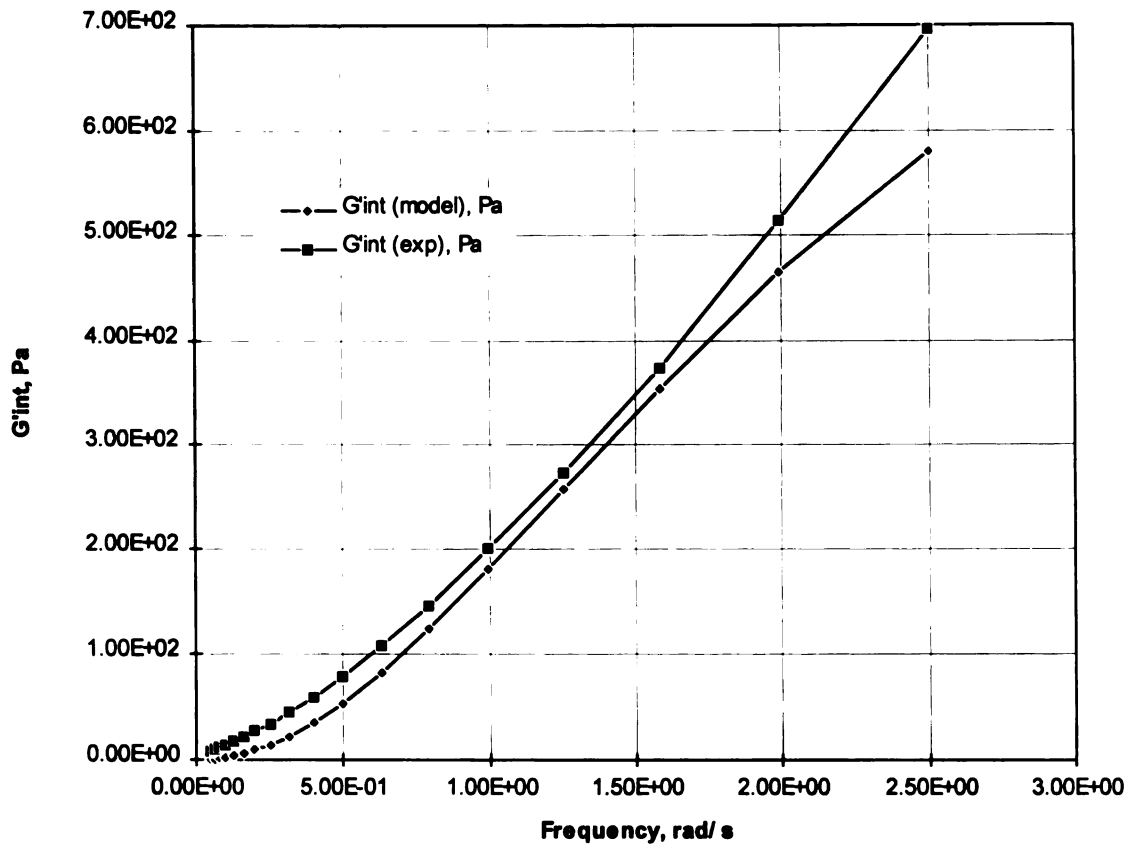
Figure 4.16: Comparison of the G'$_{int}$ values obtained from the model with that obtained experimentally for B3/ 3150 (80/ 20) (Γ^0 = 4 mN/ m, R = 1.5 μm).
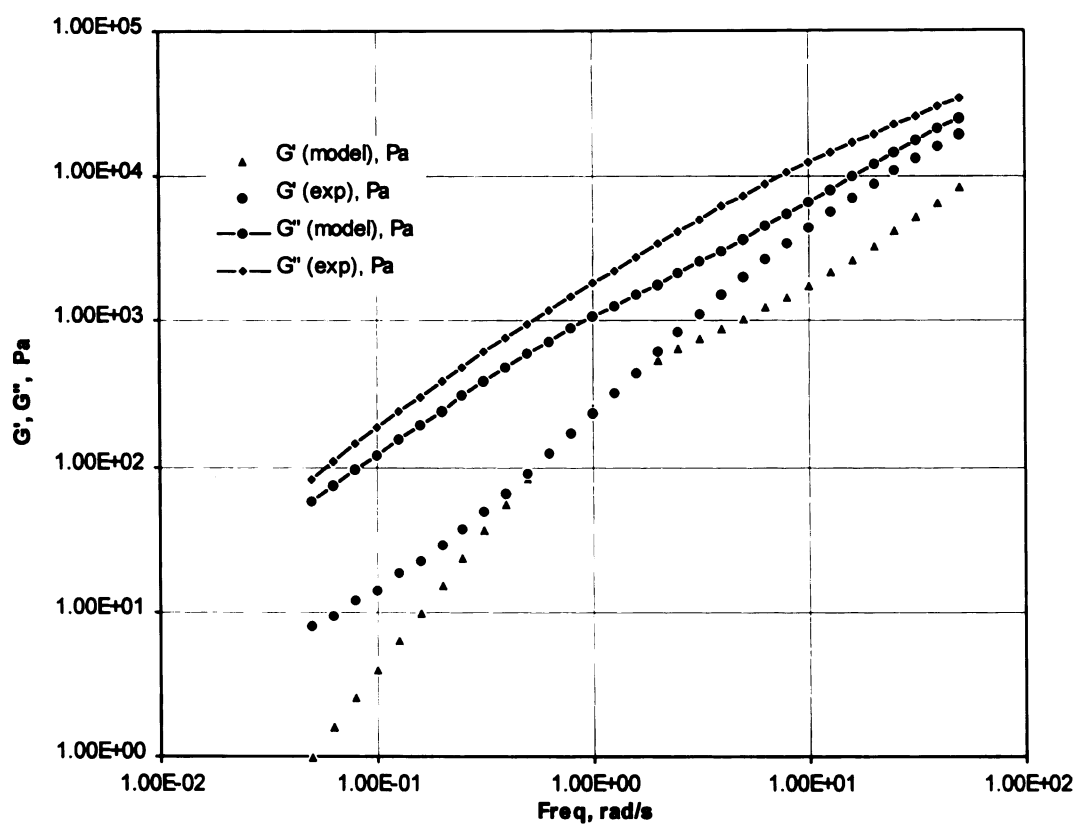
Figure 4.17: Comparison of the G' values obtained from the model with that obtained experimentally for B3/ 3150 (80/ 20) (Γ^0 = 4 mN/ m, R = 1.5 μm, β_0 = 0 mN/ m).
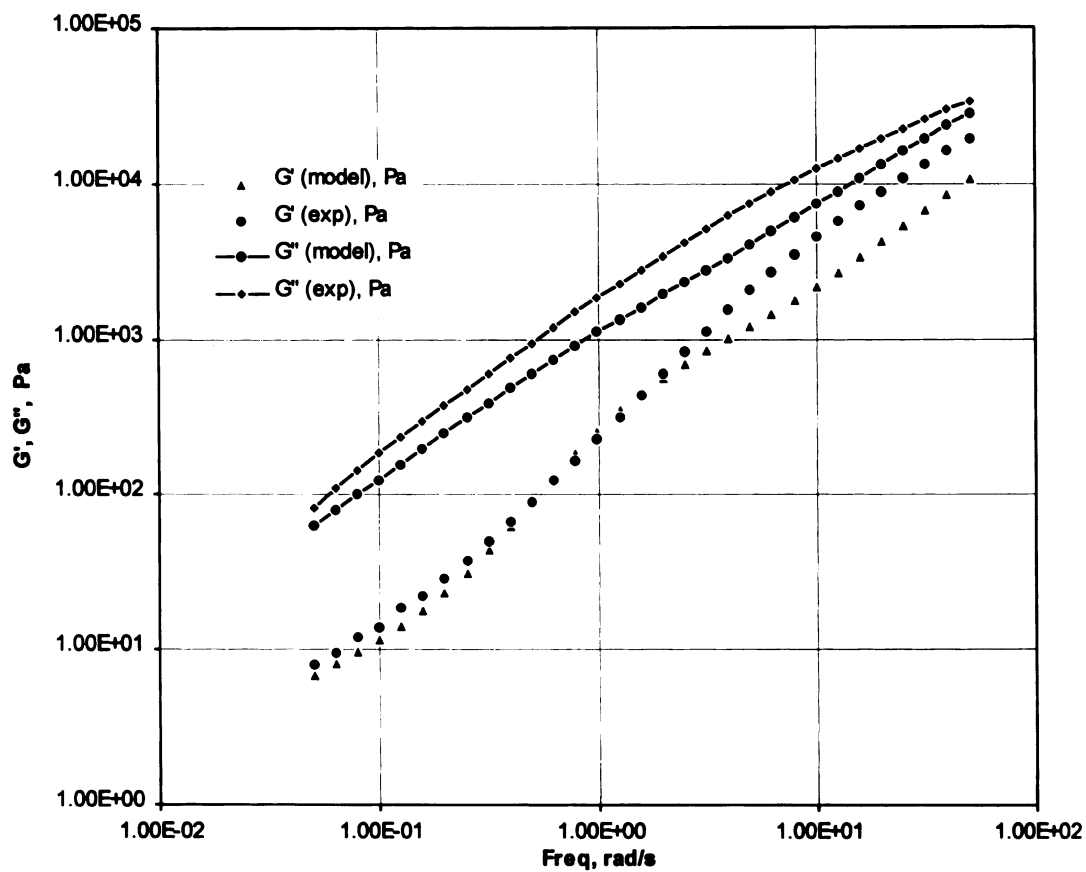
Figure 4.18: Comparison of the G' values obtained from the model with that obtained experimentally for B3/ 3150 (80/ 20) (Γ^0 = 4 mN/ m, R = 1.5 μm, β_0 = 0.1 mN/ m).
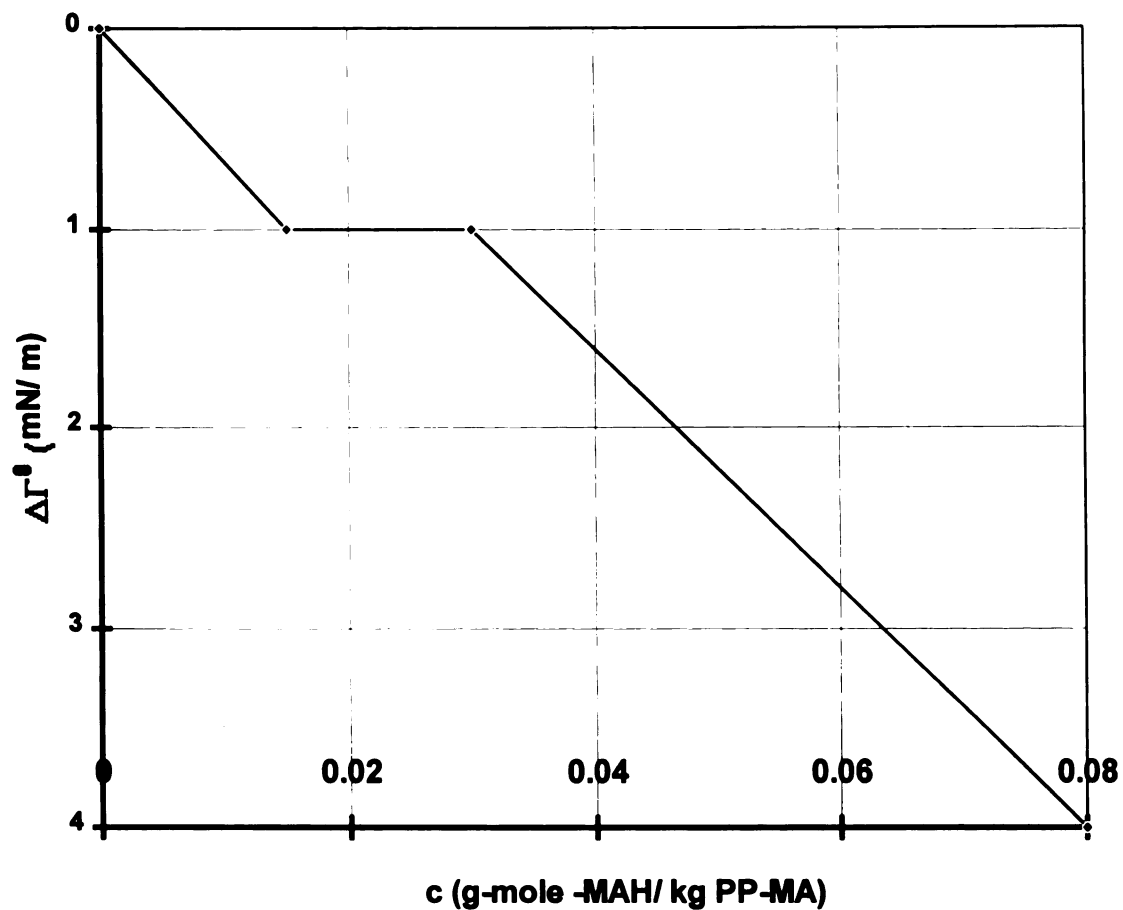
Figure 4.19: The plot showing the reduction of equilibrium interfacial tension with progressively increasing extent of maleation.

THE EFFECT OF COMPATIBILIZATION OF POLYPROPYLENE AND POLYSTYRNE WITH A DI-BLOCK COPOLYMER ON THE RHEOLOGY AND THE MORPHOLOGY OF THEIR BLENDS

Chapter 5

5.1 INTRODUCTION

Most polymers are thermodynamically immiscible. As a result, they phase separate on mixing. In order to circumvent the problem of phase separation, the component polymers are compatibilized. This is achieved by addition of an external compatibilizer or by carrying out an in-situ reaction between the complementary groups of the components. The resulting blend has a fine dispersion of the minor phase in the major phase. The particle size (distribution) of the blend depends on the processing conditions and the interfacial tension between the components. The governing parameter is the capillary number given in Equation 5.1. It is a dimensionless ratio of the shape deforming viscous forces and the shape retaining interfacial tension forces.

$$Ca = \frac{\overset{\bullet}{\gamma}\, \eta_m d}{\Gamma^0} \qquad (5.1)$$

According to this relation, a reduced equilibrium interfacial tension leads to a higher capillary number which promotes break-up of drops. In polymeric blends this is achieved by the addition of an external compatibilizer or the in-situ reaction which leads to a reduction in interfacial tension [Graebling et. al., 1993; Chapters 3 and 4]. The Chapters 3 and 4 show that besides a reduction in interfacial tension, interfacial reaction also leads to a fundamental change in the rheology of the blend. An additional elasticity

is imparted to the system. They attributed this effect to the product of the interfacial reaction. In this study, a similar effect has been observed with externally compatibilized systems. The compatibilizer is located at the interface or it phase separates as micelles. In either case, it brings about a change in rheology of the blend [Brahimi et. al., 1991; Germain et. al., 1994] .

Graebling et. al. [1993] carried out a study on rheology of polystyrene blended with PMMA compatibilized by an external agent. In the same study, results for PDMS blended with POE in presence of an external compatibilizer were presented. It was shown that equilibrium interfacial tension drops due to the presence of the compatibilizer. The study by Brahimi et. al. [1991] shows that a blend of polyethylene and polystyrene conforms to the rheological model of Palierne, but the compatibilized blend does not. However, the HIPS used in that study is itself a two phase system and can alter the behavior of the blend. The present study uses neat polystyrene to eliminate the effects which could have been caused by the dual phase nature of HIPS itself. Germain et. al. [1994] also observed a disagreement between the model and the experimentally obtained values. This discrepancy was attributed to the properties associated with the interface. In a non-compatibilized blend, the interface is 2-5 nm thick. However, as the study by Fayt et. al. [1986] shows, in a compatibilized blend, the compatibilizing agent occupies the interface and thickens it. The thickness of this interface was estimated around 10 nm. The properties associated with the material in this layer affect the rheology of the blend. In light of this, Germain et. al. [1994] attempted to explain the blend rheology on the basis of a core-shell model. They said that the properties of the dispersed phase play a

minimal role in the blend rheology. Since the compatibilizer is located at the interface, its properties will dominate those of the disperse phase. The results with this assumption improved, but there was still disagreement with the model behavior. The aim of this work is to systematically study the effect of progressive addition of the compatibilizing agent on the rheology of the blend. The main focus would be understand the changes brought about in the rheology of the blend by the compatibilization and determine the reason for those changes. In order to do this, the role of the interface and the equilibrium interfacial tension will be investigated. The model of Palierne [1990] will be used to fit the observed rheology of the blend with appropriate values of the equilibrium interfacial tension. Equations 5.2 and 5.3 describe the model.

$$G^*(\omega) = G_m^*(\omega) \frac{1 + 3\sum_i \phi_i H_i(\omega)}{1 - 2\sum_i \phi_i H_i(\omega)} \qquad (5.2)$$

where,

$$H_i(\omega) = \frac{(4\Gamma^0 / R_i)(2G_m^* + 5G_d^*) + (G_d^* - G_m^*)(16G_m^* + 19G_d^*)}{(40\Gamma^0 / R_i)(G_m^* + G_d^*) + (2G_d^* + 3G_m^*)(16G_m^* + 19G_d^*)} \qquad (5.3)$$

5.2 EXPERIMENTAL

5.2.1 Materials

Polypropylene (Profax 6523 from Montell Polyolefins) was used as the matrix phase. It was blended with polystyrene (Huntsman Polycom) which was the disperse phase. A di-block copolymer -S-EP- (Kraton G1702 from Shell Chemicals) was used as the compatibilizing agent. The propylene units on the di-block are physically compatible with the polypropylene and styrene units are compatible with the polystyrene. The molecular weights of the respective components have been shown in Table 5.1.

Blends were prepared with 10 wt. % and 20 wt. % of the polystyrene as the dispersed phase and 0 wt.%, 2 wt.%, 4 wt.% and 6 wt.% compatibilizing agent. Blending was carried out in a ZSK-30 twin screw extruder at a temperature of 180 °C for all the zones. The extrudate strands were quenched in a water bath and pelletized. These were then air dried. The density used for calculations was 0.93 g/ cc for polypropylene and the compatibilizer and 1.11 g/ cc for polystyrene [Immergut et. al., 1989]

5.2.2 Rheological

Rheological characterization was carried out on an RMS-800 rheometer (Rheometrics Scientific, Inc., New Jersey, USA) using a 50 mm parallel plate arrangement. The disks were prepared by compression molding the pellets in a Carver press under a force of 6 tons and 180 °C. The instrument oven was purged with dry nitrogen during measurements to avoid degradation. A frequency range of 0.05-50 rad/s

and strains of 10-15% were applied during the measurements. A strain sweep was carried out to determine the viscoelastic limits on the strain.

5.2.3 Morphological

The samples for morphological examination were prepared by placing the pre-notched disks in the RMS 800 oven, heating them to 180 °C and placing them directly in liquid nitrogen. Those were then fractured under liquid nitrogen. These samples were then examined in a Phillips Electroscan 2020 environmental scanning microscope. Water vapor at a pressure of 2-3 Torr was used as the imaging gas. The measurements were made directly from the micrographs and the volume average radii were calculated.

5.3 RESULTS AND DISCUSSION

5.3.1 Blend Morphology

Figures 1a and 1b show the micrographs for the non-compatibilized blends while Figures 1c thru 1i show the micrographs for the compatibilized blends. In all cases, the particles are spherical. The volume average radii of the various dispersed phase particles are shown in Table 5.2. The particle size increases in case of non-compatibilized blends as the polystyrene content is raised from 10 wt.% to 20 wt.%. This effect is due to coalescence. In non-compatibilized blends the interface is highly mobile and during blending the probability of the droplets coming in contact with each other and coalescing is high. On compatibilization, this effect is reduced as can be observed from the data in Table 5.2. This behavior can be attributed to the reduced mobility of the interface in presence of the compatibilizer (at the interface) [Macosko et. al., 1996]. A reduced mobility leads to a decrease in the probability of coalescence [Janssen et. al., 1993]. Besides, another effect of the presence of the block copolymer at the interface is to reduce the interfacial tension. This in turn, imparts stability to the interface and reduces the drive to coalesce.

5.3.2 Rheological Observations

Figures 5.2a and 5.2b show a comparison of the storage and loss moduli of the components of the blend respectively. It can be seen that the storage modulus of the polystyrene (the disperse phase) is higher than that of the polypropylene (the matrix

phase). As shown in Table 5.1, the viscosity of polystyrene is about 4.5 times the

viscosity of the polypropylene. This ensures that the dispersed phase particles are

spherical. The storage modulus of the compatibilizer is higher in comparison to the

matrix and the dispersed phase. Also, as can be observed from Figure 5.2a, the curve is

relatively flat over the frequency range under investigation while those for polypropylene

and polystyrene rise steadily with increasing frequency. It appears that the compatibilizer

is in the rubbery plateau region and has a high degree of elasticity compared to

polystyrene and polypropylene, in the frequency range under investigation.

Using the experimental data, the first effort will be to gather the main changes

brought about by the addition of the compatibilizer to the components. Figure 5.3 is a

comparison of the storage moduli of the compatibilized and non-compatibilized 90/ 10

blends. It is observed that the storage modulus of the PP/ PS/ 1702 (90/ 10/ 2) falls

below PP/ PS (90/ 10) and then rises for the 90/ 10/ 4 and 90/ 10/ 6 blends. Also, the

difference between 90/ 10/ 4 and 90/ 10/ 6 is small. In case of PP/ PS (80/ 20) blend, 80/

20/ 2 rises, then drop occurs for 80/ 20/ 4 and then rises again for 80/ 20/ 6 curve. Refer

to Figure 5.4. Brahimi et. al. [1991] also observed a trend in their study on

compatibilization of HDPE with HIPS depending on the compatibilizer they used. For

the tapered block copolymer, the storage moduli fell as the extent of compatibilizer added

was increased while for a straight block copolymer, the storage moduli decreases and

then increases. Asthana and Jayaraman on the other hand have observed a distinct trend

in their studies on the compatibilization of nylon 6 with polypropylene by in-situ reaction

[Chapter 3 and Chapter 4]. The observations of Chapter 3 and Chapter 4 show that as the

extent of reaction and the volume fraction increased, the storage moduli also increased progressively. What is the reason for the drop in the modulus value in externally compatibilized blend, while in in-situ reactively compatibilized blend the elasticity is enhanced progressively with the extent of reaction? This can be understood if the physical events occurring at the interface are analyzed.

Figure 5.5 is a comparison of the storage moduli of the PP/ PS (90/ 10) blend with its components. The blend curve falls between those of the components. But, a comparison in case of 90/ 10/ 2 shows that the blend curve matches the curve for polypropylene. Refer to Figure 5.6. The storage modulus has fallen due to compatibilization. On increasing the concentration to 90/ 10/ 4, the blend curve rises again and actually crosses the polystyrene at higher frequencies (Figure 5.7). Similar observation was made for 90/ 10/ 6 as shown in Figure 5.8. A similar analysis was carried out for 80/ 20 blends. Results are shown in Figures 5.9 thru 5.12. It is seen that in the non compatibilized blend itself the blend curve crosses over the polystyrene curve. This cross over behavior was observed in all the compatibilized 80/ 20 blends. The data presented until now shows that there are two effects occurring simultaneously in the blends. The effect of the polystyrene volume fraction and the effect of the concentration of the compatibilizer. The next section discusses the events occurring at the interface and explains the observations made above on the basis of these events.

5.3.3 Physical Events at the interface and the value of interfacial tension

An important effect of adding the compatibilizer to the blend is to change the nature of the interface between the dispersed and the continuous phase. The interface goes from being 'bare' to 'occupied'. The blocks of the compatibilizer hook up with the individual components leading to compatibilization. It has been shown that if the modulus of the compatibilizer is higher than that of the diffusing component (polypropylene in this case), the net result is a lowering of the overall modulus. Now, the diffusion of the component continues until the interface is saturated with the linkages between the compatibilizer and the diffusing species. After this, further addition of the compatibilizer leads to an enhancement in the elasticity of the blend. In the results of Brahimi et. al. [1993], the interface with the tapered block copolymer did not get saturated with the amount of compatibilzer added. This led to a continuous fall in the storage modulus curve. But, for the straight di-block copolymer it did get saturated after 1% compatibilizer was added which led to an increase after the initial decrease.

Similar observations have been made in this study also. The storage modulus curve shifts down for the 90/ 10/ 2 blend compared to the 90/ 10 blend but then the curves move up. The reason is that the interface possible is saturated by the diffusing PP chains into the -[S- EP] - copolymer. Further addition of compatibilizer does not promote diffusion of the PP chains into the interface. The copolymer merely sits in the interface, leading to an increased storage modulus. Now, the compatibilizer in the

interface has a surfactant effect also. This leads to reduced values of equilibrium

interfacial tension.

For non compatibilized polypropylene/ polystyrene system a value of 5 mN/ m

has been obtained experimentally [Sundraraj and Macosko, 1993]. This was checked by

using the dispersive and polar component of the components as well as the

thermodynamic theory of Helfand and Tagami [1971]. Table 5.3 shows the dispersive

and polar components for polypropylene and polystyrene [Paul, 1978]. Equation 5.4 was

used for determining the value of interfacial tension.

$$\Gamma^0 = \Gamma_1^0 + \Gamma_2^0 - \frac{4\Gamma_1^d \Gamma_2^d}{\Gamma_1^d + \Gamma_2^d} - \frac{4\Gamma_1^P \Gamma_2^P}{\Gamma_1^P + \Gamma_2^P} \qquad (5.4)$$

This gives a value of 6 mN/ m. The estimates from the thermodynamic theory using

Equation 5.5 lead to a value of 2.7 mN/ m. The values of the parameters used in this

theory are shown in Table 5.4 [Rudin; Immergut, 1989]. Thus, the experimentally

measured value of 5 mN/ m is reasonable.

$$\Gamma^0 = k_B T (\rho_0 \chi)^{1/2} \left[\frac{\beta_A + \beta_B}{2} + \frac{1}{6} \frac{(\beta_A - \beta_B)^2}{\beta_A + \beta_B} \right] \qquad (5.5)$$

The parameter χ is estimated from the Hilderbrand solubility parameters. The relation is

$$\chi = \frac{1}{\rho_0 k_B T} (\delta_A - \delta_B)^2 \qquad (5.6)$$

To estimate the interfacial tension values in this study, the storage moduli curves were used. The storage modulus is the most sensitive to the values of the interfacial tension [Graebling et. al., 1993]. Figure 5.13 shows a comparison of the experimentally obtained storage moduli curve with that obtained from the model of Equation 5.2 and 5.3 for non compatibilized PP/ PS (90/ 10) blend for an equilibrium interfacial tension value of 5 mN/ m. The agreement is good. For the non-compatibilized PP/ PS (80/ 20) system also the agreement was reasonable for a value of 5 mN/ m for the equilibrium interfacial tension, as shown in Figure 5.14. When a similar calculation was done for the PP/ PS / 1702 (90/ 10/ 2) blend, once again a value of 1 mN/ m was found to give a good estimate as shown in Figure 5.15. That is, the interfacial tension has reduced from 5 mN/ m to 1 mN/ m while the particle size has fallen from 1.1 μm to 0.9 μm. For PP/ PS / 1702 (90/ 10/ 4) blend however, there was disagreement over the entire frequency range even for an interfacial tension values as low as 1 mN/ m, as shown in Figure 5.16. This observation is similar to that of Brahimi et. al. [1991]. This behavior was noted in all the cases except for the PP/ PS/ 1702 (80/ 20/ 4) blend. Thus, how does one estimate the value of the interfacial tension in these blends ?

In order to estimate the interfacial tension values from the storage moduli data, one has to focus on the low frequency plateau as suggested by Graebling et. al. [1993]. In the observations of the present system, there is no clear cut evidence of such a plateau. In order to delineate the low frequency transitions, it became crucial to abstract the

contributions due to the interface alone. To do this, an empirical relation shown in Equation 5.7 was used. It subtracts the weighted average of the components from the storage moduli of the blend.

$$G'_{int} = G'_{blend} - [\phi G'_d + (1 - \phi)G'_m]$$ (5.7)

This was used for the storage moduli values obtained experimentally as well as from the model. In order to determine the transition frequency, tangents were drawn on the G'_{int} obtained experimentally. An example is shown in Figure 5.17 for PP/ PS/ 1702 (90/ 10/ 6) blend. Using this frequency and relation shown in Equation 5.8 [Graebling et. al., 1993] the values of the equilibrium interfacial tension were obtained.

$$\lambda_D = \left(\frac{R\eta_m}{4\Gamma^0}\right)\left[\frac{(19k + 16)(2k + 3 - 2\phi(k - 1))}{10(k + 1) - 2\phi(5k + 2)}\right]$$ (5.8)

It is seen that the values do not follow a trend. Moreover, even these values did not give a good agreement between the model and the experimentally obtained storage moduli curves. The addition of the compatibilizing agent has changed the rheological behavior such that it fundamentally differs from the non-compatibilized blends. This change can be attributed to two factors:

• The changes due to the interfacial product

• The changes due to the formation of micelles

5.3.4 The issue of extent of coverage

Assuming all the block copolymer to be at the interface the interface area

occupied by the copolymer chains is given by Equation 5.9. It is similar to that defined in

directly reacted blends between nylon 6 and maleated polypropylene.

$$\Sigma = \frac{\text{interface area / volume}}{\text{copolymer chains / volume}} = \frac{M_c S_{sp}}{N_A \rho_c \phi_c} \qquad (5.9)$$

In Equation 5.9, S_{sp} is the specific interfacial area (m^2/ m^3) which is given by Equation

5.10.

$$S_{sp} = \frac{6\phi_d}{D} \qquad (5.10)$$

Table 5.5 shows the values calculated for Σ for the different blends. For a given

weight fraction of the dispersed phase, as the amount of copolymer is increased the value

of Σ falls as it should as the number of di block grafts formed in the interface also

increases. However, the values of equilibrium interfacial tension do not reduce

correspondingly. This has been shown in Figure 5.18. The equilibrium interfacial

tension falls with the addition of a small amount of the compatibilizing agent. Further

addition does not cause a decrease in the equilibrium interfacial tension. As the

observations show, after a critical point, the effect of adding the block copolymer is to

enhance the elasticity. This observation is similar to that in the directly compatibilized

blends. But, the fundamental difference is that this increase is not monotonic. In the

earlier stages of the addition in fact there is a reduction in the elasticity. This effect is

attributed to the dissolution of the matrix in the copolymer. Moreover, as observed from

Figure 5.2a , the storage moduli of the compatibilizer is much higher than those of the components and hence the larger relaxation times as compared to those of the components. That is, the relaxation effects due to the interface have been masked. In addition to this, the ratio of the viscosities of the disperse phase to the matrix is around 3.5, and the ratio of the relaxation times is 1.5. The analysis by Graebling and co-workers [1993] shows that as the viscosity ratio increases, the position of the secondary plateau also falls to lower values of the storage moduli. Also, the frequency of onset of this secondary plateau also is reduced. A combination of this factor along with the high elasticity of the compatibilizer have not allowed the appearance of the secondary plateau in the observable frequency range. As shown in a related work in Chapters 3 and 4, to capture the secondary plateau, it is essential that the materials be chosen such that their relaxation times are very low. This permits the unmasking of the relaxation due to the interface and brings it in the observable frequency range.

5.4 CONCLUSION

This study has investigated the role of progressive addition of an -S-EP- di block copolymer to a blend of PP and PS on its rheology, with focus on the nature of the interface and the value of interfacial tension. The data show that the equilibrium interfacial tension is reduced from a value of 5 mN/ m to 1 mN/ m. But, in addition to this reduction, an enhanced elasticity is imparted to the system due to the addition of the compatibilizer. This elasticity is due to the two factors. Firstly, the compatibilizer which is located at the interface and secondly the compatibilizer in the form of micelles. This

observation is similar to that observed in reactively compatibilized nylon 6 and maleated polypropylene the results of which are shown in Chapters 3 and 4 respectively. However, in directly reacted blends the increase was monotonic which is not the case in externally compatibilized blends.

Table 5.1: The properties of the components used in the study.

	M_n (kg/ kg-mole)	η_0 (Pa-s)	λ_r (s)
Polypropylene	54000	3700	3
Polystyrene	220000	14000	4.5

Table 5.2: The volume average radii of the disperse phase in the various blends.

	R_v (μm)	$S_{sp} \times 10^{-5}$ (m^2/ m^3)
PP/ PS (90/ 10)	1.12	0
PP/ PS/ 1702 (90/ 10/ 2)	0.9	2.7
PP/ PS/ 1702 (90/ 10/ 4)	0.8	3.0
PP/ PS/ 1702 (90/ 10/ 6)	0.6	3.7
PP/ PS (80/ 20)	1.86	0
PP/ PS/ 1702 (80/ 20/ 2)	1.0	5.0
PP/ PS/ 1702 (80/ 20/ 4)	1.0	4.9
PP/ PS/ 1702 (80/ 20/ 6)	0.8	6.1

Table 5.3: The polar and dispersive component of polystyrene and polypropylene [Paul, 1978].

	Γ^0 (mN/ m)	Γ^0_P (mN/ m)	Γ^0_D (mN/ m)
Polypropylene	21.0	0	21.0
Polystyrene	32.1	5.4	26.7

Table 5.4: The values of the parameters used in to estimate the interfacial tension using the thermodynamic theory [Rudin 1993; Immergut et. al., 1989]

	δ_i (cal/ cc)$^{1/2}$	$(r_0/ M^{1/2})_i$ nm)	m_i (g/ mole)	density (g/ cc)
Polypropylene	8.3	835 x 10^{-4}	42	0.93
Polystyrene	9.0	670 x 10^{-4}	105	1.11

Table 5.5: The variation of the extent of coverage and the equilibrium interfacial tension with progressive addition of the compatibilizing agent.

	c (g-mole SEP/ kg-PS)	Σ x 10^{14} (m^2/ no. of copolymer)	Γ^0 (mN/ m)
PP/ PS (90/ 10)	0	0	5
PP/ PS (90/ 10/ 2)	0.001	0.35	1
PP/ PS (90/ 10/ 4)	0.003	0.18	1
PP/ PS (90/ 10/ 6)	0.004	0.15	1
PP/ PS (80/ 20)	0	0	5
PP/ PS (80/ 20/ 2)	0.0007	0.62	1
PP/ PS (80/ 20/ 4)	0.001	0.31	1
PP/ PS (80/ 20/ 6)	0.002	0.24	1

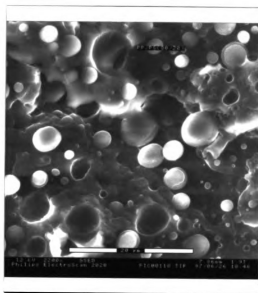Figure 5.1a: Micrograph showing the morphology of PP/ PS (90/ 10).

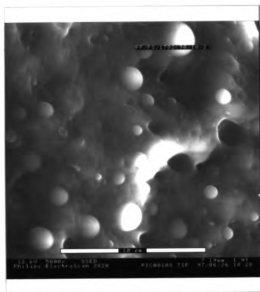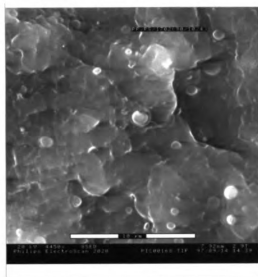Figure 5.1b: Micrograph showing the morphology of PP/ PS (80/ 20).

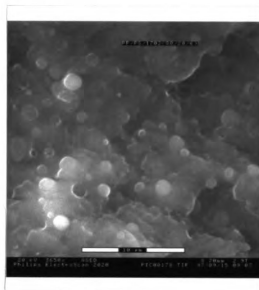Figure 5.1c: Micrograph showing the morphology of PP/ PS/ 1702 (90/ 10/ 2).

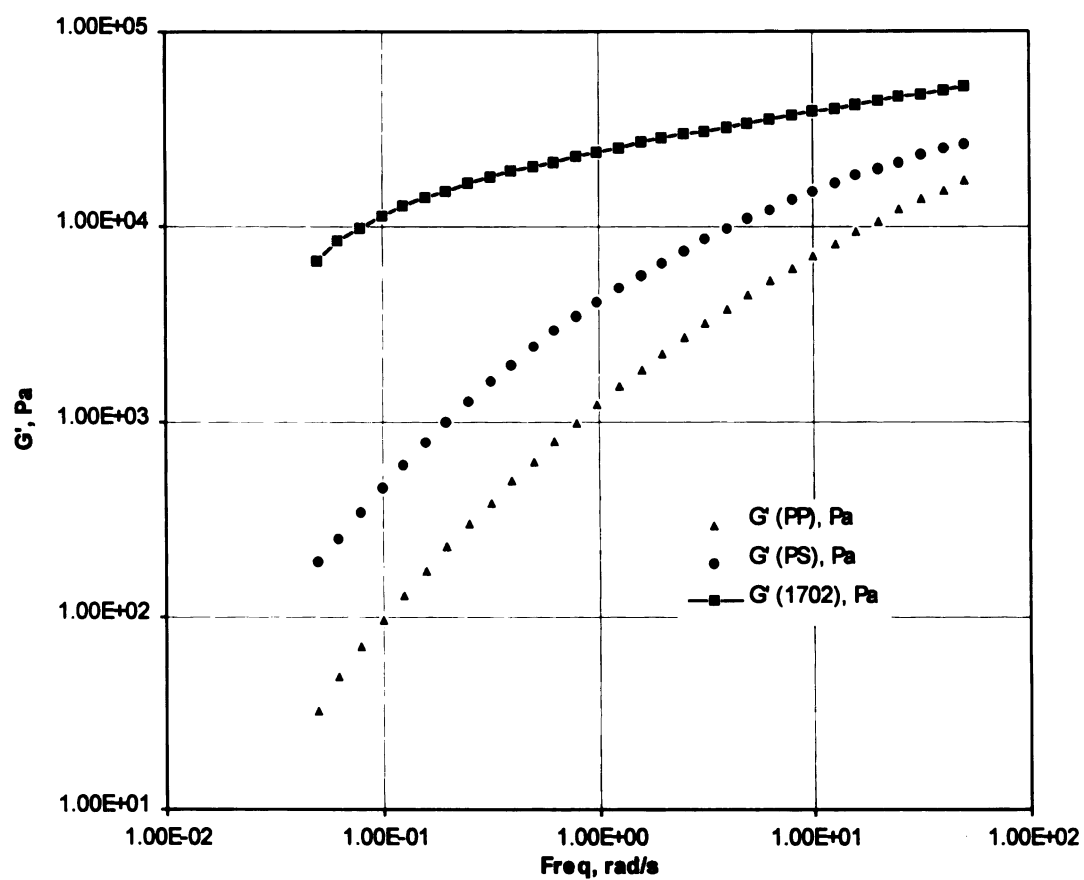Figure 5.1d: Micrograph showing the morphology of PP/ PS/ 1702 (90/ 10/ 4).

Figure 5.1e: Micrograph showing the morphology of PP/ PS/ 1702 (90/ 10/ 6).

Figure 5.1f: Micrograph showing the morphology of PP/ PS/ 1702 (80/ 20/ 2).

Figure 5.1g: Micrograph showing the morphology of PP/ PS/ 1702 (80/ 20/ 4).

Figure 5.1h: Micrograph showing the morphology of PP/ PS/ 1702 (80/ 20/ 6).

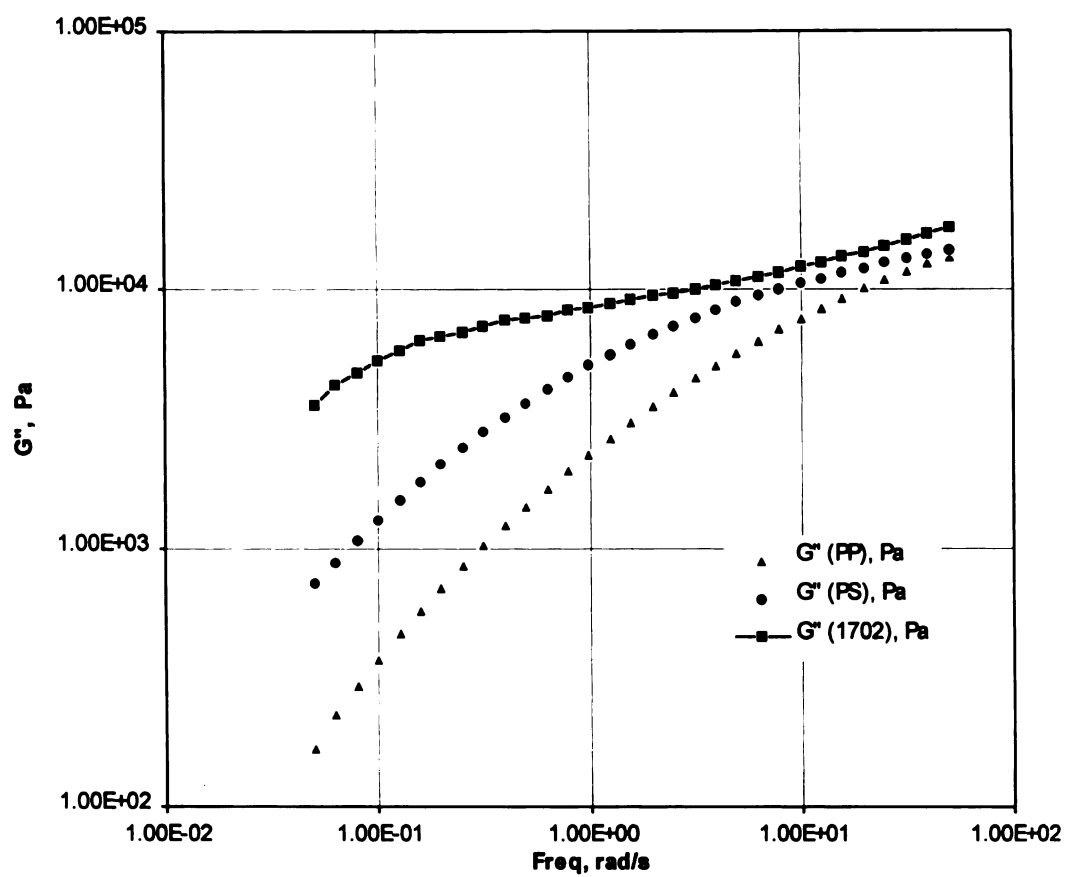Figure 5.2a: Comparison of the storage moduli of the components of the blend.

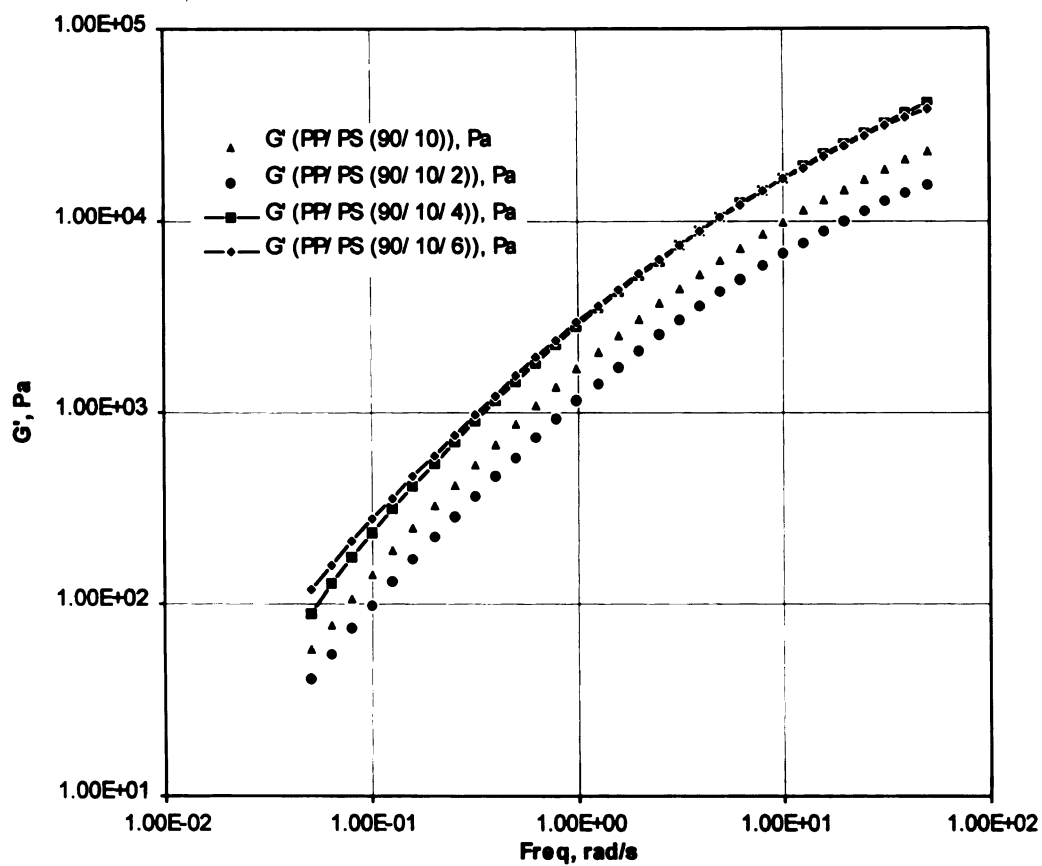Figure 5.2b: Comparison of the loss moduli of the components of the blend.

Figure 5.3: Comparison of the storage moduli of the 90/ 10 blends with different amounts of the compatibilizing agent.
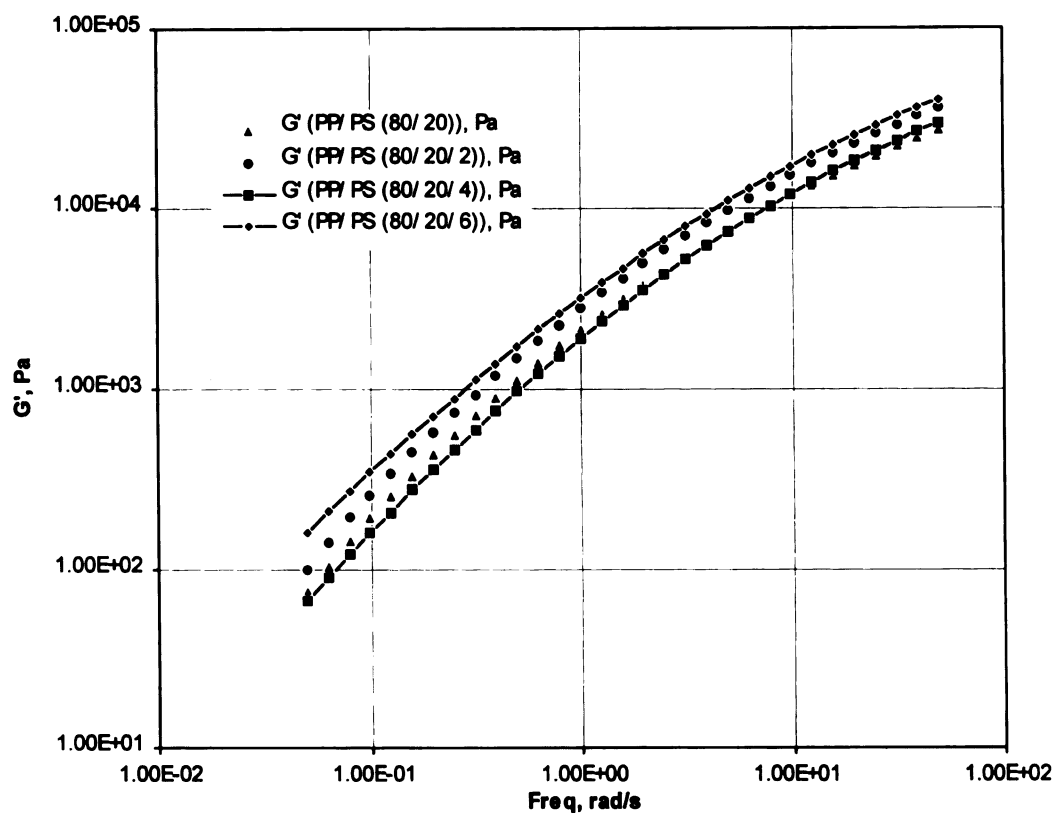
Figure 5.4: Comparison of the storage moduli of the 80/ 20 blends with different amounts of the compatibilizing agent
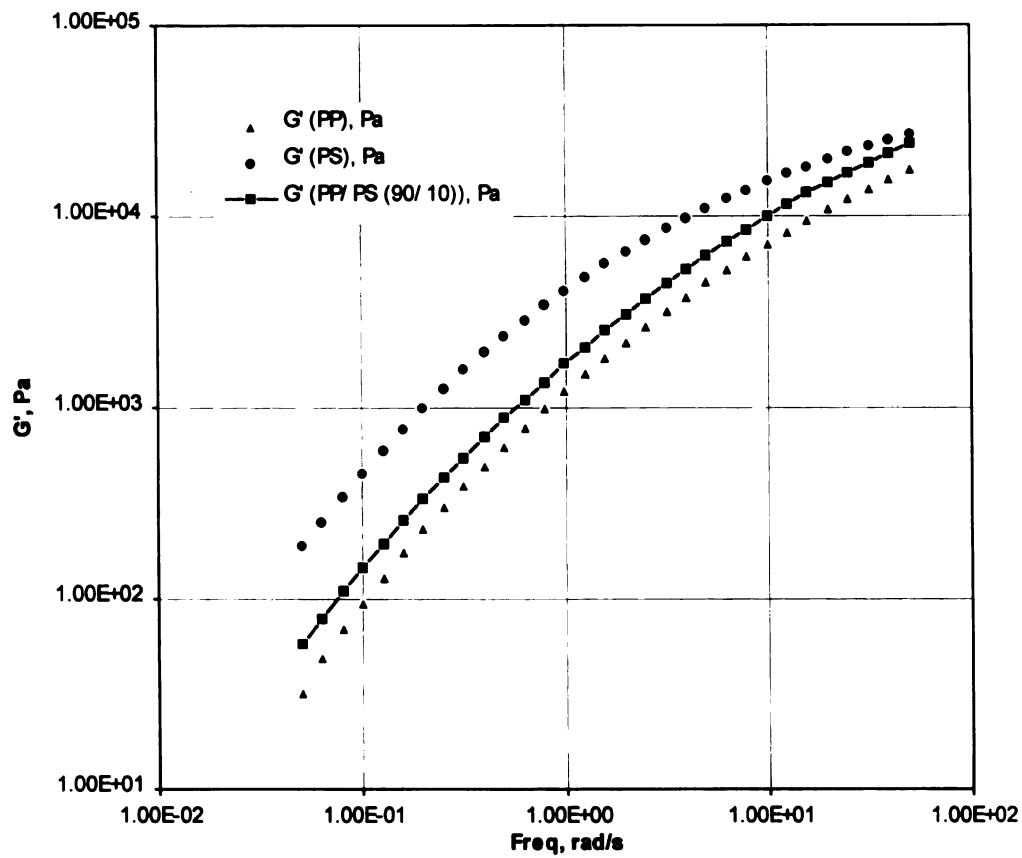
Figure 5.5: Comparison of the storage moduli of the PP/ PS (90/ 10) blend with its components.
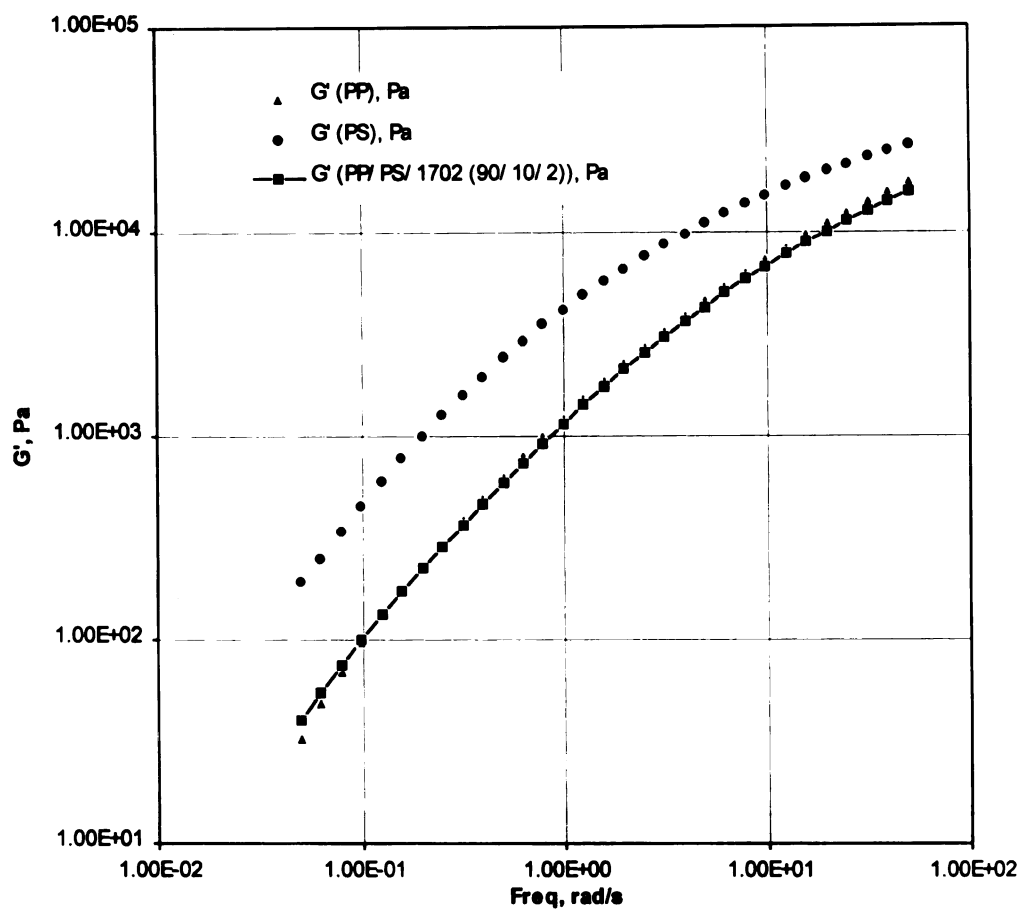
Figure 5.6: Comparison of the storage moduli of the PP/ PS/ 1702 (90/ 10/ 2) blend with its components.

Figure 5.7: Comparison of the storage moduli of the PP/ PS/ 1702 (90/ 10/ 4) blend with its components.

Figure 5.8: Comparison of the storage moduli of the PP/ PS/ 1702 (90/ 10/ 6) blend with its components.

Figure 5.9: Comparison of the storage moduli of the PP/ PS (80/ 20) blend with its components.

Figure 5.10: Comparison of the storage moduli of the PP/ PS/ 1702 (80/ 20/ 2) blend with its components.
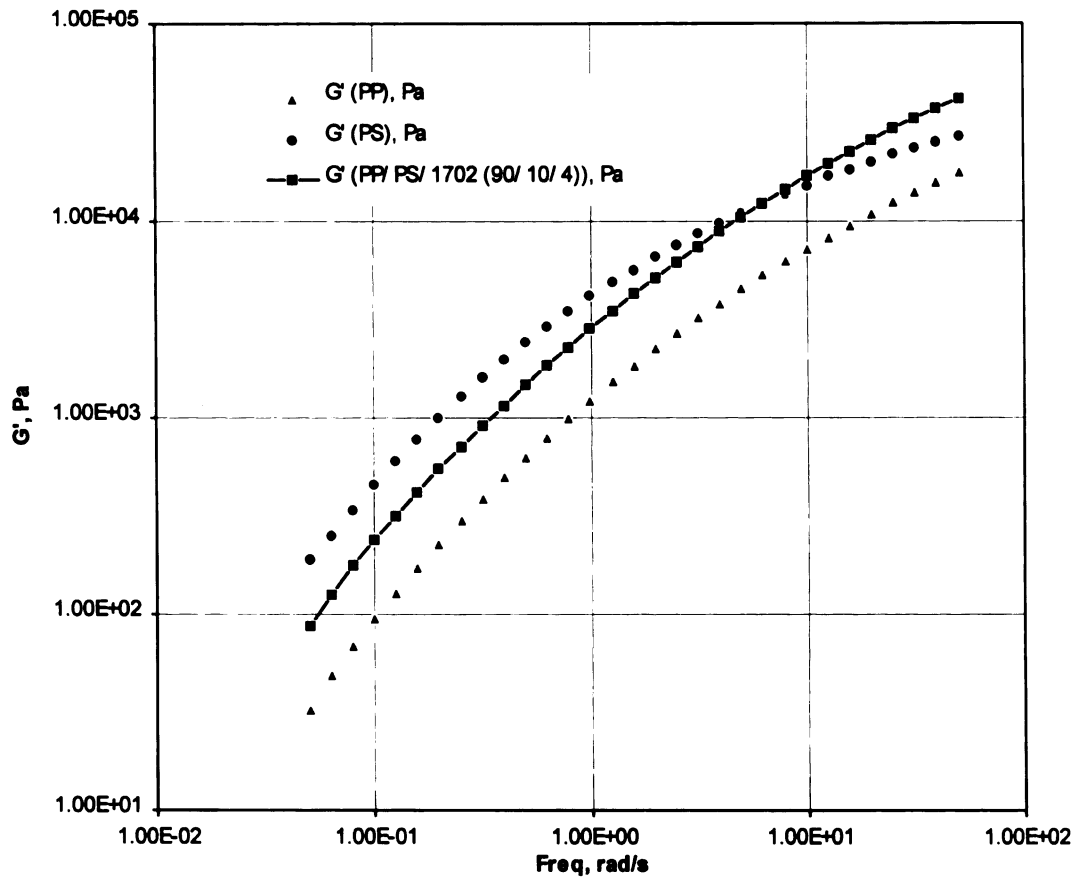
Figure 5.11: Comparison of the storage moduli of the PP/ PS/ 1702 (80/ 20/ 4) blend with its components.
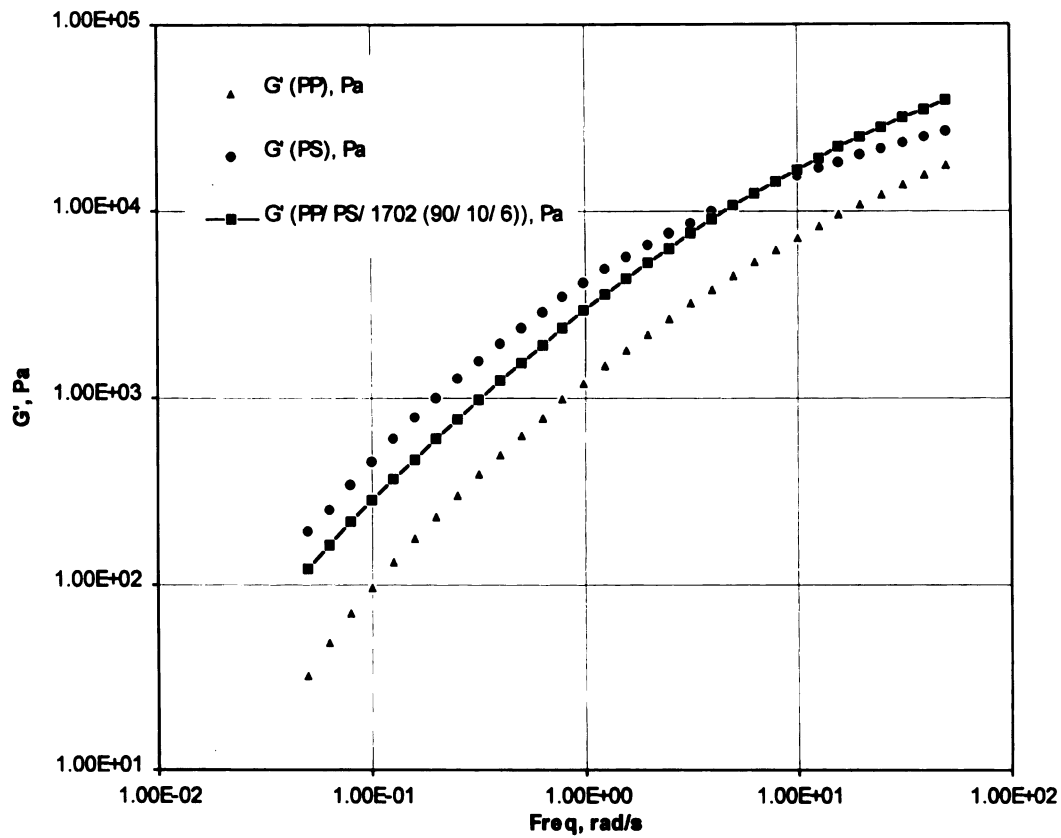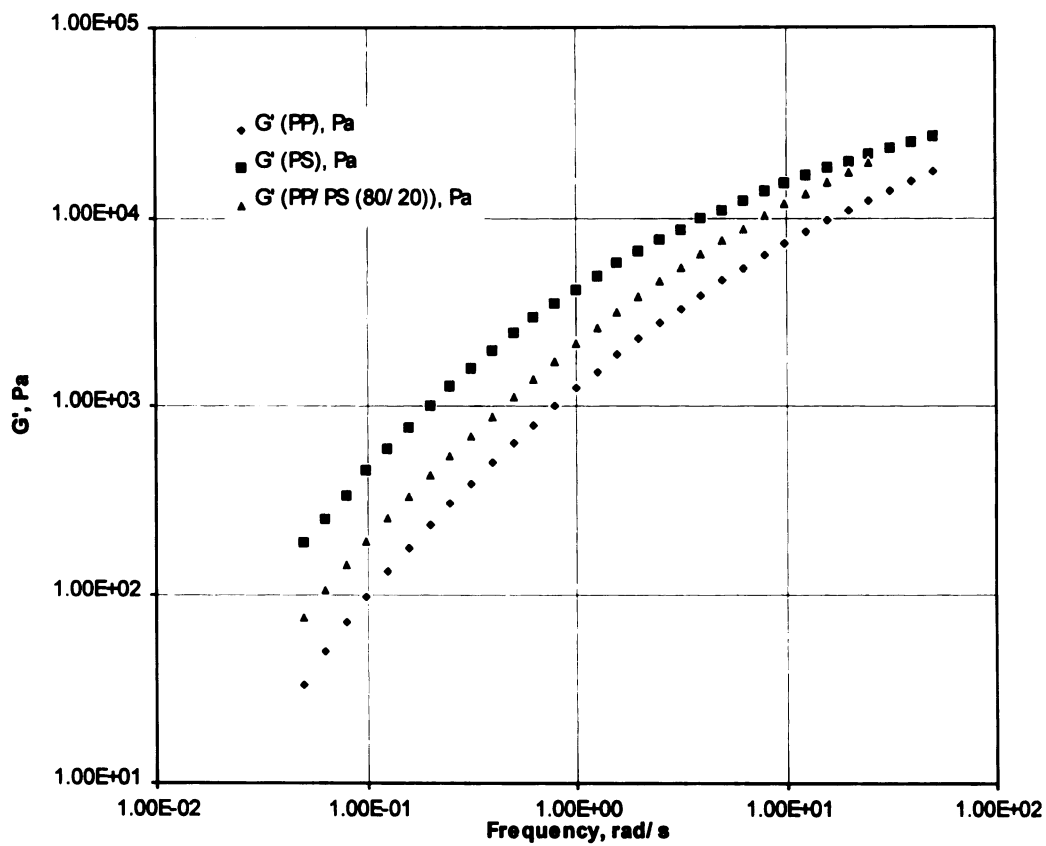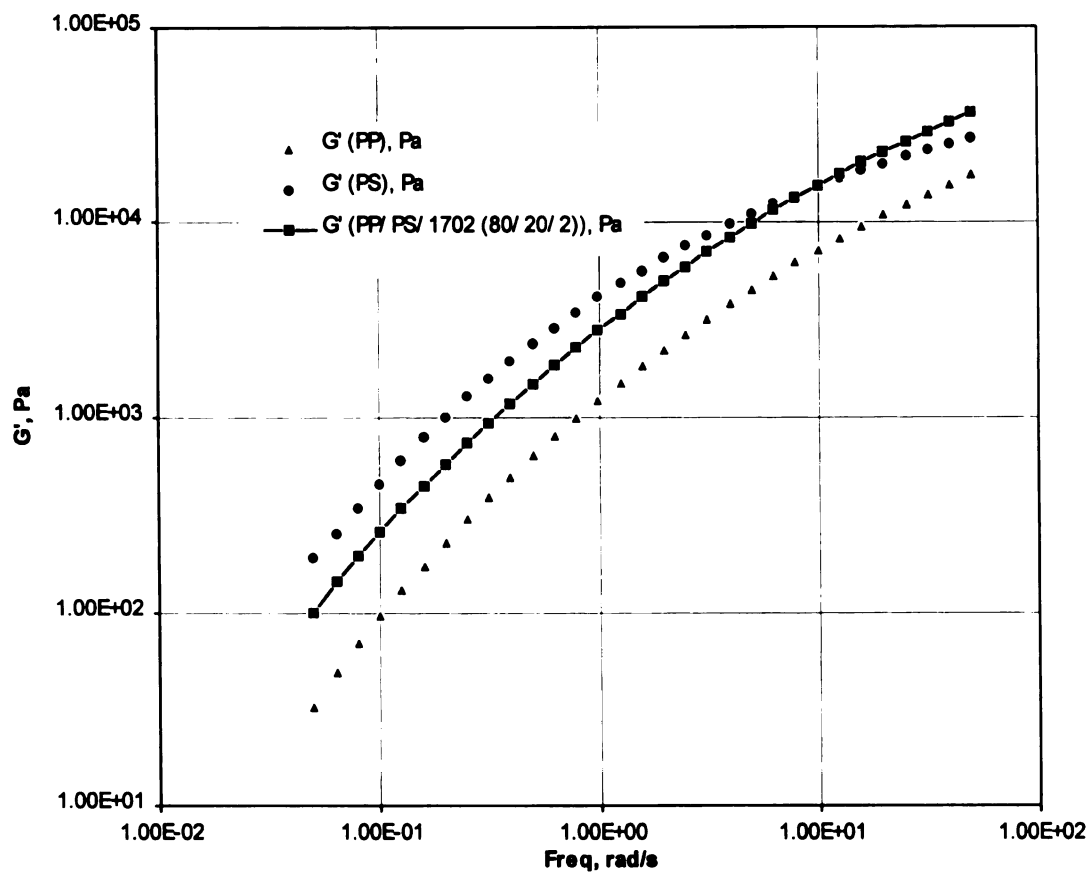
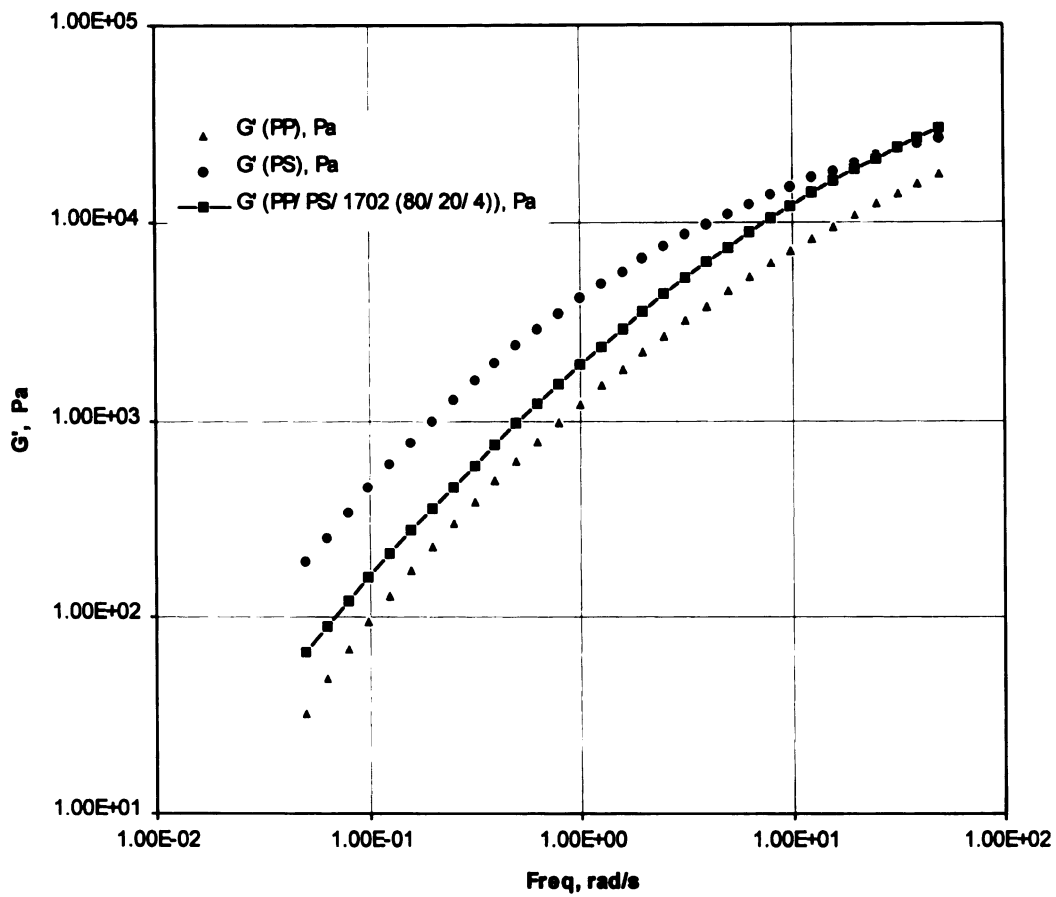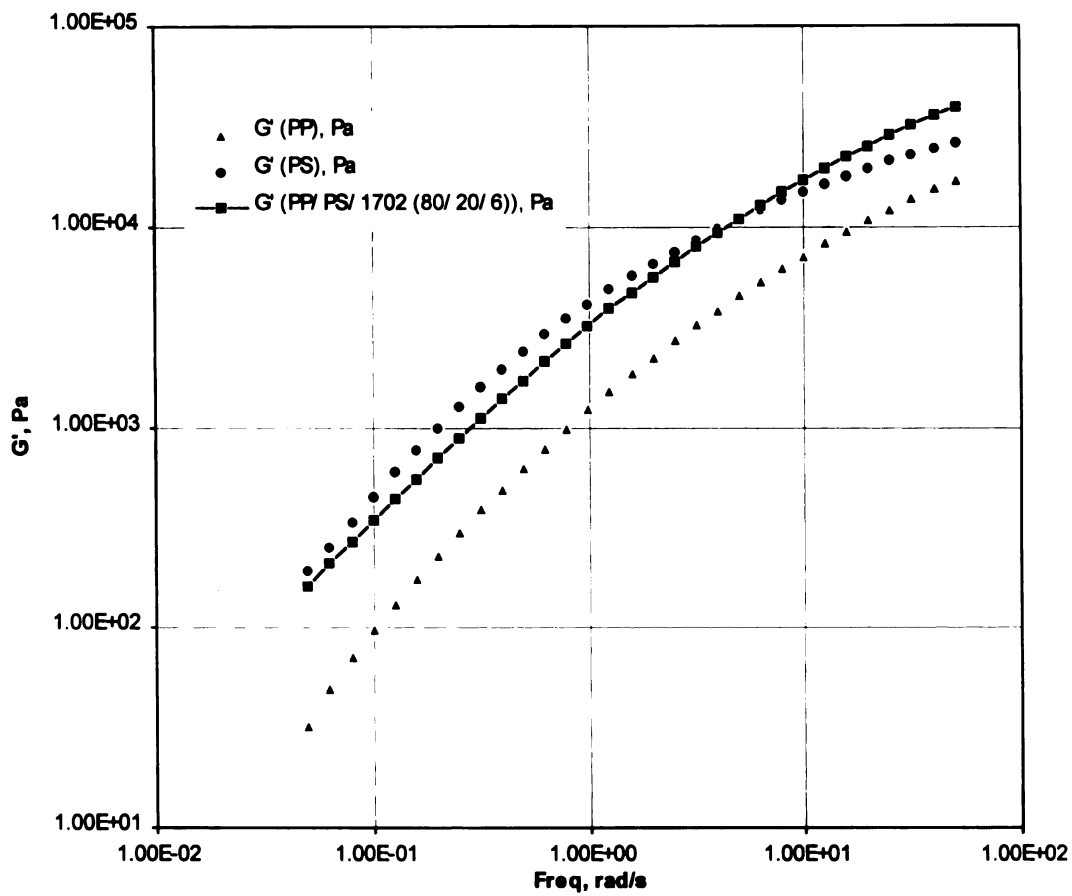Figure 5.12: Comparison of the storage moduli of the PP/ PS/ 1702 (80/ 20/ 6) blend with its components.

Figure 5.13: Comparison of the storage moduli obtained from the model with that obtained experimentally for PP/ PS (90/ 10) (Γ^0 = 5 mN/ m, R= 1.12 µm).

Figure 5.14: Comparison of the storage moduli obtained from the model with that obtained experimentally for PP/ PS (80/ 20) (Γ^0 = 5 mN/ m, R= 1.86 μm).

Figure 5.15: Comparison of the storage and loss moduli obtained from the model with that obtained experimentally for PP/ PS/ 1702 (90/ 10/ 2) (Γ^0 = 1 mN/ m, R= 0.9 μm).

Figure 5.16: Comparison of the storage moduli obtained from the model with that obtained experimentally for PP/ PS/ 1702 (90/ 10/ 4) for different values of equilibrium interfacial tension (R= 0.8 μm).
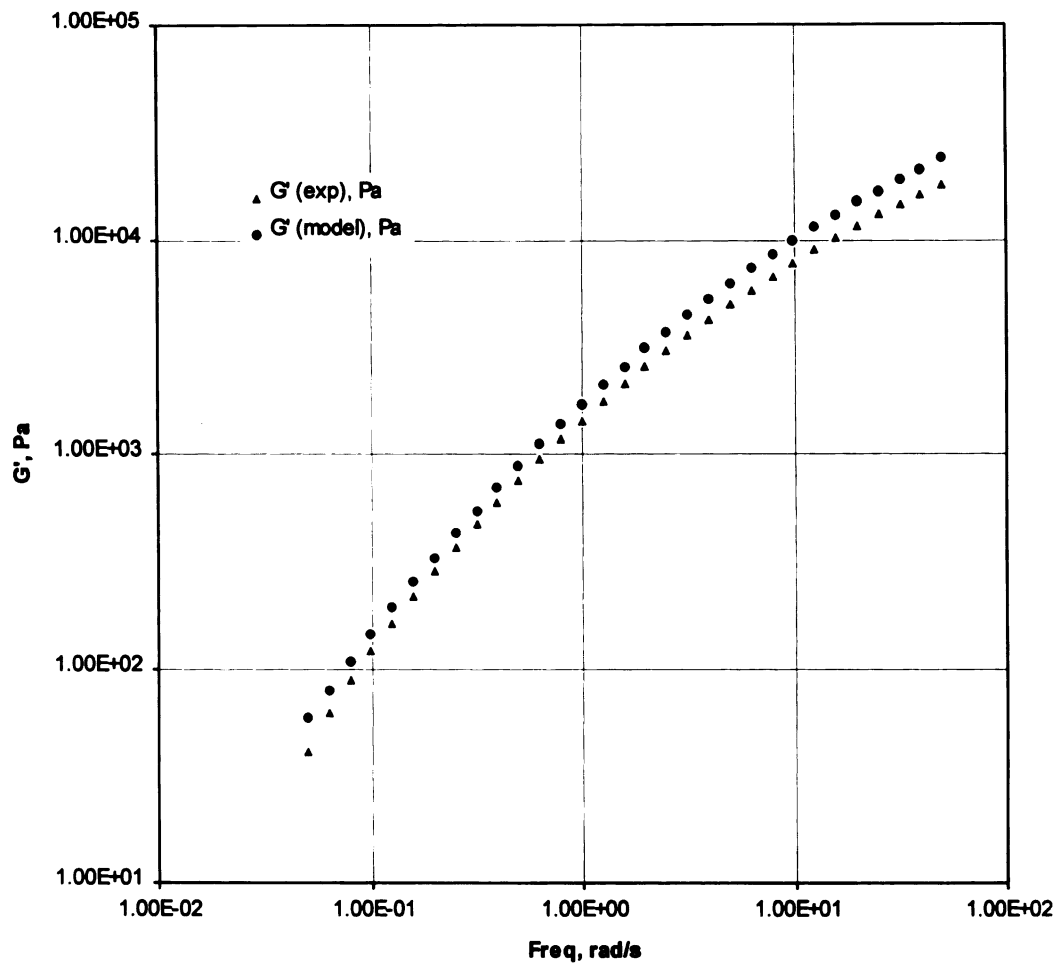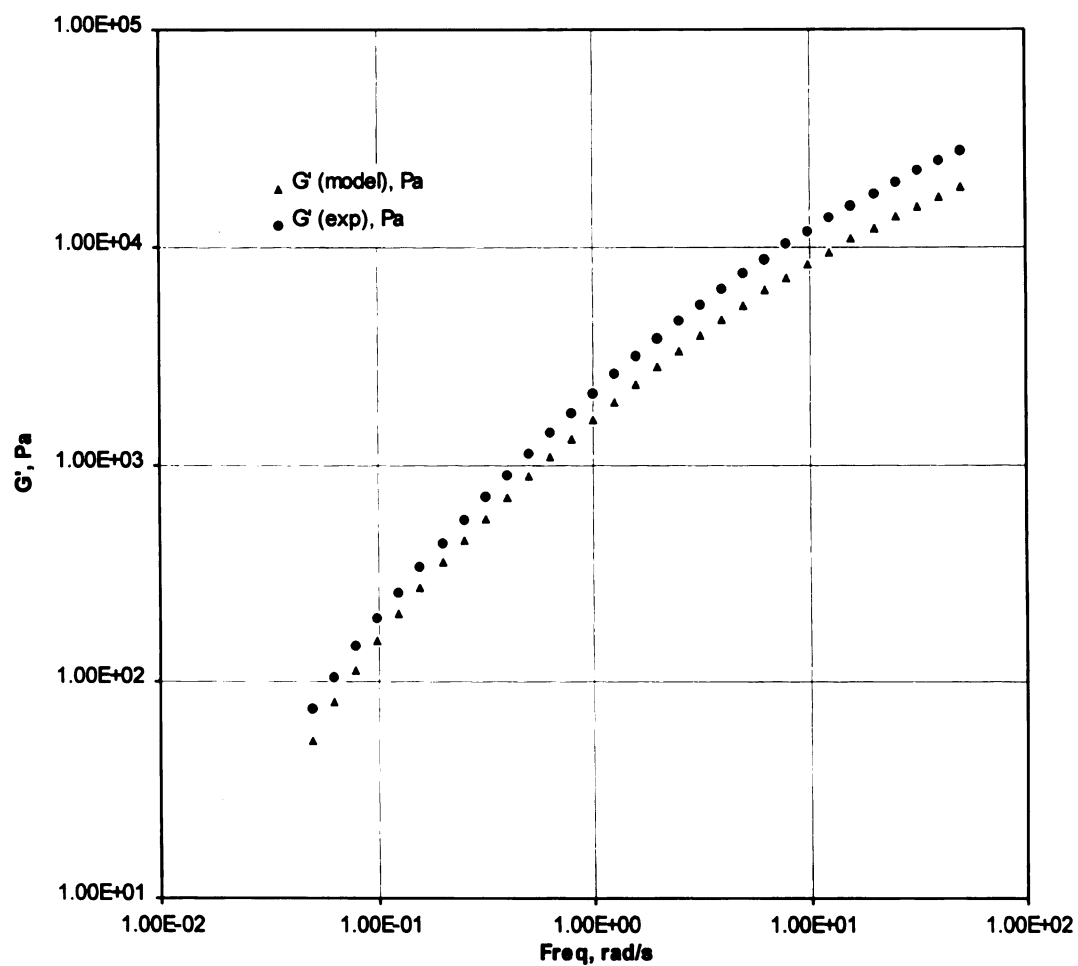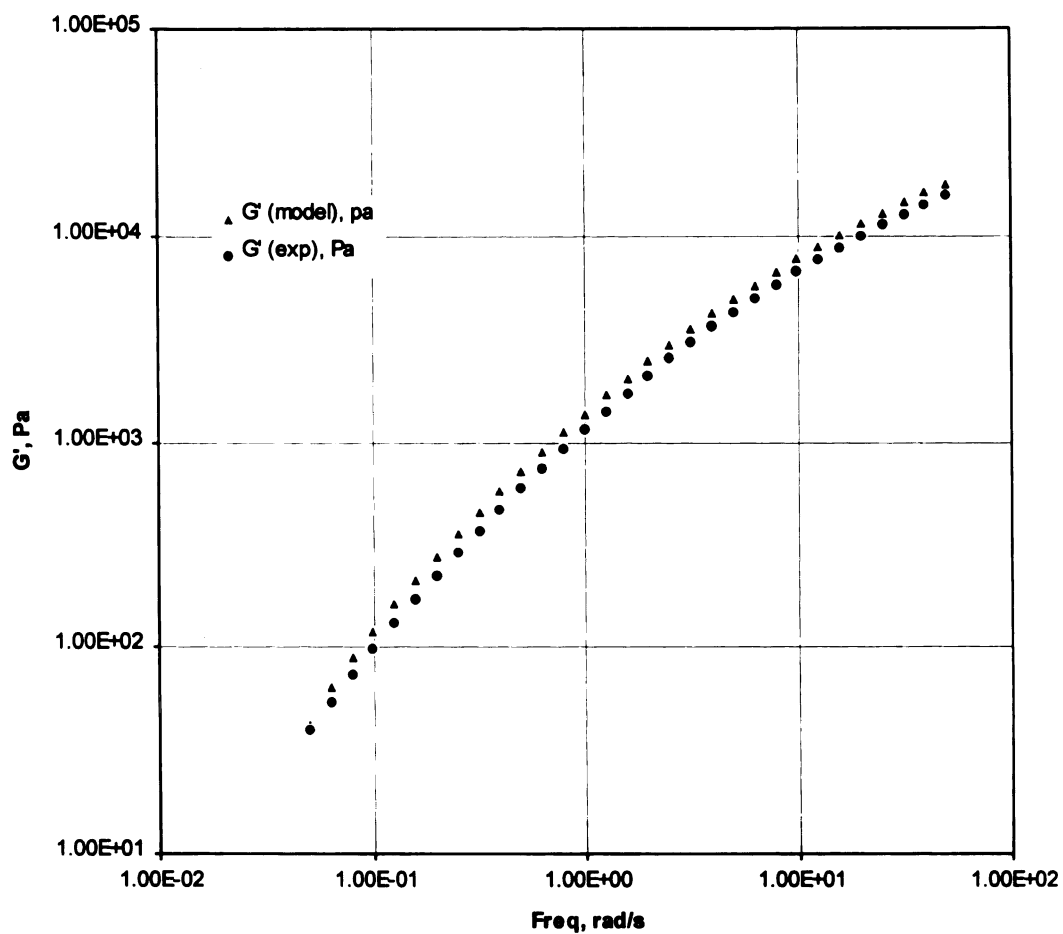
Figure 5.17: Comparison of the G'$_{int}$ obtained from the model with that obtained experimentally for PP/ PS/ 1702 (90/ 10/ 6) (Γ^0= 1 mN/ m, R= 0.6 µm).

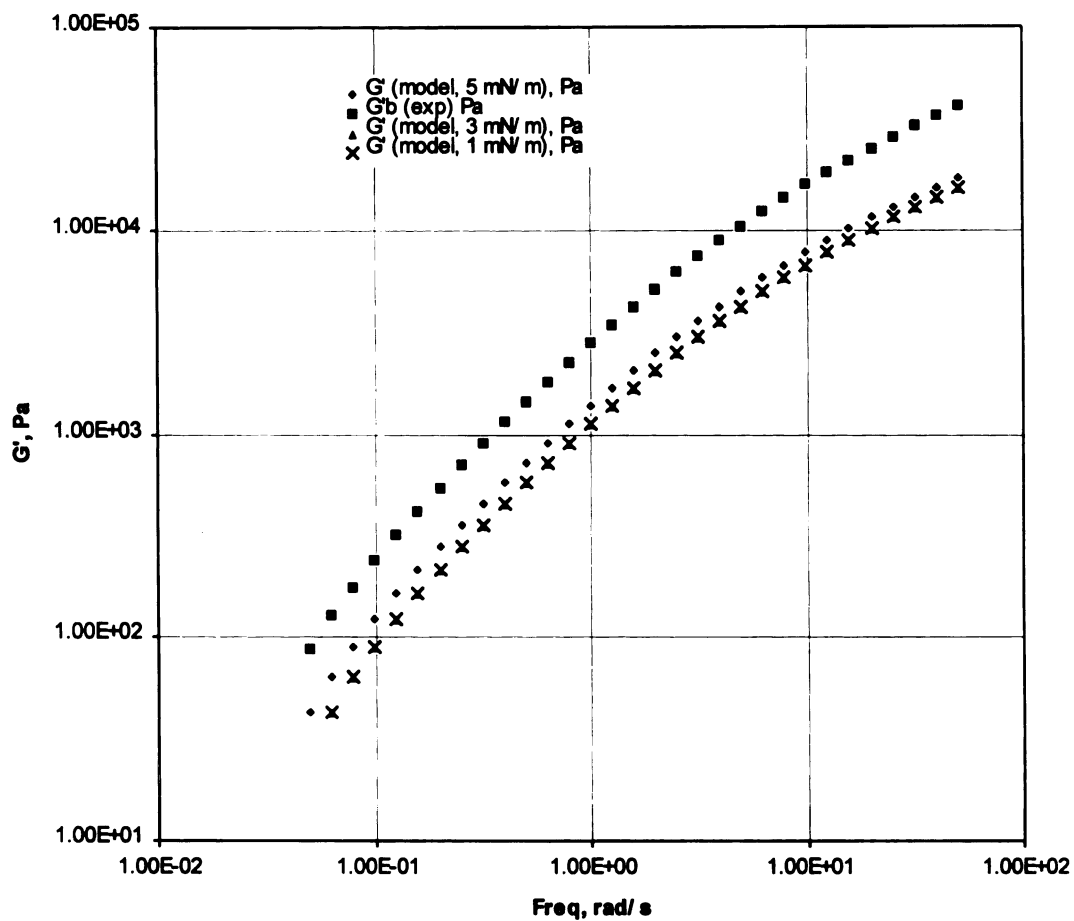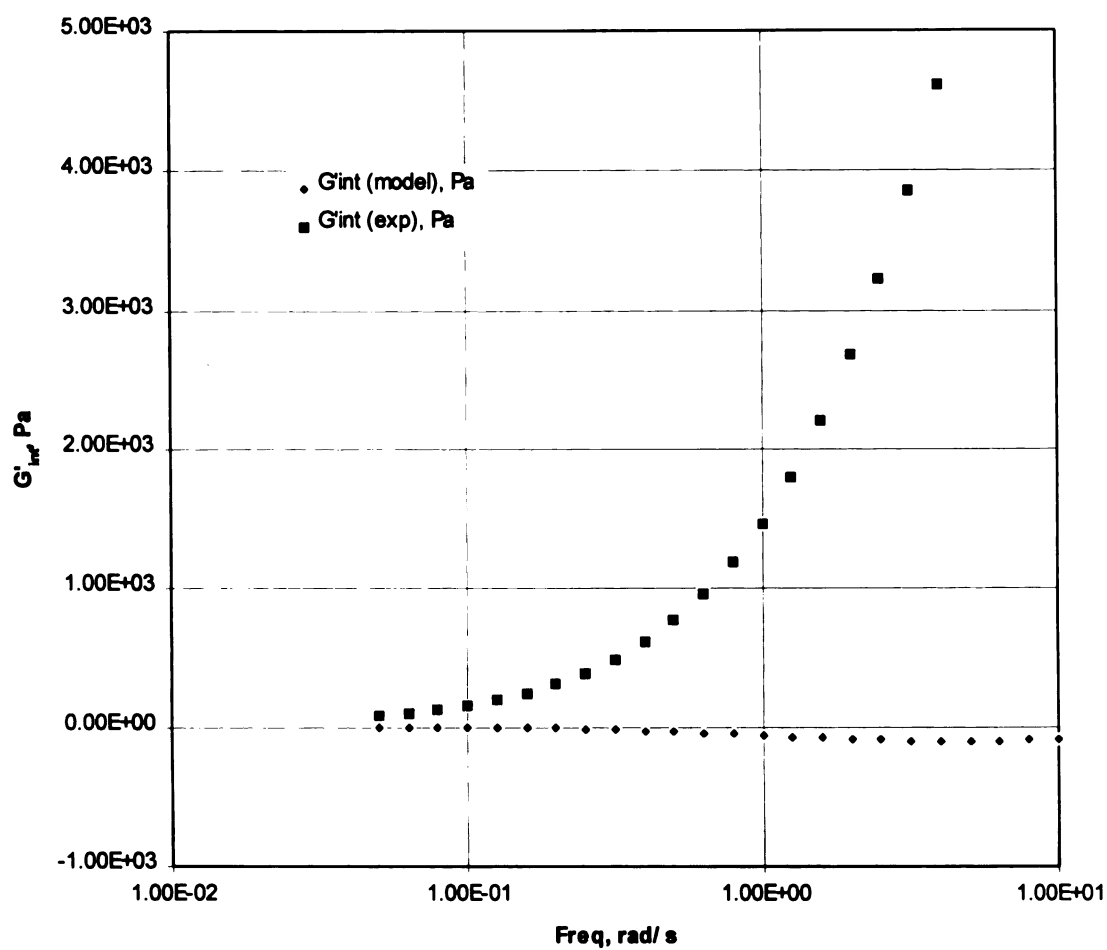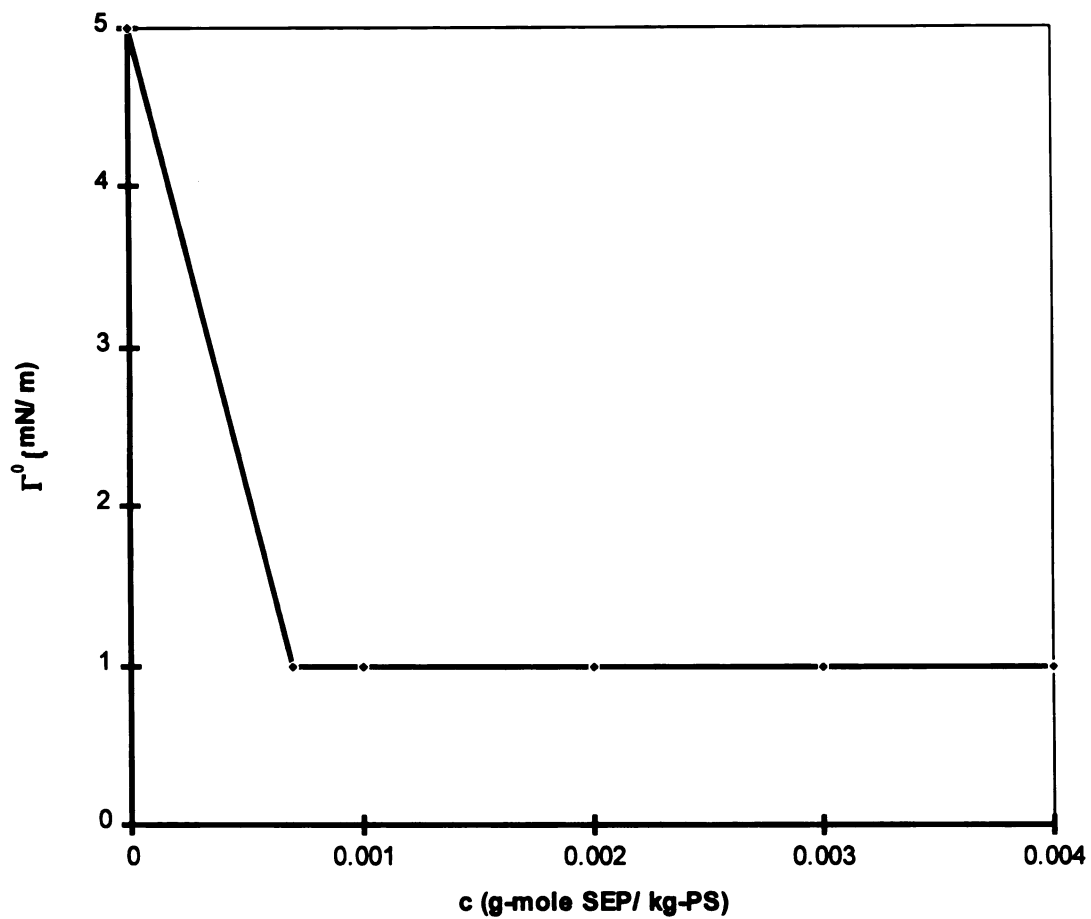Figure 5.18: The variation of the equilibrium interfacial tension with varying amount of the compatibilizing agent.

CONCLUSIONS AND RECOMMENDATIONS

Chapter 6

6.1 CONCLUSIONS

The main questions investigated in this work center around the effect of the nature of the interface the changes in which are brought about by the interfacial reaction.

- Does the equilibrium interfacial tension in reactively compatibilized blends fall due to interfacial reaction?

The results in Chapters 3 and 4 respectively show that the value of equilibrium interfacial tension in reactively compatibilized nylon 6 and maleated polypropylene fall due to interfacial reaction. In Chapter 3 a study of nylon 6 (containing lubricants) blended with neat polypropylene and maleated polypropylene containing 0.8 wt% of maleic anhydride was carried out. The value of equilibrium interfacial tension fell from 4 mN/m to 1 mN/m. In addition, it was seen that interfacial reaction imparts an additional elasticity to the blend.

The study presented in Chapter 4 investigates the effect of progressive extent of interfacial reaction on the equilibrium interfacial tension. It was carried out by blending nylon 6 (containing no lubricants) with neat polypropylene and three different grades of maleated polypropylene containing 0.15 wt%, 0.30 wt.% and 0.80 wt.% of maleic anhydride respectively. The measurements show that the equilibrium interfacial tension falls from 8 mN/m to 7 mN/m to 4 mN/m for progressively increasing extents of maleation.

- What are the accompanying effects (in rheology and morphology) besides the reduction in equilibrium interfacial tension in reactively compatibilized blends?

The observations in Chapter 3 and Chapter 4 show that interfacial reaction leads to a finer morphology. The particle size reduces from a few microns to sub-microns range. It has been shown that one important effect of interfacial reaction is the suppression of coalescence. Interfacial reaction imparts immobility to the interface and thus a reduced rate of coalescence. In addition, a lower value of interfacial tension reduces the thermodynamic drive to coalesce. It is seen that a very small amount of reaction is required to attain a finer morphology. Increased extents of reaction does not necessarily lead to a correspondingly finer morphology. The increasing extent of reaction however did effect the rheological behavior. The reaction imparted an elasticity to the blend. The model values under predicted the storage moduli in such blends. To account for this additional elasticity surface shear modulus as defined by the model of Palierne was employed. In absence of actual measurements of this modulus and the interfacial thickness estimates of this parameter were made. On using this parameter the results showed a considerable improvement.

- How do the trends compare with externally compatibilized blends?

The results of Chapter 5 present the trends obtained in blends of polypropylene and polystyrene compatibilized with -[S-EP]- di block copolymer. It is observed that the equilibrium interfacial tension falls from 5 mN/ m in non compatibilized blends to 1 mN/

m in compatibilized blends. In addition, similar to the directly reacted blends the compatibilized blends exhibited an enhanced elasticity.

- How good is the rheological model of Palierne applied in this work?

The results of Chapter 3, 4 and 5 show that the model of Palierne is applicable in reactive blends for a given range of the concentration of the dispersed phase. For non compatibilized blends however the agreement is good with the experimental values for a more concentrated blend. An important limitation of the model is that the components have to be chosen carefully so that the secondary plateau (a result of the equilibrium interfacial tension) is accessible.

6.2 RECOMMENDATIONS AND FURTHER WORK

- Quantify the extent of interfacial reaction

In this study the extent of interfacial reaction was not quantified. It was assumed that all the maleic anhydride in the interface is reacted with the amine. This is a reasonable assumption since there is 15. 74 g-mole of amine/ kg- nylon 6 compared to a maximum of 0.008 g-mole of -MAH/ kg- PP-MA. However, in order to actually quantify this effect it is important to make direct measurements of the extent of interfacial reaction and relate it to the equilibrium interfacial tension.

- Measure the interfacial thickness

The results in Chapter 4 indicate that in order to understand the issue of the extent of coverage of the interface, thickness of the interface must be directly measured.

Theoretical work [O' Shaughnessy and Sawhney, 1996] shows that interfacial reaction should lead to a reduction in the interfacial thickness. This must be verified by using techniques such as ellipsometry.

- Delineate the visco-elastic effects from the interfacial effects

In order to delineate the effects of the viscoelastic nature of the polymer from the interfacial effect, the following experiments should be designed:

1. Synthesize polymers such that the viscosity stays constant and the number of reactive sites is varied.

2. Synthesize polymers such that the number of reactive sites is a constant while the viscosity is varied.

BIBLIOGRAPHY

1. "Polymer Handbook", Ed. Brandrup J., Immergut E.H., Third Edition, Wiley Interscience Publication, New York, NY 1989.

2. "Reactive Extrusion. Principles and Practices", Ed. M. Xanthos, Hanser Publishers, New York, NY 1992.

3. "The Elements of Polymer Science and Engineering", A. Rudin, Academic Press, New York, 1993.

4. Anastasiadis S.H., Gancarz I., Koberstein J.T., Macromolecules 1988, 21, 2980-2987.

5. Bentley B.J., Leal L.G., J. Fluid Mech., 167:219-240, 1986.

6. Bentley B.J., Leal L.G., J. Fluid Mech., 167:241-283, 1986.

7. Borggreve R.J.M., Gaymans R.J., Polymer, 30, 63(1989).

8. Brahimi B., Ait-Khadi A., Ajji A., Jerome R., Fayt R., J. Rheol., 35(6), 1991.

9. Broseta D., Fredrickson G.H., Helfand E., Leibler, Macromolecules 1990, 23, 132-139.

10. Carriere C.J., Cohen A., Arends C.B., J. Rheology 33(5), 681-689(1989).

11. Cho K., Jeon H.K., Park C.E., Jim J., Kim K.U., Polymer, 37(7), 1117-1122 (1996).

12. Choi S.J., Schowalter W.R., Phys. Fluids 18, 420-427(1975).

13. Cohen A., Carriere C.J., Rheologica Acta 28:223-232 (1989).

14. Cox R.G., J. Fluid Mech. (1969), 37(3), 601-623.

15. Elemans P.H.M., Janssen J.M.H., Meijer H.E.H., J. Rheol., 34(8), 1311-1325(1991).

16. Elmendorp J.J., Polym. Eng. Sci.26(6), March 1986, 418.

17. Fayt R., Jerome R., Ph. Teyssie, J. Polym. Sci., Polym. Lett. Ed., 24, 25(1986).

18. Ferry J.D. in "Viscoelastic Properties of Polymers", John-Wiley and Sons, Inc., New York, NY 1961.

19. Frankel N.A., Acrivos A., Chem. Eng. Sc., 22, 847-853(1967).

20. Germain Y.B., Ernst B., Genelot O., Dhamani L., J. Rheol. 38(3), 1994.

21. Grace H.P., Chem. Eng. Commun. Vol. 14, p. 225.

22. Graebling D., Muller R., Colloids and Surfaces, (89-103)1991.

23. Graebling D., Muller R., J. Rheology 34(2), Feb. 1990.

24. Graebling D., Muller R., Palierne J.F., Macromolecules, 26, 320-329(1993).

25. Gramespacher H., Meissner R., J. Rheol., 36(6), 1127(1992).

26. Helfand E., Sapse A.M., J. Chem. Phys., 62, 1327 (1975).

27. Helfand E., Tagami Y., J. Chemical Phys., 56(7), Apr. 1971.

28. Helfand E., Tagami Y., J. Chemical Phys., 62(4), Feb. 1975.

29. Helfand E., Tagami Y., Polym. Lett., 9(1971), 741-746.

30. Helfand S., Bhattacharjee S.M., Fredrickson G.H., J. Chem. Phys. 91, 7200(1989).

31. Hosoda S., Kojima K., Kanda Y., Aoyagi M., Polym. Networks Blends, 1,51-59 (1991).

32. Ide F., Hasegawa A., J. Appl. Polym. Sc., Vol. 18, 963(1974).

33. Janssen J.M.H., Meijer H.E.H., Polym. Eng. Sci.35(22), Nov. 1995, 1766.

34. Kennedy M.R., Pozrikdis C., Skalak R., Comp. Fluids, 23, 251-254(1994).

35. Lee J., Yang S., Polym. Eng. Sci., Mid-Dec. 1995, 35(23), p. 1821.

36. Lim S., White J.L., Polym. Eng. Sci., Mid-Feb. 1994, 34(3), p. 221.

37. Loewenberg M., Hinch E.J., J. Fluid Mech., 321, 395-419(1996).

38. Matsumoto T., Chiyoji H., Onogi S., Transactions of the Society of Rheology 19:4 541-555 (1975).

39. Nishio T., Suzuki Y., Kojima K., Kakugo M., J. Polym. Eng., Vol. 10, Nos.1-3, 1991.

40. O' Shaughnessy B., Sawhney U., Macromolecules, 29, 7230(1996).

41. Okamoto M., Inoue T., Polym. Eng. Sci., Mid-Feb. 1993, 33(9), p. 175.

42. Oldroyd J.G., Proc. Roy. Soc. London Ser. A 218, 122-132 (1953).

43. Palierne J.F., Rheologica Acta 29:204-214 (1990).

44. Paul D.R., Barlow J.W., Keskkula H., in "Encyclopedia of Polymer Science and Engineering", 2nd Edition, Ed. Kroschwitz J.I., Wiley, New York, 1988, Vol. 12.

45. "Polymer Blends", Paul D.R., Newman S., Academic Press, New York, 1978, Vol. 1.

46. Rayleigh Lord, Proc. London Math. Soc. 10, 4(1878).

47. Rumscheidt F.D., Mason S.G., J. Colloid Sci., 17, 260(1962).

48. Sangani A.S., Mo G., Phys. Fluids, 6(5), 1994.

49. Scholz P., Froelich D., Muller R., J. Rheology 33(3), 481-499 (1989).

50. Scott C.E., Macosko C.W., Intern. Polym. Proc. X (1995) 1, p36.

51. Scott C.E., Macosko C.W., Polym. Eng. Sci.35, 1938(1995).

52. Serpe G., Jarrin J., Dawans F., Polym. Eng. Sci.30, 553(1990).

53. Sperling L.H. in "Introduction to Physical Polymer Science", 2nd Edition, Wiley, New York, 1992.

54. Stone H.A., Ann. Rev. Fluid Mech. 1994, 26:65-102.

55. Sundraraj U., Macosko C.W., Macromolecules, 28, 2647(1995).

56. Taylor G.I., Proc. Roy. Soc. London, A138, 41(1938).

57. Taylor G.I., Proc. Roy. Soc. London, A146, 501(1934).

58. Tjahjadi M., Ottino J.M., Stone H.A., AIChE J., 40, 3(385).

59. Tomotika S., Proc. Roy. Soc. London, A150, 302(1936).

60. Tomotika S., Proc. Roy. Soc. London, A150, 322(1935).

61. Wu S. in "Polymer Interface and Adhesion", Marcel-Dekker, New York, NY 1982.

62. Wu S., Polym. Eng. Sci.27, 335(1987).

63. Wu S., Polym. Sci. Polym Phys. Ed., 21, 699(1983).

.